Quantifying the system balancing cost when wind energy is incorporated into electricity generation system

Natalia Issaeva

Contents

List of Figures

iv

List of Tables

Abstract

Incorporation of wind energy into the electricity generation system requires a detailed analysis of wind speed in order to minimize system balancing cost and avoid a significant mismatch between supply and demand. Power generation and consumption in the electricity networks have to be balanced every minute, therefore it is necessary to study wind speed on a one-minute time scale. In this thesis, we examine the statistical characteristics of one-minute average values of wind speed. One-minute wind speed is available from a single site in Great Britain while there are records of ten-minute wind speed available. We apply a modified Gibbs sampling algorithm to generate one-minute wind speed required for optimization modelling from the available ten-minute wind speed.

System balancing costs are estimated through optimization modelling of the short-term electricity generation with wind energy contributing to the total supply. Two main drivers of additional system cost caused by wind energy are variability and unpredictability of one-minute wind speed. Further, a linear mathematical optimization model for a problem of short-term electricity generation is presented to calculate an additional balancing cost that appears as a result of wind energy variability. It is then shown that this additional balancing cost can be estimated using the statistical characteristics of wind energy present in the system. The unpredictable characteristic of wind speed is analysed with the techniques of stochastic programming. Uncertainty of the expected wind speed is represented through scenario trees and stochastic linear optimization models are used to calculate the extra cost due to uncertainty. Alternative optimization models are compared by calculating the additional balancing cost and the extent of imbalance between power generation and consumption in the system.

Notation

G	a set of all generators
C	a set of conventional generators
W	a set of wind generators
T	a number of time periods
T_Υ	a number of time periods in one year
T^S	a modelling horizon
T_n	a number of intervals associated with node
N	a number of nodes
S	a number of scenarios
V	a number of intervals of mismatch between the electricity supply and demand
α	power law exponent
$t, \tau, \nu, d, \delta, m$	a single period of time
l, L	a lag
i, j, k	an index
g	an index of generator
n	a node
a_n	an ancestor of node
p_n	a path probability
κ	a number of thermal generators
f_w^+	saving in fuel cost
f_w^-	additional fuel cost
S_i, S_j	a set of indices
z, z_r	height where wind speed was recorded
θ, q, s_g, k_1, k_2	parameters
λ	a parameter of Lagrangian function
$\beta^{\pm}$	percent of cost band
ϵ	an error term

b_1, b_2, b_3	parameters of quadratic function
β_i, ς_i	parameter of an exponential curve
$a_1, a_2, ..., a_{T_\Upsilon}$	deseasonal scaling curve
$r_1^\pm, r_2^\pm, r_3^\pm$	Run-Up and Run-Down export rates
$e_1^\pm, e_2^\pm$	"elbows" of Run-Up and Run-Down export rates
$D_1, D_2, ..., D_T$	the electricity demand
c_g, c_{coal}, c_{gas}	fuel costs
c_m	fuel cost of the marginal generator
$\zeta_1^\pm, \zeta_2^\pm, ..., \zeta_V^\pm$	cost of imbalance between the electricity supply and demand
k_{dm}	a weight in calculation of deseasonal scaling curve
Δ_D	a percent mismatch allowed between
	the electricity supply and demand
h_w	height of wind energy curve
γ_w	the average of the absolute value of gradients of wind energy curve
γ_g	the average of the absolute value of gradients of thermal plants
$\overline{\gamma_g}$	maximum of the absolute gradients of thermal plants
γ^*	sum of the absolute value of gradients of thermal plants
σ_x	standard deviation of wind energy
σ_γ	standard deviation of the absolute value of gradients
μ	mean value
σ	standard deviation
φ	covariance matrix
ψ	an inverse to covariance matrix
M	a matrix such that $MM^T = \varphi$
$\mathbf{1}$	vector consisting of scalers 1 only
$Y_1, Y_2, ..., Y_k$	a vector of normal variable (normally includes 10 values)
$U_1, U_2, ..., U_k$	a vector of a standard normal variable (normally includes 10 values)
$X_1, X_2, ..., X_k$	a vector of decision variable (normally includes 10 values)
$W_1^s, W_2^s, ..., W_k^s$	a vector of wind speed (normally includes 10 values)
$W_1^d, W_2^d, ..., W_k^d$	a vector of deseasonalised wind speed (normally includes 10 values)
$W_1^e, W_2^e, ..., W_k^e$	a vector of wind energy (normally includes 10 values)
$y_1, y_2, ..., y_k$	one-minute normal variable
$u_1, u_2, ..., u_k$	one-minute standard normal variable
$x_1, x_2, ..., x_k$	one-minute decision variable
$w_1^s, w_2^s, ..., w_k^s$	one-minute wind speed
$w_1^d, w_2^d, ..., w_k^d$	one-minute deseasonalised wind speed
$w_1^e, w_2^e, ..., w_k^e$	one-minute wind energy

$d_1^\pm, d_2^\pm, ..., d_V^\pm$	mismatch between the electricity supply and demand
$\overline{W^s}, \overline{w^s}$	the average of wind speed over a period of time
$\overline{x_g}, \underline{x_g}$	maximal and minimal capacity limits
$\overline{d^\pm}, \underline{d^\pm}$	upper and lower limits of mismatch intervals
Y^A, Y^B, Y^C, Y^D	vectors
$\hat{y}$	a value of normal variable
$f(*), h(*)$	a function
$P(*)$	a probability function
$\phi(*)$	probability density function
$\Phi(*)$	cumulative distribution function
$\Theta_d(W^s, a_\nu)$	function transferring original wind speed into deseasonal
$\Theta_n(W^d)$	function transferring deseasonalised wind speed into normal variable
$F_0, F_w^{flat}, F_w^{var}$	accumulated fuel cost of the deterministic optimization model
$F_{stoch}^{(a)}, F_{stoch}^{(b)}$	accumulated fuel cost of the stochastic optimization model
F_A	actual accumulated fuel cost
F_m	marginal fuel cost
$[Y_1, Y_2], [Y_1|Y_2], [Y]$	joint, conditional and marginal densities

Chapter 1

Introduction

How expensive is the operating of the electricity generation system when wind energy is introduced into it? This issue is becoming important as the amount of renewables in the system increases in order to meet the target that the Government of United Kingdom has set. In 2002 the Government introduced the Renewable Obligation (RO) to encourage development of renewable sources of energy[1, 2] and aimed to reach 15.4% of renewables in the overall electricity supply by 2015. Generators receive an RO Certificate (ROC) for each 1MWh of renewable electricity they generate. These are sold to electricity suppliers (defined in Appendix A) that pay the fixed penalty for each MWh it falls short of its obligation[1].

Various renewable technologies can contribute to the goal set by the Government but wind resource takes a leading competitive position among other renewable sources of energy (solar, tidal, wave, hydro) by the availability and efficiency. However, using wind for the electricity generation introduces a problem of intermittency and unpredictability of wind energy that will be studied in this work. The problem of meeting a target set by the Government of United Kingdom was investigated by the researchers of the Environmental Change Institute at Oxford University. In the report "Wind power and the UK wind resource"[10], Sinden states that in order to integrate wind power into electricity networks it is essential to understand the characteristics of wind resources. He believes variability of the wind energy is one of the obstacles to its extensive use by an electricity supplier and suggests a diversified renewable energy portfolio that includes wave and tidal steam combined with wind power. Such a combination reduces effect of variability in wind speed and consequently the cost of balancing electricity supply and demand.

1.1 Benefits of wind energy

In the 21st century the use of modern wind turbines for electricity generation has been growing very rapidly in Europe and this growth is expected to continue. Integration of wind generation in the operation and development of the electricity system is associated with both benefits and costs. The following reasons create plenty of opportunities to realise the technical potential of renewable energy, particularly wind power:

- Wind turbines produce green energy unlike conventional generators that produce CO_2 emissions;

- Renewable sources of energy do not have fuel costs that contribute the most to the expenses of the conventional generators;

- In spite of high percentages of natural gas and coal in British electricity generation, these resources are limited and their long-term supply can be disrupted. Meanwhile wind, tides, solar are known as renewable sources of energy.

1.2 Challenges of wind energy

However desirable the incorporation of wind energy into the electricity system there are a number of issues associated with its installation and management of the system. Detailed estimation of additional costs associated with the presence of the wind energy in the electricity generation system was performed by a few researchers since 2002 ([8, 9, 10, 11, 12]). Strbac et al. wrote a detailed paper on "Quantifying the system costs of additional renewables by 2020"[8] that examined the issue of challenges that incorporation of additional renewable sources faces. Besides the high investment cost of renewable sources of electricity, there is additional cost that occurs when balancing intermittent and variable wind energy. The work of Strbac et al. shows that in the current system wind energy is not able to replace fully the capacity and flexibility of conventional generating plants.

This thesis concentrates on the system costs associated with the balancing of supply and demand, however, there are also system costs appearing in transmission and distribution of electricity. Strbac et al.[8, 9] state different system cost drivers, such as location of the generation sources in relation to the source of demand, lack of flexibility in generation as well as intermittency and variability

of supply. Moreover, wind turbines are generally not able to provide the range of system support services (eg. voltage and frequency regulation) that are provided by conventional thermal and hydro plant. At relatively low levels of penetration this can usually be tolerated, but at the higher levels indicated by the Renewables Obligation target, it will require systematic solutions in order to maintain stability and integrity of the transmission system. These issues reduce the value of wind generation that displaces conventional generation.

1.3 Balancing of the electricity system

Electricity generation and delivery to the customers is a complex process. It is described in detail by the National Grid and Balancing and Settlement Codes[3, 4] that we refer to while formulating a problem of scheduling the electricity generation.

The main groups included into the electricity generation and distribution system are presented on Figure 1.1.
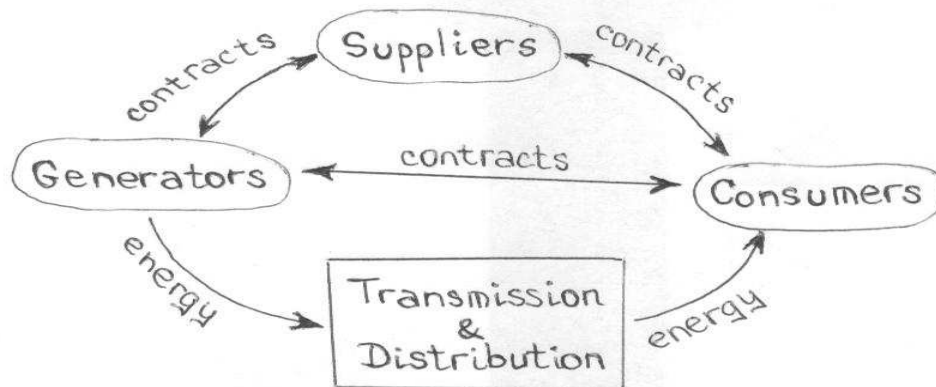
Figure 1.1: Schematic description of the power system

Most of the electricity in the power system is contracted. Some of the contracts are signed directly between the Generating companies and large industrial consumers. Residential consumers pay for their electricity through the Suppliers, companies like EDF, Scottish power or npower. Suppliers sign agreements to deliver contracted amounts of power to the Consumers. At the same time the Generators have an obligation to provide this power to the transmission system.

This section explains general terms of the system functioning while formal definitions of what these participants represent are given in Appendix A.

The interaction process of different participants in the electricity generation, transmission and consumption is complex and contains many procedures. Let us give a general description of this process in terms of a **Settlement Period**, a half-hour period of time when real-time balancing of the electricity supply and demand takes place (Figure 1.2).
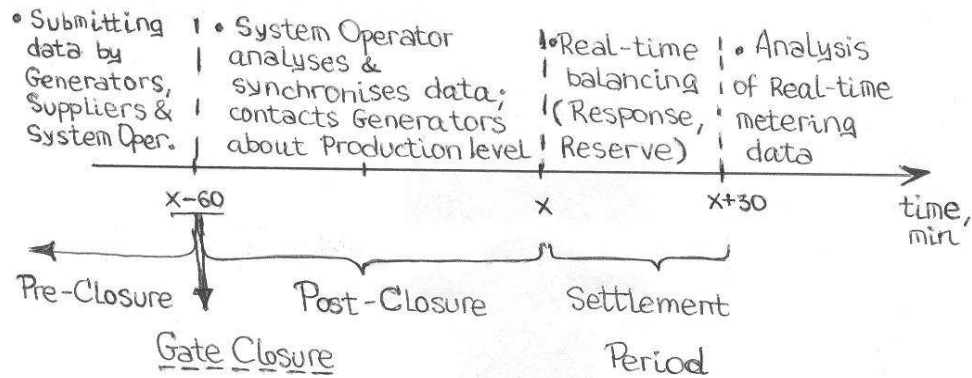
Figure 1.2: Process of balancing power system shown in terms of the Settlement Period

In order to manage the electricity transmission system efficiently National Grid Electricity Transmission (NGET), company that stands for the System Operator, collects the necessary data from the appointed parties. **Pre Gate closure** procedures are intended for the submission of Balancing Mechanism (BM) Unit Data (as defined in Appendix A) which includes characteristics of each generator such as maximum and minimum power output, ramp up rates, availability and other. This information would enable NGET to assess which BM Units are expected to be operating in order that NGET can ensure (so far as possible) the integrity of the Great Britain Transmission System, and the security and quality of supply [4]. From the information provided by BM Units the System Operator has an insight into how much it can vary their generation above or below their submitted profile and what price must be paid for every possible amount of deviation from the planned generation.

Gate Closure takes place one hour before the beginning of the Settlement Period. Data for any Operational Day may be submitted to NGET up to several

days in advance of the day to which it applies, as provided in the Data Validation, Consistency and Defaulting Rules. The data to be used by NGET for operational planning will be determined from the most recent data that has been received by NGET by 11:00 hours on the day before the Operational Day to which the data applies, or if no data has been submitted by 11:00 hours on that day by the default data values. The individual data items that Generators and Suppliers submit include Physical Notifications, Quiescent Physical Notifications, Export and Import Limits, Bid-Offer Data and Dynamic Parameters (all defined in Appendix A).

NGET as the System Operator has the responsibility of providing the information on the Demand Estimates. On the basis of historic trends in the availability of generating capacity and the data submitted by the generating units NGET also decides on the necessary Contingency and Operating Reserve, as well as System Margins.

Electricity transmission and distribution system of Great Britain operates with a certain **Target Frequency**. The frequency is allowed to vary 1% up or down from 50Hz. As long as the amount of produced electricity equals the demand, frequency in the transmission system stays at 50Hz. If the the generation exceeds demand frequency would rise above 50Hz and if demand exceeds generation then frequency in the system drops. The System Operator balances the supply and the demand in the system every moment of the real time through different procedures and is responsible for keeping the system frequency in the target range.

In order to deal with unpredicted variations in demand and generation, the System Operator requires an appropriate automatic Response, to neutralise rapid variations from a few seconds to a few minutes, and operating Reserve to deal with slow variations over time horizons from several minutes to several hours [24]. Response is defined as an automatic change in active power output by the large generating units that effects the frequency in the system. Response is used as an earliest available instrument of the balancing mechanism. It supports the system from the first second up to 30 minutes after the imbalance was recorded. By that time the operating Reserve is ready to change the Export (Import) level (as defined in Appendix A). Some of the generating units acting as the Reserve are operating at part-time load, some are off-line but able to start within a short time. Pumped storage, for example, can respond very rapidly to counteract any loss of generation or surge in demand. Gas turbines are able to provide generation on timescale of few minutes while steam plant would require a few hours to warm

up. The participants need to ensure that each of their BM units, applying **Good Industry Practise**, follows the submitted notification of export or import level.

Balancing costs appear when the System Operator uses or keeps on standby flexible but expensive generating units in order to deal with an unexpected mismatch between the electricity supply and demand or operates generators at non-optimal generation levels so as to provide flexibility for rapid change in output level. The levels of reserve required at any given time depend partly on uncertainties in the predictions of demand, but also on the need to deal with the sudden loss of substantial amounts of generation, either due to a power station faults or the loss of transmission circuits. In England and Wales, for example, key criteria are possible loss of one circuit of the cross-Channel link (1000 MW), or of Sizewell B nuclear power station (1320 MW). The value of possible loss of generating capacity can significantly increase after wind energy is introduced into the power system.

1.4   Timescale

Electricity supply and demand in the transmission and distribution power systems need to be balanced every single moment of time. On the scale of seconds it is managed through the automated process of frequency response. At the same time, scheduling of electricity generation reserve on hourly and daily basis has been extensively studied by various researchers, for example in [29, 30, 31, 32, 33]. Hourly and daily production planning of power systems involves start-up and maintenance of the thermal plants. This leads to dynamic, mixed-integer programming problems, and methods of solving these models were analysed by Römisch, Möller, Dentcheva, Feltenmark and other researchers ([29, 30, 31]) in the 1990s. Later, mixed-integer programming problems were extended by capturing the uncertainty in thermal power systems and the stochastic mixed-integer programming was applied to solve complex models ([32, 33]).

We wish to study scheduling of the electricity generation at time intervals that were not well-researched before but have an important application in the industry. This work focuses on short-term variability of the wind energy and the electricity generation with one-minute frequency. At this short scale there can be no decision made on the start-up or maintenance of thermal plants, therefore, we avoid the complexity of mixed-integer programming problems.

When scheduling the operating Reserve, the System Operator takes into account the uncertainties in demand and generation on various timescales. Uncer-

tainty increases with the time horizon, but broadly speaking, the costs of the appropriate Reserve decrease as the time scale over which they have to respond increases. Operating Reserve (as defined in Appendix A), for example, may cost around £1/MWh, but fast Response plant may cost up to £5/MWh, or more[24].

Figure 1.3 plots an example of the wind power that would have been generated by a small wind farm in Aberystwyth based on the recorded wind speed. It varies significantly from minute to minute[1] which makes variability of wind energy one of the strongest drivers of the balancing cost. One possible solution for this problem involves diversifying locations of wind farms. Another solution suggested by Sinden in his work on diversified renewable energy portfolios[12], was to combine wind energy with more predictable tidal and wave energy.
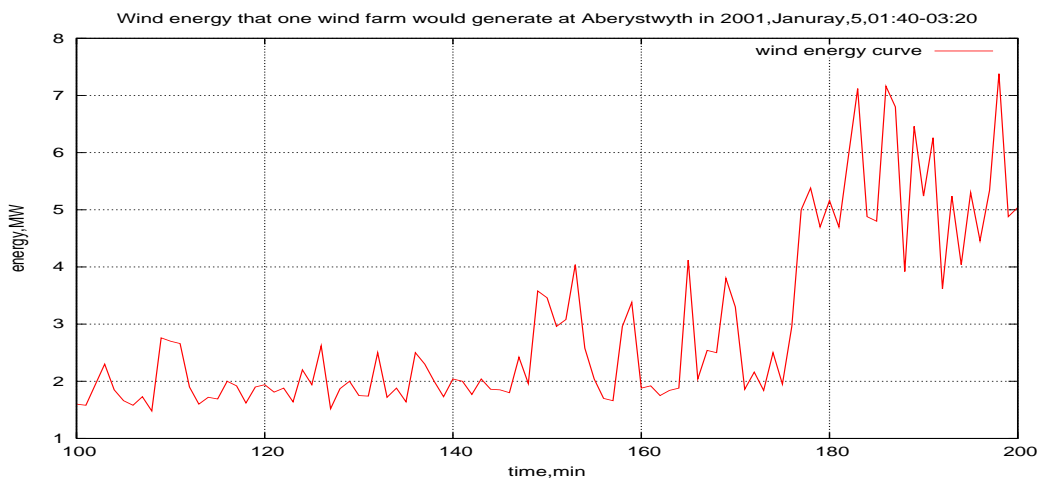
Figure 1.3: Wind energy that would have been generated by a small wind farm in Aberystwyth on the 5th of January,2001

1.5   Aim of the research

Different participants of the electricity industry (Figure 1.1) can benefit from the efficient operation and planning of electric power generation systems. On the one hand, suppliers of energy reduce the cost of mismatch between the reported and actual electricity load. On the other hand consumers receive uninterrupted electricity flow in their houses and offices. This thesis is aiming at the vertically integrated utilities (like Scottish Power or EDF) that are capable of combining

---

[1]The MST Radar Facility at Aberystwyth is funded by the UK Natural Environment Research Council and the data are provided through the British Atmospheric Data Centre

different energy portfolios and, thus, minimize their costs of meeting the contracted demand.

NGET acting as the System Operator manages the electricity generation system of the United Kingdom. Its profit is independent of the operational cost of the electricity generation, however the System Operator has to ensure the integrity of the Great Britain Transmission System while minimizing the balancing costs.

1.6   Structure of thesis

In Chapter 2 we investigate how the wind speed varies and how this affects the wind power generation. There is only one publicly available site of wind speed one-minute averages. In order to obtain a wind power output from the geographically diverse sources we will develop a Gibbs sampling algorithm to generate one-minute average wind speed from available average ten-minute values of wind speed at geographically dispersed locations.

Obtained in Chapter 2, wind power output is used later in the thesis when testing the optimization model of the electricity generation. Chapter 3 describes the power system of the United Kingdom and how it can be modelled using linear programming. By setting different parameters of the deterministic model, the system balancing cost of wind power variability is calculated. In deterministic models we assume that wind can be predicted exactly, so the costs of incorporating the wind power into the electricity generation system originate only in variability of wind speed.

The additional system balancing cost that appears after the wind power is introduced into the electricity generation system can be modelled as a function depending on the statistical parameters of one-minute wind power output. There is a number of tests performed in Chapter 4 that derives a model approximating the operational cost of the electricity generation.

In practise it is not possible to predict the wind speed accurately even over a short time period of 30 minutes. Chapter 5 investigates into the additional system balancing cost that comes from coping with the unpredictable nature of wind speed. The problem of electricity generation is then solved using stochastic programming methods where the uncertainty is represented with a scenario tree. The issue is complicated by a possible loss of the generating capacity. This uncertainty can also be pictured on the scenario tree and resolved along with the uncertainty of the wind power output using stochastic programming.

Deterministic and stochastic models formulated in this work are implemented using a mathematical programming modelling language (AMPL)[47]. Data used for the solving of the electricity scheduling problem are managed using JAVA programming language.

Chapter 2

Wind Speed Analysis

The aim of this thesis is to study electricity generation on one-minute time scale. Implementation of optimization models requires data with the appropriate resolution, however, there is no one-minute wind speed available on the country level. Least frequent data is provided by two sources: the Meteorological Office of the United Kingdom that publishes wind speed averaged over one hour for different sites in the UK and Utah Geological Survey (USA) [21] that gives an access to ten-minute average wind speed with standard deviation known.

To obtain the necessary data, in this chapter we wish to study the only available source of one-minute wind speed recorded in the UK ([20]) and apply this information to generating an unbiased sample conditional on a given average value. Samples generated for different sites of a geographically diverse territory are further transformed into power that can be used for optimization modelling of the electricity generation system.

2.1   Generating wind energy

United Kingdom is situated on an island with a unique location that defines its climate. Due to the proximity to the Atlantic Ocean and the North Sea, weather on the British islands frequently changes producing high wind speeds. As a result the United Kingdom has some of the best wind resources in Europe, if not the world, in both onshore and offshore locations. This makes the country a very attractive location for wind developments, as high average wind speeds and good reliability result in more power output and lower costs[6].

Currently there are over 200 onshore and offshore wind farm projects operating in Great Britain with a total installed capacity of 3.3GW. Wind energy contributes around 2.2% of the total electricity generation in the United King-

dom and this number is expected to grow as more wind farms are connected to the grid. Rapidly developing technology introduces more efficient wind turbines built with the towers up to 100m tall that can capture strong winds. The average turbine size in 2008 was considered as 2MW that produces energy with the average output of 40% of the maximum possible capacity[6].

In order to estimate wind energy produced by a turbine, the available wind speed is transformed into power using a wind-power curve. These curves are uniquely determined for the different wind turbine type. Let us take NEG Micon 2750/92 as a typical wind turbine with the capacity 2.75MW, 3m/s cut in and 25m/s cut out wind speed. Its hub height is 70m and rotor diameter is 92m. The wind-power curve for this wind turbine is plotted in Figure 2.1.
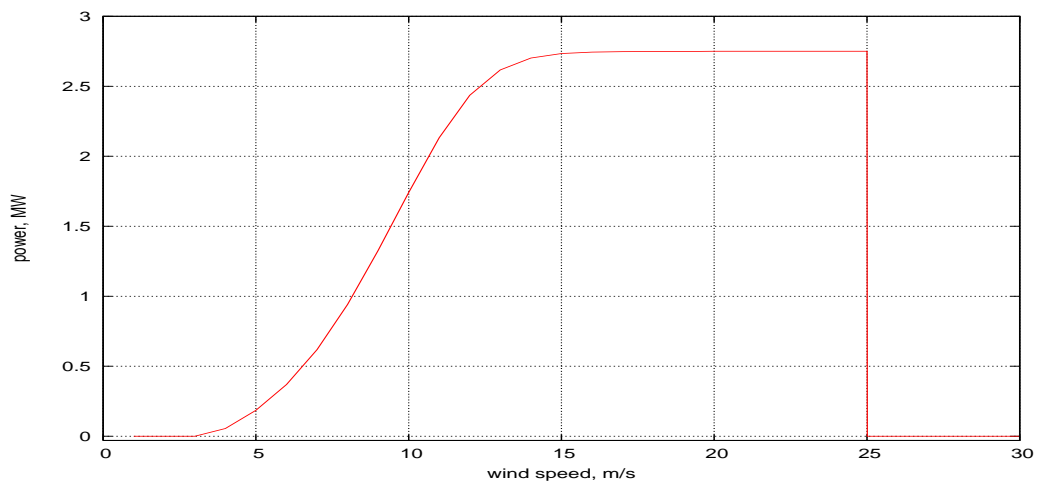
Figure 2.1: Transformation function between the wind speed and the wind power

2.2 Generating wind speed data

This section starts with the analysis of the available source of one-minute wind speed recorded in the United Kingdom ([20]) that is used to identify the probability distribution required for sampling one-minute wind speed. Further, we wish to develop a unique method that generates an unbiased sample from the wind speed stochastic process conditional on each consecutive group of wind speeds having a given average value. A new algorithm includes Monte Carlo Markov Chain method, Gibbs sampling algorithm, originally adapted to a problem of generating one-minute wind speed data.

2.2.1 One-minute wind speed data

The one-minute resolution wind speed stochastic process is based on the statistical properties of one-minute wind speed measurements made at one location. The one-minute wind speed measurements required for this work are provided by Mesosphere-Stratosphere-Troposphere (MST) Radar located at Frongoch farm near Aberystwyth (140 m above mean sea level, 52.42N, 4.05W; British National Grid Reference SN 604826) funded by the Natural Environment Research Council (NERC). Wind speed and direction are recorded at one-minute intervals using vector instruments, an A100R anemometer and a W200P wind vane[20]. This research uses 12 years of data for the period between 1996 and 2007.

Further adjustments are necessary. Wind speed read by the MST Radar is registered at 5-meter height, however, a hub height of NEG Micon 2750/92 (a typical wind turbine for this research) is 70 meters. Thus, it is necessary to transfer available 1-minute wind speed to this height. The power law represents a simple model for the vertical wind speed profile. Its basic form is provided by Manwell, McGowan and Rogers in [22]:

$$\frac{W^s(z)}{W^s(z_r)} = \left(\frac{z}{z_r}\right)^\alpha$$

where $W^s(z)$ is the wind speed at height z, $W^s(z_r)$ is the reference wind speed at height z_r, and α is the power law exponent.

In practise, the exponent α is a highly variable quantity. It has been found that α varies with such parameters as height above the sea level, time of day, season, nature of terrain, wind speed, temperature, and various thermal and mechanical mixing parameters. Some researchers have developed methods for calculating α from the parameters of the log law. Many researchers, however, feel that these complicated approximations reduce the simplicity and applicability of the general power law and that wind energy specialists should accept the empirical nature of the power law and choose values of α that best fit available wind data. For flat and open areas α equals $\frac{1}{7}$, which is what expected for a flow over a flat plane.

In what follows the wind speeds have been transformed to correspond to a height of 70m above ground level.

Definition Let $W_1^s, ..., W_T^s$ be *a vector of wind speed* corresponding to a height of 70m above ground level. T is a number of minutes in 12 years of one-minute records. We assume 360 days in a year so that $T = 6220800$.

Let us test the wind speed data for periodicity, as this can interfere with the

15

probability distribution of the wind speed data later. There are two different types of periodicity affecting original records. There is a daily pattern which may be caused by the interaction between warm and cold air of the land and the sea consequently (geographical feature of the United Kingdom) or due to heating during the day over land (even when there is no sea involved). There is also a seasonal pattern which affects a strength of the wind speed during different months of the year. We use a multiplicative model to evaluate the seasonal and daily effect in order to preserve a non-negative property of the data.

Definition Let $\{a_\nu\}_{\nu=1,\dots,T_\Upsilon}$ be a *deseasonal scaling curve* that carries the information on daily and seasonal patterns of the wind speed. T_Υ is a number of minutes in a year. We assume 360 days in a year so that $T_\Upsilon = 518400$.

For a convenience of further calculations every minute ν of a year can be described by a δ day of the year and a τ minute of the day:

$$\nu = 1440(\delta - 1) + \tau,$$

where $\delta = 1, \dots, 360$ and $\tau = 1, \dots, 1440$. Similarly, every minute t of the 12-year data can be described by a δ day of an Υ year and a τ minute of the day:

$$t = 518400(\Upsilon - 1) + 1440(\delta - 1) + \tau,$$

where $\Upsilon = 1, \dots, 12$, $\delta = 1, \dots, 360$ and $\tau = 1, \dots, 1440$.

Then a_ν is obtained by calculating a weighted average of the wind speeds over all 12 years for a day $\delta - 10$ to $\delta + 10$ and for each of these days over minutes $\tau - 20$ to $\tau + 20$.

$$a_\nu = a_{1440\cdot\delta+\tau} = \sum_{\Upsilon=1}^{12} \sum_{d=-10}^{10} \sum_{m=-20}^{20} k_{dm} W^s_{\Upsilon,(\delta+d),(\tau+m)} \tag{2.1}$$

where k_{dm} is a weight of the wind speed $W^s_{\Upsilon,(\delta+d),(\tau+m)}$ in minute $(\tau + m)$ of day $(\delta + d)$ in year Υ. In (2.1) $\nu = 1, \dots, T_\Upsilon$ is a minute of a year and an average value a_ν is assumed to be effected by the preceding and the following 20 minutes of the preceding and the following 10 days to the current.

Weight k_{dm} varies depending on the distance between the current minute (δ, τ) and a minute effecting it $(\delta + d, \tau + m)$. If plotted in terms of day d or minute m, weights k_{dm} form a shape of an isosceles triangle with the middle vertex at the current time moment of τ minute of δ day. Every weight k_{dm} can be defined

as follows:
$$k_{dm} = \frac{(10 - |d| + 1)(20 - |m| + 1)}{12 * (20 + 1)^2 * (10 + 1)^2} \qquad (2.2)$$

In (2.2) values 10 and 20 correspond to intervals of 10 days and 20 minutes assumed to contribute to an average value a_ν. Note, that all 12 years are given the same weight in the average.

As a result a deseasonal scaling curve a_ν can be constructed, each value of which is a weighted average over 12 years of data.

Definition Let us denote $W_1^d, ..., W_T^d$ as *deseasonalised wind speed*, or the wind speed with removed daily and seasonal components. T again is a number of minutes in 12 years.

To estimate deseasonalised wind speed W_t^d we remove daily and seasonal effects from the wind speed W_t^s dividing the latter by a corresponding value of the deseasonal scaling curve. For a convenience of calculation we assume a linear connection between a minute of a year ν and a minute t of the 12-yearly data:

$$t = 518400(\Upsilon - 1) + 1440(\delta - 1) + \tau \Rightarrow \nu = 1440(\delta - 1) + \tau, \qquad \forall \Upsilon$$

Definition Let us denote $\Theta_d(W_t^s, a_\nu)$ as a function transferring original wind speed W_t^s into deseasonalised wind speed W_t^d for $\forall t = 1, ..., T$.

By defining a time position of a wind speed t with a minute τ of a day δ in year Υ the deseasonilised value W_t^d can be found as follows:

$$W_t^d = \Theta_d(W_t^s, a_\nu) = \Theta_d(W_{\Upsilon\delta\tau}^s, a_{\delta\tau}) = \frac{W_{\Upsilon\delta\tau}^s}{a_{\delta\tau}}$$

where $a_{\delta\tau} = a_\nu$ is the deseasonal scaling curve.

Notice, that the hypothesis about daily periodicity of wind speed is supported by the autocorrelation of the original data. The series of autocorrelation coefficients measure the correlation, if any, between observations at different distances apart and provide useful descriptive information [43]. Given T observations of wind speed $W_1^s, ..., W_T^s$, on a time series, for every integer l we can form $T - l$ pairs of observations, namely, $(W_1^s, W_{1+l}^s), ..., (W_t^s, W_{t+l}^s), ..., (W_{T-l}^s, W_T^s)$, where each pair of observations is separated by a time lag l. Regarding the first observation in each pair as one variable, and the second observation in each pair as a second variable, then, we can measure the autocorrelation coefficient between

adjacent observations, W^s and W^s_l, using the formula:

$$corr(W^s, W^s_l) = \frac{\sum_{t=1}^{T-l}(W^s_t - \overline{W}^s)(W^s_{t+l} - \overline{W}^s)}{\sum_{t=1}^{T}(W^s_t - \overline{W}^s)^2} \cdot \frac{T}{T-l} \qquad (2.3)$$

where $\overline{W}^s$ is the mean value of the series $W^s_1, \ldots, W^s_T$.
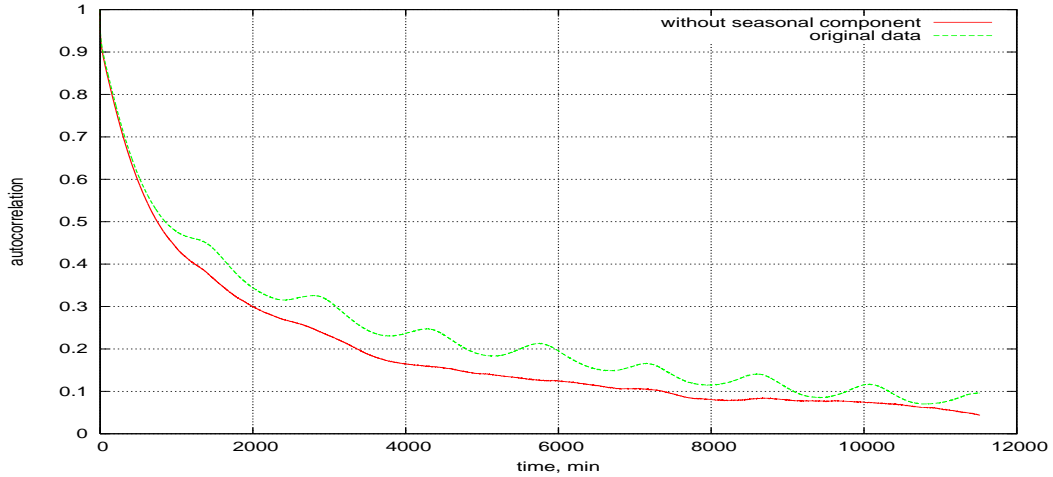
Figure 2.2: Autocorrelation of the original and the deseasonalised wind speed data

Figure 2.2 plots the autocorrelation of one-minute wind speed recorded with MST Radar located near Aberystwyth and the autocorrelation of the same deseasonalised data. The fluctuations of the autocorrelation function for the original data repeat every 1440 minutes, which supports the presence of a daily periodic component in the wind speed, however this pattern is not visible in the deseasonalised data.

2.2.2   Methods of generating missing data

After wind energy is incorporated into the the electricity generation system its optimization modelling requires geographically distributed samples of one-minute wind speed data. US Geological Survey provides sample of ten-minute wind speed recorded over a large territory of Utah state. In this section we wish to describe an algorithm that would allow us to sample one-minute wind speed from a known distribution when an average value over ten minutes is given.

To ensure a generated set of data values reflects the properties of one-minute wind speed distribution, one-minute records from MST Radar located near Aberystwyth are analysed. However, it is hard to describe this distribution analytically. A survey of existing techniques on data sampling identified Monte Carlo Markov Chain (MCMC) methods as a group of methods that can be applied to generate one-minute wind speed when the distribution is not fully formulated. One of the MCMC algorithms, Metropolis-Hastings produces a sequence of random samples from a probability distribution, however it requires a joint probability distribution of one-minute wind speed which is hard to find. Meanwhile, it is possible to find a conditional distribution of wind speed at every minute depending on the past realisations and, hence, to use a special case of Metropolis-Hastings algorithm - Gibbs sampling algorithm. This method ensures that as a number of iterations of sampling from known conditional distributions increases, the density of a resulting set of variables converges to the required one.

Gibbs sampling algorithm was developed during the last 30 years. In the 1980s two important papers were published that discussed a question of computing an estimate of a posterior distribution. Tanner and Wong (1987)[15] estimated a distribution of the set of missing and observed values by data-augmentation. Shortly before this, in 1984 Geman and Geman[13] offered a new restoration algorithm for computing the maximum a posteriori estimate of the original image given a degraded image. In 1990, Gelfand and Smith[14] showed a close relationship between the Gibbs sampler introduced by Geman and Geman (1984) and the data-augmentation algorithm proposed by Tanner and Wong. In their paper "Sampling-based approaches to calculating marginal densities", Gelfand and Smith gave a description of a sampling technique that we shall extend for the generation of one-minute wind speed when the average value over each ten minutes is known.

Glasbey et al. in ([16, 17, 18, 19]) applied Gibbs sampling to a problem of sampling hourly rainfall when a daily value is given. It worked better for dry days as Glasbey required repeated sampling until the desired average value appeared. We wish to apply Gibbs sampling to the sites with the highest wind speed, hence, the algorithm is originally adapted to preserve good samples and reduce their number.

2.2.3   Description of Gibbs sampling

Let us formulate an algorithm of Gibbs sampling for a problem of generating T variables correlated with the variables in a certain "neighbourhood" [14]. In a

relation to a collection of random vectors, $Y_1, Y_2, \ldots, Y_T$, suppose that for $i = 1, \ldots, T$, the conditional distributions $[Y_i | Y_1, \ldots, Y_{i-1}, Y_{i+1}, \ldots, Y_T]$ are available in reduced forms, i.e. depend only on $\{Y_j\}_{j \in S_i}$, where $S_i \subset \{1, \ldots, T\}$:

$$[Y_i | Y_1, \ldots, Y_{i-1}, Y_{i+1}, \ldots, Y_T] = [Y_i | Y_j; j \in S_i \subset \{1 \ldots T\}], \qquad i = 1, \ldots, T \quad (2.4)$$

In (2.4), brackets denote densities, so joint, conditional, and marginal forms, for example, can be written as $[Y_1, Y_2]$, $[Y_1 | Y_2]$, and $[Y]$. We denote by S_i a certain "neighbourhood" subset of $\{1, \ldots, T\}$.

Gibbs sampler is an iterative Markov Chain Monte Carlo method. The algorithm uses the following representation of the desired posterior density:

$$[Y_1] = \int [Y_1 | Y_T, \ldots, Y_2] * [Y_T | Y_{T-1}, \ldots, Y_2] * \ldots * [Y_3 | Y_2] * [Y_2] \qquad (2.5)$$

$$[Y_2] = \int [Y_2 | Y_1, Y_T, \ldots, Y_3] * [Y_1 | Y_T, \ldots, Y_3] * \ldots * [Y_4 | Y_3] * [Y_3] \qquad (2.6)$$

$$[Y_3] = \int [Y_3 | Y_2, Y_1, Y_T, \ldots, Y_4] * [Y_2 | Y_1, Y_T, \ldots, Y_4] * \ldots * [Y_5 | Y_4] * [Y_4] \qquad (2.7)$$

$$\cdots \qquad (2.8)$$

$$[Y_{T-1}] = \int [Y_{T-1} | Y_{T-2}, \ldots, Y_1, Y_T] * [Y_{T-2} | Y_{T-3}, \ldots, Y_1, Y_T] * \ldots * [Y_1 | Y_T] * [Y_T]$$

$$(2.9)$$

$$[Y_T] = \int [Y_T | Y_{T-1}, Y_{T-2} \ldots, T_1] * [Y_{T-1} | Y_{T-2}, \ldots, Y_1] * \ldots * [Y_2 | Y_1] * [Y_1] \quad (2.10)$$

In $(2.5) - (2.10)$, $*$ denotes a multiplication of densities, for example $[Y_1, Y_2] = [Y_1 | Y_2] * [Y_2]$. The process of marginalisation (i.e. integration) is denoted by forms such as $[Y_1 | Y_2] = \int [Y_1 | Y_2, Y_3, Y_4] * [Y_3 | Y_4, Y_2] * [Y_4 | Y_2]$, with the convention that all variables appearing in the integrand but not in the resulting density have been integrated out. Therefore, for this example the integration is with respect to Y_3 and Y_4 [14].

Substitution of (2.10) into (2.9) and further up into (2.5) produces a marginal distribution for Y_1 [14]:

$$[Y_1] = \int h(Y_1, \hat{Y}_1) * [\hat{Y}_1]$$

where $h(Y_1, \hat{Y}_1)$ is an integral that was resulted from the substitutions with $\hat{Y}_1 \equiv Y_1$. By similar substitutions, marginal distributions of all the random vectors

$Y_1, Y_2, \ldots, Y_T$ are found:

$$[Y_i] = \int h(Y_i, \hat{Y}_i) * [\hat{Y}_i] \qquad (2.11)$$

The method of successive substitution for solving (2.11) suggests an iterative method for the estimation of marginal distributions $[Y_i], i \in 1, ..., T$. Its implementation by Tanner and Wong[15] requires, however, the availability of all conditional distributions on the right-hand side of $(2.5) - (2.10)$, which are not known in our case. The full conditional distributions uniquely determine the joint distribution $[Y_1, \ldots, Y_T]$ that we wish to estimate by marginal distributions using Gibbs sampling algorithm.
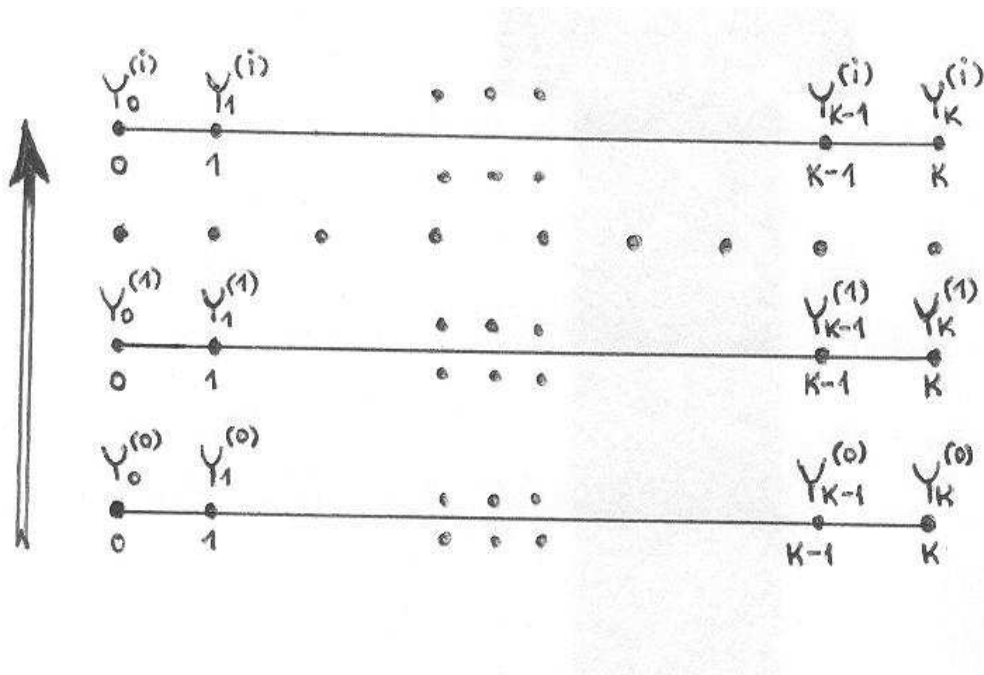
Figure 2.3: Schematic description of Gibbs sampler as a Markov-chain process

Gibbs sampling can be described as the following sequence of actions schematically presented in Figure 2.3.

Step 1:   Given an arbitrary starting set of values $Y_1^{(j)}, \ldots, Y_T^{(j)}$
              we draw $Y_1^{(j+1)} \sim [Y_1 | Y_2^{(j)}, \ldots, Y_T^{(j)}]$

Step 2:   After the value of $Y_1^{(j+1)}$ is found
              we draw $Y_2^{(j+1)} \sim [Y_2 | Y_1^{(j+1)}, Y_3^{(j)}, \ldots, Y_T^{(j)}]$

$\ldots$: $\ldots$

21

Step T: After the values of $Y_1^{(j+1)}, \ldots, Y_{T-1}^{(j+1)}$ are found
we draw $Y_T^{(j+1)} \sim [Y_T | Y_1^{(j+1)}, Y_2^{(j+1)}, \ldots, Y_{T-1}^{(j+1)}]$

Thus, each variable is visited in the natural order and a cycle requires T random variate generations. After i such iterations, results a set of variables $(Y_1^{(i)}, \ldots, Y_T^{(i)})$.

Under mild conditions, Geman and Geman showed that the following results hold[13, 14]:

Convergence. $[Y_1^{(i)}, \ldots, Y_T^{(i)}] \to [Y_1, \ldots, Y_T]$ as $i \to \infty$, and so $[Y_j^{(i)}] \to [Y_j]$ for $j \in 1, \ldots, T$. In fact, a slightly stronger result is proved. Rather than requiring that each variable is visited in repetitions of the natural order, convergence still follows under any visiting scheme, provided that each variable is visited infinitely often.

Rate. Using the sup norm, rather than L_1 norm, the joint density of $(Y_1^{(i)}, \ldots, Y_T^{(i)})$ converges to the true joint density at a geometric rate in i, under visiting in the natural order. A minor adjustment to the rate is required for an arbitrary "infinitely often" visiting scheme.

For i sufficiently large, the resulting set of variables $(Y_1^{(i)}, \ldots, Y_T^{(i)})$ is a sufficiently accurate sequence of wind speed values. It does not reflect, however, our property that the average value of wind speed over each group of 10 one-minute values should equal a given ten-minute measured value. Let us denote $\{Y_j\}_{j=1,\ldots,T}$ as a vector consisting of 10 scalars, or in other words $Y_j = (y_{j,1}, \ldots, y_{j,10}), j = 1, \ldots, T$. Then, we can write an additional condition required in the probability density function to reflect the fact that we require 10 sampled values of one-minute wind speed having the measured ten-minute wind speed average:

$$Y_j \sim [Y_j | Y_1, Y_2, \ldots, Y_{j-1}, Y_{j+1}, \ldots, Y_T, f(Y_j) = \overline{W_j^s}] \qquad (2.12)$$

where $f(Y_j)$ is a function of 10 components of Y_j and $\overline{W_j^s}$ is the ten-minute measured value.

Glasbey and Allcroft in [16] performed spatio-temporal rainfall disaggregation using Gibbs sampler for a truncated Gaussian Markov random field model. In order to satisfy (2.12) they suggested repeating sampling from the conditional distributions (2.4) until the right average value is reached within a specified tolerance. Dry blocks were easier to match but approximately 0.1% of blocks that described intense rainfall needed more than 1000 attempts. For the purpose of electricity generation using wind speed turbines it is in the interest of producers to locate wind farms in windy places. Therefore, we would like to suggest a modification to Gibbs sampling of one minute wind speed that reduces a number

of iterations. Later in subsection 2.2.5, a technique is described that shifts every generated point towards the required average wind speed value in a way that does not bias the sampling. This reduces a number of samples required by using samples that initially do not satisfy the condition $f(Y_j) = \overline{W_j^s}$.

2.2.4 Transformation to normal variable

This section presents transformation of the deseasonalised one-minute wind speed data so that the marginal distribution is normal. If the stochastic process describing the deseasonalised wind speed was fully known, then in theory we could generate the samples from this. However, there is not enough data to decide on a unique stochastic process for the deseasonalised wind speed so we proceed as follows.

1. We do a non-linear transformation of the deseasonalised wind speed so that the distribution of wind speeds at any time is normal and so that when the normalised wind speed falls below a threshold, the corresponding deseasonalised wind speed is zero. In the normalised wind speed variable the distribution of wind speed at any one time is truncated normal.

2. We assume that the stochastic process in the normalised variables is multivariate normal with the same autocorrelation function as the measured data.

Points 1 and 2 make the generation of data computationally tractable.
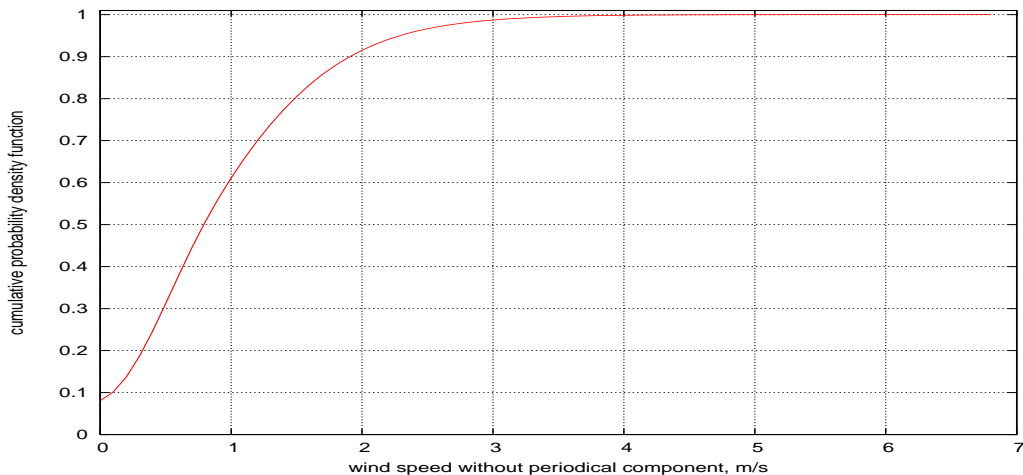
Figure 2.4: Cumulative probability distribution of one-minute wind speed recorded with MST Radar located at Frongoch farm

The nature of wind speed is such that there can be no negative values. Further, typical measurements show a big number of values zero. This is due to the fact that the measurements are recorded in discrete quantities. These features are depicted with the distribution of 1-minute wind speed plotted in the Figure 2.4. As a multiplicative model was applied to remove seasonal effect from the data, the non-negative property of the original data is still present. Since 8% of the wind speeds are zero we require:

$$P(W^d \equiv 0) = 0.08 \tag{2.13}$$

where W^d is a deseasonalised wind speed.

Definition Let us denote $Y_1, \ldots, Y_T$ as *normalised wind speed*, or the deseasonalised wind speed transfered to the normal variable. T again is a number of minutes in 12 years.
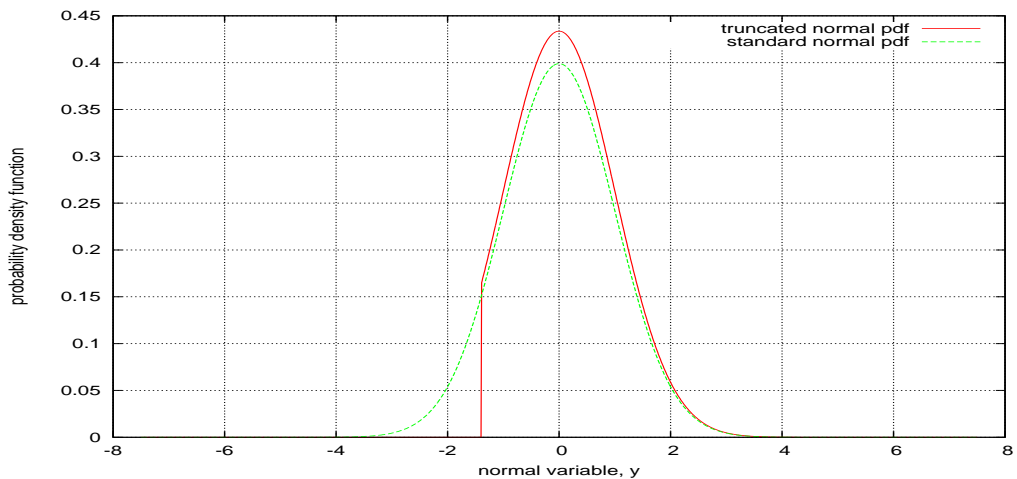
Figure 2.5: Truncated and full plot of normal probability density function

Let us consider standard normal distribution $N(0, 1)$ with mean equals 0 and standard deviation 1. Eight percent of wind speed data equals zero, hence we wish to transform the standard normal distribution so that it is truncated from the left (Figure 2.5). Single truncation means that certain outcomes are constrained, in our case these are the wind speeds recorded at zero.

The corresponding lowest value of the normal variable can be found from the equation:

$$P(Y \leq \hat{y}) \equiv P(W^d \equiv 0) = 0.08 \tag{2.14}$$

From (2.14) we have $\hat{y}$ equals -1.1225.

There is a large body of literature on the subject of estimation of the parameters of the original data (μ, σ) based upon data from truncated samples. For our work Schneider provides an excellent overview of parameter estimation of truncated normal distributions in his detailed work "Truncated and Censored samples from Normal Populations" [44]. Johnson and Thomopoulos applied most of the analysis to a special case of left truncated normal distribution [45].

Definition Let us denote $U_1, \ldots, U_T$ as standard normal random variable with mean equals 0 and standard deviation 1.

The probability density function (pdf) of U is given by

$$\phi(U) = \frac{1}{\sqrt{2\pi}} e^{-\frac{U^2}{2}} \qquad -\infty \leq U \leq \infty$$

Let $\Phi(U)$ denote the cumulative distribution function (cdf) of U. The cdf of a normal random variable Y with mean μ and variance σ^2 is $\Phi(\frac{Y-\mu}{\sigma})$. The random variables Y and U are linearly related and the relationship is given by $U = \frac{Y-\mu}{\sigma}$. A random variable Y has a single truncation from the left normal distribution if its probability density function is:

$$f(Y; \mu, \sigma, \hat{y}) = \begin{cases} \frac{\phi(\frac{Y-\mu}{\sigma})}{\sigma(1-\Phi(\hat{y}))} & \hat{y} \leq \frac{Y-\mu}{\sigma} \\ 0 & \text{otherwise} \end{cases}$$

where $\hat{y} = -1.1225$ is left (lower) truncation point and a degree of truncation is $\Phi(\hat{y}) = 0.08$ for the considered dataset.

Let us define θ for a singly truncated from the left normal distribution:

$$\theta = \frac{\phi(\hat{y})}{1 - \Phi(\hat{y})}$$

Then the expected value and variance of Y can be obtained in the following way:

$$E(Y) = \mu + \sigma\theta \tag{2.15}$$

$$V(Y) = \sigma^2(1 - \theta^2 + \theta\hat{y}) \tag{2.16}$$

Every variable from the truncated normal distribution described by (2.15) and (2.16) corresponds to a single value of the deseasonalised one-minute wind speed.

$$Y(W^d) : P(Y < \bar{y}) \equiv P(W^d < \bar{w}) \tag{2.17}$$

where $\bar{y}$ and $\bar{w}$ are the corresponding values of the normal variable and the deseasonalised wind speed respectively.

Wind speed is normalised according to the cumulative density function of the left truncated normal distribution. If we write now a normalised wind speed in discrete form with a step equal to 0.01, it has a "one-to-one" relation with the deseasonalised wind speed. Hence, it is possible to look for an analytic fit that can simplify further calculations.

Figure 2.6 plots the original empirical relation between normalised and deseasonalised wind speed. It appears a simple function can be used as an analytic monotonic fit to the transformation function between the normalised and deseasonalised wind speed (Monotonicity is a necessary condition for this transformation. If transformation function were not monotonic there would be a possibility of multiple solutions, this would prevent the method working). In ([16, 17, 18, 19]) Glasbey et al. suggest using a quadratic as the function to transform the rainfall to normal.
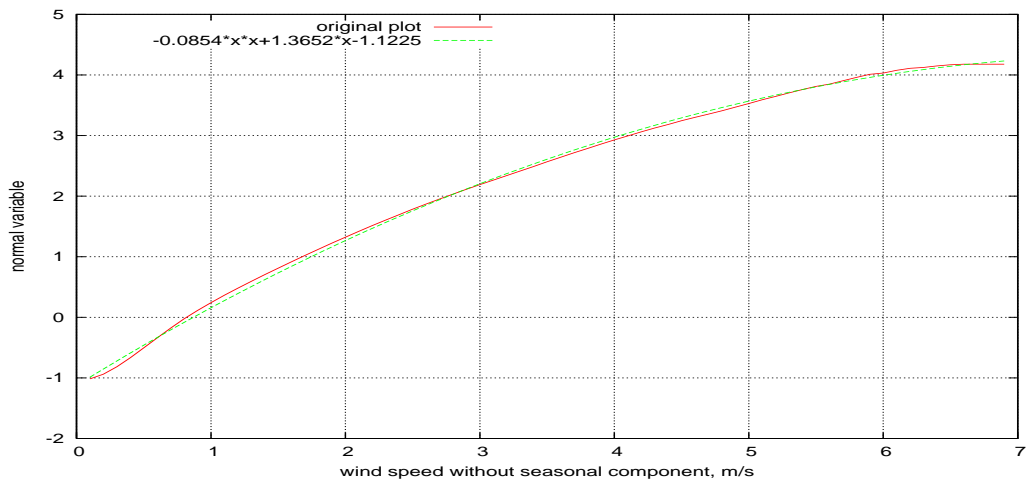
Figure 2.6: Normal variable plot with respect to the deseasonalised wind speed

Definition Let us denote $\Theta_n(W_t^d)$ as a function transferring deseasonalised wind speed W_t^d into normalised wind speed Y_t for $\forall t = 1, \ldots, T$.

We wish to find an analytical fit to $\Theta_n(W_t^d)$ so that during sampling it is easy to calculate its inverse $W_t^d = \Theta_n^{-1}(Y_t)$. We assumed $\Theta_n(W_t^d)$ to be a logarithmic or quadratic function from a plot on figure 2.6 and tested a set of points $\{(W_t^d, Y_t)\}_{t=1,\ldots,T}$ for a best fit. During the test quadratic function gave a better

26

result, therefore, we write a function $\Theta_n(W_t^d)$ as a full square:

$$Y_t = \Theta_n(W_t^d) = b_1(W_t^d + b_2)^2 + b_3, \quad \forall t = 1, \ldots, T \quad (2.18)$$

where W_t^d denotes the deseasonalised one-minute wind speed and Y_t denotes the normalised wind speed, i.e. a variable from the normal distribution truncated to the left. Using a quadratic function formulated as a full square it is straightforward to find the inverse to $\Theta_n(W_t^d)$:

$$W_t^d = \Theta_n^{-1}(Y_t) = \pm\sqrt{\frac{Y_t - b_3}{b_1}} - b_2, \quad \forall t = 1, \ldots, T \quad (2.19)$$

Parameters of the equation (2.18), b_1, b_2 and b_3 can be estimated by solving simultaneously three linear equations for the points from the original plot (W_t^d, Y_t), giving $b = (-0.0854, -7.993, 4.3335)$. With these parameter values, the function is monotonic along all the period $[0 : 6]$ (m/s) with a range for the normalised wind speed $[-1.1225 : 4.3335]$ and probability of the deseasonalised wind speed exceeding 6m/s at a single site is only $1.6 * 10^{-5}$, which is small enough to ignore. Plus or minus in front of the square root in (2.19) is chosen so that a value of the deaseasonalised wind speed W_t^d is in a range $[0 : 7.993]$ (m/s). The estimated transformation function is plotted on Figure 2.6 along with the original plot.

2.2.5 Suggested modifications to Gibbs sampler

Let us now reformulate the Gibbs sampling algorithm for the normalised wind speed. On page 19 of the current work we introduced Y_t as a vector containing 10 normalised wind speeds or $Y_t = (y_{t,1}, \ldots, y_{t,10}), t = 1, \ldots, T$. Then $f(Y_t)$ represents the average of the wind speeds corresponding to the components of Y_t, i.e.

$$f(Y_t) = \frac{1}{10}\sum_{j=1}^{10} \Theta_d^{-1}(\Theta_n^{-1}(y_{t,j})),$$

where $y_{t,j}$ is normalised wind speed that is transfered into one-minute wind speed with inverse functions to Θ_n and Θ_d defined on page 23 and page 14 accordingly.

We wish to sample a collection of random normalised wind speed variables, $Y_1, Y_2, \ldots, Y_T$ from the available conditional distributions:

$$[Y_t \sim [Y_t|Y_1, Y_2, \ldots, Y_{t-1}, Y_{t+1}, \ldots, Y_T, f(Y_t) = \overline{W_t^s}], \quad t = 1, \ldots, T$$

To achieve this, first Y_t is sampled from the distribution $[Y_t|Y_1, Y_2, \ldots, Y_T]$ and

then shifted to $\tilde{Y}_t$ in the space to satisfy the equation $f(\tilde{Y}_t) = \overline{W_t^s}$.

Assume a vector Y_t is generated. We wish to preserve a chance of this vector to appear. So Y_t is shifted along a vector of maximum probabilities for the desired normal probability distribution function. Let us consider a matrix form of the probability density function for the normalised wind speed.

$$\phi(Y) = \frac{1}{\sqrt{2\pi}} e^{-\frac{1}{2}(Y^T \varphi^{-1} Y - 2Y^T \varphi^{-1}\mu - \mu^T \varphi^{-1}\mu)} \tag{2.20}$$

where Y is the normalised wind speed with the covariance matrix φ and the mean μ.

Then a point Y which maximizes $\phi(Y)$ subject to satisfying the constraint $f(Y) = \overline{W^s}$ can be found by solving an optimization problem:

$$\arg\max \left[\frac{1}{\sqrt{2\pi}} e^{-\frac{1}{2}(Y^T \varphi^{-1} Y - 2Y^T \varphi^{-1}\mu - \mu^T \varphi^{-1}\mu)} \right]$$

subject to:
$$f(Y) = \overline{W^s}$$

which occur at the same

$$\arg\min \left[\frac{1}{2}(Y^T \varphi^{-1} Y - 2Y^T \varphi^{-1}\mu - \mu^T \varphi^{-1}\mu) \right]$$

subject to:
$$f(Y) = \overline{W^s}$$

Write Lagrangian for this minimization problem to solve it:

$$L(Y, \lambda) = \frac{1}{2}(Y^T \varphi^{-1} Y - 2Y^T \varphi^{-1}\mu - \mu^T \varphi^{-1}\mu) + \lambda(f(Y) - \overline{W^s}) \tag{2.21}$$

Function $f(Y)$ in (2.21) is complex, every normalised wind speed is transformed to one-minute wind speed using two inverse functions Θ_n^{-1} and Θ_d^{-1}. In order to work in the space of the normalised wind speed we assume further that the equation $f(Y) = \overline{W^s}$ can be replaced with its linear approximation $\mathbf{1}^T Y = \overline{Y}$, where $\mathbf{1}$ is a vector of the same size as vector Y and consists of scalars 1 only. Value of $\overline{Y}$ is found so that $\mathbf{1}^T Y$ is situated closer to the center of the distribution

[Y]:

 If $\mathbf{1}^T Y \leq \mathbf{1}^T \mu,$ $\mathbf{1}^T Y$ is the tangent to $f(Y) - \overline{W^s}$ at the point of

         the shortest distance between $f(Y) - \overline{W^s}$ and μ, and

 If $\mathbf{1}^T Y > \mathbf{1}^T \mu,$ we assume $\overline{Y} = b_3,$

where μ is mean value of the distribution $[Y]$ and b_3 is a parameter in a quadratic function at (2.18).

When using a linear approximation of the equation $f(Y) = \overline{W^s}$, the resulting Lagrangian function obtained from (2.21) is easily differentiated with respect to Y:

$$\nabla_Y L = \frac{\partial L}{\partial Y} = \frac{\partial[\frac{1}{2}(Y^T \varphi^{-1} Y - 2Y^T \varphi^{-1} \mu - \mu^T \varphi^{-1} \mu) + \lambda(\mathbf{1}^T Y - \overline{Y})]}{\partial Y}$$
$$= \varphi^{-1} Y - \varphi^{-1} \mu + \lambda \mathbf{1}^T$$

First-order necessary condition for Y to be a minimum for the above optimization problem stipulates that $\nabla_Y L = 0$. From here we can find an equation for Y:

$$\varphi^{-1}(Y - \mu) = -\lambda \mathbf{1}^T \tag{2.22}$$
$$Y = -\lambda \mathbf{1}^T \varphi + \mu \tag{2.23}$$

In (2.23) φ and μ denote the covariance matrix and the mean vector, they describe the probability distribution of the normalised wind speed. The scalar λ is a Lagrangian constant and defines a position of Y on a vector of maximum probabilities. Parameter λ is found so that Y in (2.23) satisfies a linear equation $\mathbf{1}^T Y = \overline{Y}$.

In the context of the Gibbs sampling, a generated vector Y_t is shifted along the vector described by (2.23). This means that $\tilde{Y}_t$ acquires a value from the vector

$$\tilde{Y}_t = -\lambda \mathbf{1}^T \varphi + Y_t \tag{2.24}$$

where Y_t is the original generated variable and $\tilde{Y}_t$ is a shifted normalised value of wind speed so that it satisfies now the condition $\mathbf{1}^T \tilde{Y}_t = \overline{Y}$.

A shifted variable $\tilde{Y}_t$ is found so that it satisfies $f(Y) = \overline{W^s}$ within a certain tolerance as the equation $f(Y) = \overline{W^s}$ is close to its linear approximation $\mathbf{1}^T Y = \overline{Y}$ which $\tilde{Y}_t$ satisfies exactly. Assume, there exists a vector Y_t^* such that it satisfies both equations exactly, $f(Y_t^*) = \overline{W^s}$ and $Y_t^* = -\lambda \mathbf{1}^T \varphi + Y_t$. Then $\tilde{Y}_t$ is accepted as a valid normalised wind speed if the probability of $\tilde{Y}_t$ is within a specified

tolerance of the probability of Y_t^*. The values of the one-minute wind speed W_t^s in this case are found using $W_t^s = \Theta_d(\Theta_n(\tilde{Y}_t))$.

2.3   Implementation of modified Gibbs sampler

We wish to generate an unbiased sample from the wind stochastic process conditional on each consecutive group of wind speeds having a given average value. Assume the group size is q and we wish to generate $T \cdot q$ values:

$$\underbrace{w_1^s, \ldots, w_q^s,}_{t=1} \qquad \underbrace{w_{q+1}^s, \ldots, w_{2q}^s,}_{t=2} \qquad \ldots, \qquad \underbrace{w_{(T-1)q+1}^s, \ldots, w_{Tq}^s,}_{t=T}$$

such that

$$\frac{1}{q}(w_{(t-1)q+1}^s + w_{(t-1)q+2}^s + \ldots + w_{tq}^s) = \overline{W_t^s}$$

where w_i^s, $i = 1, \ldots, Tq$ are the one-minute wind speeds and $\overline{W_t^s}$ is the measured average wind speed for times $i = (t-1)q+1, \ldots, tq$. For the real problems we are dealing with $q = 10$, but we will also illustrate the case $q = 2$.

Instead of operating with wind speed variables w_i^s directly, we work with the transformed stochastic process when the periodicity (seasonal and daily effects) has been removed so that their marginal distribution is a truncated normal. We will do this in two steps, first the removal of periodic effects by transforming to new variables $w_i^d = \Theta_d(w_i^s)$ followed by a transformation to variables $y_i = \Theta_n(w_i^d)$ which have a truncated normal distribution.

Definition Let us denote Θ as a compound function, such that

$$y_i = \Theta_n(\Theta_d(w_i^s)) := \Theta(w_i^s)$$

and since the transformation will be "one-to-one",

$$w_i^s = \Theta_d^{-1}(\Theta_n^{-1}(y_i)) := \Theta^{-1}(y_i)$$

Transformation functions Θ_d and Θ_n were described earlier in this Chapter. Section 2.2.1 dealt with daily and seasonal periodical components of the original wind speed data. Section 2.2.4 discussed transformation to the normalised wind speed. Given these functions are known and given μ and φ as described in Section 2.2.4, the algorithm of generating one-minute wind speed values is the following:

Step 1:   Start with $t = 1$.

Step 2: Generate normalised wind speed $Y_t = (y_{(t-1)q+1}, \ldots, y_{tq})$ from $N_q(\mu, \varphi)$.

Step 3: Find $w_i^s = \Theta^{-1}(y_i)$, $i = [(t-1)q+1 \ldots tq]$.

Step 4: If $\frac{1}{q}(w_{(t-1)q+1}^s + w_{(t-1)q+2}^s + \ldots + w_{tq}^s) = \overline{W_t^s}$ within a specified tolerance
Go to Step 8

Step 5: Shift $(y_{(t-1)q+1}, \ldots, y_{tq})$ along the vector of maximum probabilities to find $(\tilde{y}_{(t-1)q+1}, \ldots, \tilde{y}_{tq})$

Step 6: If a probability of $(\tilde{y}_{(t-1)q+1}, \ldots, \tilde{y}_{tq})$ is within a specified tolerance of a probability of $(y_{(t-1)q+1}^*, \ldots, y_{tq}^*)$, which if transferred to the wind speed satisfies
$\frac{1}{q}(w_{(t-1)q+1}^s + w_{(t-1)q+2}^s + \ldots + w_{tq}^s) = \overline{W_t^s}$ exactly,
Go to Step 8

Step 7: Go to Step 2

Step 8: $t = t + 1$

Step 9: If $t > T$ Stop
else Go to Step 2

This algorithm describes a single iteration of the Gibbs sampler. To generate a sample with the required probability density function we wish to perform a significantly big number of such iterations.

2.3.1 Multivariate normal distribution

Section 2.2 of this Chapter introduced the Gibbs sampling technique for a collection of normalised wind speed variables $Y_1, Y_2, \ldots, Y_T$. Every generated variable $Y_t = (y_{t,1}, \ldots, y_{t,10}), t = 1, \ldots, T$ has to satisfy $f(Y_t) = \overline{W_t^s}$, which is ten wind speed values have to add up to the measured average ten-minute wind speed. The fact that Y_t includes 10 univariate variables defines a vector Y_t as a **multivariate** variable.

A stochastic process can be described with the moments of the process, particularly the first and second moments, mean and autocovariance function respectively. Let us find mean and autocovariance of the univariate one-minute normalised wind speed that can be used further to define a stochastic process for multivariate normalised wind speed. First moment of the stochastic process of

wind speed generation is described earlier as the expected value of the truncated normal distribution. It can be found using the formula (2.15).

Given Tq variables $y_1, \ldots, y_{Tq}$, autocovariance coefficients can be found:

$$cov(y, y_l) = \frac{1}{Tq - l} \sum_{i=1}^{Tq-l} (y_i - \overline{y})(y_{i+l} - \overline{y}) \qquad (2.25)$$

where l denotes a lag between the variables and $\overline{y}$ is the mean value of the series.

Figure 2.7 plots the autocovariance function in terms of a lag l calculated for the normalised wind speed. We assume a lag up to 1440 minutes (1 day) is significant for the one minute wind speed stochastic process.

In order to use the autocovariance in the process of wind speed generation it is convenient to find a continuous function that would fit in the original plot. We assumed $cov(y, y_l)$ to be a quadratic or exponential function from a plot on figure 2.7 and tested a set of points $\{(l, cov(y, y_l))\}_{l=1,\ldots,L}$ for a best fit. During the test the exponential function gave a better result, therefore, we estimate the autocovariance function with a mixture of exponential curves:

$$cov(y, y_l) \equiv \sum_{i=1}^{m} \beta_i e^{-\varsigma_i |l|} \qquad \sum_{i=1}^{m} \beta_i = 1 \qquad (2.26)$$

According to Allcroft and Glasbey [16] a condition of all coefficients β_i being positive is sufficient for the function to be valid.
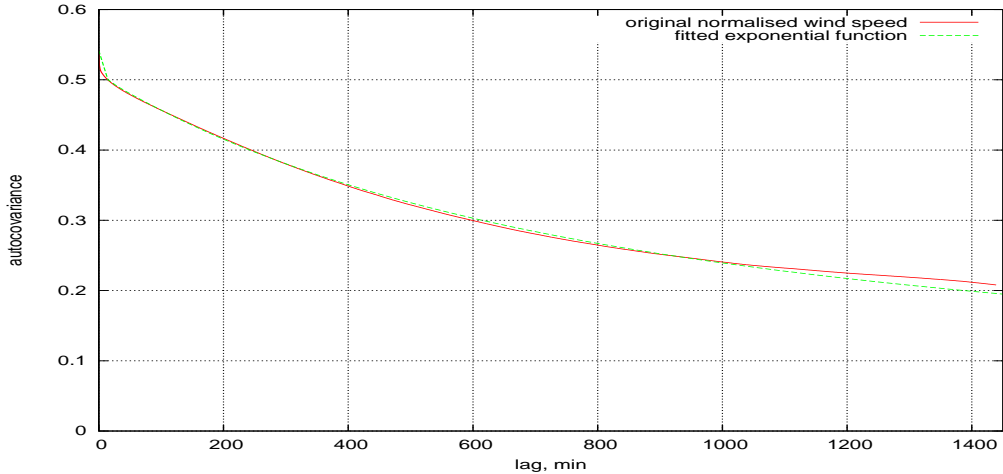
Figure 2.7: Fitted sum of exponential functions to approximate the autocovariance of the normalised wind

Figure 2.7 shows that the autocovariance of the normalised wind speed is influenced by certain processes that effect its smoothness, for example, for $l > 1000$ a gradient to the curve changes and it is hard to find a simple function to fit it perfectly. We found a good fit to the autocovariance function to be a mixture of six exponentials with the following parameters:

$$\beta = (0.04, 0.026, 0.19, 0.204, 0.25, 0.29)$$

and

$$\varsigma = (1.5, 0.13, 0.0023, 0.0018, 0.0005, 0.0002)$$

Figure 2.7 plots the original autocovariance for the normalised wind speed along with the fitted exponential function.

Calculated autocovariance and mean describe a stochastic process for the univariate normalised wind speed $y_1, \ldots, y_{Tq}$. It can be used now to formulate a multivariate stochastic process for the series $Y_1, \ldots, Y_T$.

For the convenience of further calculations a covariance can be described in a matrix form:

$$\varphi = \begin{pmatrix} \varphi_{11} & \cdots & \varphi_{1j} & \cdots & \varphi_{1L} \\ \cdots & \cdots & \cdots & \cdots & \cdots \\ \varphi_{i1} & \cdots & \varphi_{ij} & \cdots & \varphi_{iL} \\ \cdots & \cdots & \cdots & \cdots & \cdots \\ \varphi_{L1} & \cdots & \varphi_{Lj} & \cdots & \varphi_{LL} \end{pmatrix}$$

where L denotes a biggest lag of the autocovariance. Covariance matrix φ is found based on the autocovariance function described by (2.26):

$$\varphi_{ji} = \varphi_{ij} = cov(y, y_{i-j}), \qquad i \geq j \tag{2.27}$$

For a collection of multivariate normalised wind speeds $Y_1, \ldots, Y_T$ every vector Y_t follows the distribution $N_q(\mu, \varphi)$. For the case of generating ten minutes of wind speed, we take $q = 10 << L$. To find mean and covariance of a q-dimensional variable let us partition an interval of length L. Suppose that $Y \sim N_L(\mu, \varphi)$, partitioned into q and $(L - q)$ components as

$$Y = \begin{pmatrix} Y_q \\ Y_{L-q} \end{pmatrix}$$

In our case Y_q, of dimension q, is a set of ten normalised wind speeds for which we wish to find a probability distribution. Variable Y_{L-q}, of dimension $(L - q)$, is a set of variables that first q variables correlate with. Partition μ and φ analogously

as

$$\mu = \begin{pmatrix} \mu_q \\ \mu_{L-q} \end{pmatrix}$$

and

$$\varphi = \begin{pmatrix} \varphi_{qq} & \varphi_{q(L-q)} \\ \varphi_{(L-q)q} & \varphi_{(L-q)(L-q)} \end{pmatrix}$$

with dimensions of the subvectors and submatrices as induced by the partition of Y. Then $Y_q \sim N_q(\mu_q, \varphi_{qq})$ and $Y_{L-q} \sim N_{L-q}(\mu_{L-q}, \varphi_{(L-q)(L-q)})$.

Assume that $\varphi_{(L-q)(L-q)}$ is positive definite. Then the conditional distribution of Y_q given $Y_{L-q} = Y^*_{L-q}$, is q-variate normal with the following parameters:

$$\mu_{q|(L-q)} := E[Y_q|Y_{L-q} = Y^*_{L-q}] = \mu_q + \varphi_{q(L-q)}\varphi^{-1}_{(L-q)(L-q)}(y_{L-q} - \mu_{L-q}) \quad (2.28)$$

and

$$\varphi_{qq|(L-q)} := Cov[Y_q|Y_{L-q} = Y^*_{L-q}] = \varphi_{qq} - \varphi_{q(L-q)}\varphi^{-1}_{(L-q)(L-q)}\varphi_{(L-q)q} \quad (2.29)$$

Mean and covariance stated in (2.28) and (2.29) represent conditional normal probability distribution that describes the stochastic process of ten-minute wind speed generation.

For any vector $\mu \in R^q$ and positive semidefinite symmetric matrix φ of dimension $(q \times q)$, there exists a unique multivariate normal distribution with mean vector μ and covariance matrix φ [46] .

Further, to generate a multivariate normal variable with mean μ and covariance φ we sample first a multivariate vector $U \sim N_q(0, I_q)$. For any vector $\mu \in R^q$ and positive semidefinite, symmetric matrix φ of dimension $(q \times q)$, random vector Y with a $N_q(\mu, \varphi)$-distribution can be generated as

$$Y = \mu + MU \quad (2.30)$$

where $U \sim N_q(0, I_q)$, and $MM^T = \varphi$.

If φ is a positive semidefinite symmetric matrix of dimension $q \times q$, then there exists a matrix M of dimension $(q \times q)$ such that

$$\varphi = MM^T, \quad (2.31)$$

where M^T is the transposition of matrix M. Matrix M can be found precisely using different methods, for example Cholesky decomposition, since in our case covariance matrix φ is a positive definite matrix. More specifically, M can be

computed as follows:

$$M := \begin{pmatrix} M_{11} & 0 & \dots & 0 \\ M_{21} & M_{22} & \dots & 0 \\ \dots & \dots & \dots & \dots \\ M_{q1} & M_{q2} & \dots & M_{qq} \end{pmatrix}$$

where every element M_{ij}, $i \geq j$ can be found with a sequence of calculations:

Step 1: $\quad M_{11} = \sqrt{\phi_{11}}$

Step 2: $\quad M_{i1} = \frac{\phi_{i1}}{M_{11}}, i \leq q$

Step 3: $\quad$ Set $j = 2$

Step 4: $\quad M_{jj} = \sqrt{\phi_{jj} - \sum_{k=1}^{j-1} M_{jk}^2}$

Step 5: $\quad M_{ij} = \frac{\phi_{ij} - \sum_{k=1}^{j-1} M_{ik} M_{jk}}{M_{jj}}, j < i \leq q$

Step 6: $\quad$ Set $j = j + 1$

Step 7: $\quad$ If $j \leq q$ Go to Step 4
$\quad\quad\quad$ Else Finish algorithm

Matrix M is used now to generate a multivariate normal variable Y of the Gibbs sampling algorithm.

2.3.2 Two-variable sampling

We wish to generate data for each minute t where each consecutive group of ten variables has a given average value. To illustrate the method we will first derive a case where the variables are divided into groups of two. Therefore, on the interval $\{0, 1, \dots, 2T\}$ we wish to generate points w_i^s subject to a given average of two adjacent values of wind speed $\overline{W_t^s}$:

$$\frac{w_i^s + w_{i+1}^s}{2} = \overline{W_t^s}, \quad i = 0, 1, \dots, 2T, \quad t = 0, 1, \dots, T$$

This can be achieved through a sequence of steps described below in this section and illustrated in Figure 2.8. Let us start with normalising a given average wind speed by transforming it to the truncated normal variable:

$$Y_t^{(0)} := (y_i^{(0)}, y_{i+1}^{(0)}) := (\Theta(\overline{W_t^s}), \Theta(\overline{W_t^s}))$$

This gives us an initial set for Gibbs sampling.

The repeated subproblem when using Gibbs sampling algorithm to generate samples with given means, is to sample from one group of variables conditional on achieving a given average wind speed. Here are the main steps of j-th iteration:

1. Assume we wish to generate a sample $Y_t^{(j)} = (y_i^{(j)}, y_{i+1}^{(j)})$. In the normalised variables this will be a bivariate normal $Y_t^{(j)} \sim N_2(\mu, \varphi)$, where φ is the same for all samples and is given in general by, for our example,

$$\varphi = \begin{pmatrix} 0.8 & 0.6 \\ 0.6 & 0.7 \end{pmatrix}$$

and μ is calculated using the neighbouring sample values $(Y_1^{(j)}, Y_2^{(j)}, \ldots, Y_{t-1}^{(j)}, Y_{t+1}^{(j-1)}, \ldots, Y_T^{(j-1)})$.

Assume, a point $A := Y_t^{*(j)} := (y_i^{*(j)}, y_{i+1}^{*(j)}) = (1.2595, -0.3102)$ is generated (Figure 2.8) using $N_2(\mu, \varphi)$.
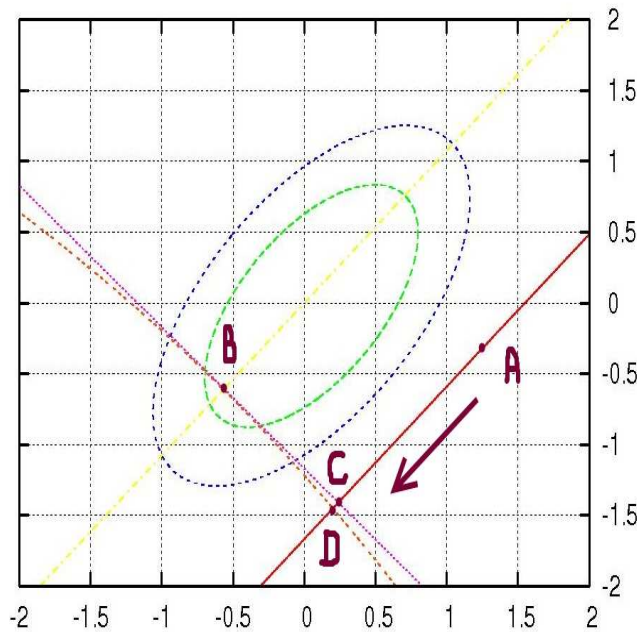
Figure 2.8: Contours of Normal distribution and four linear functions used in the modification to Gibbs algorithm

2. The generated normalised wind speeds are transformed further using inverse

function to Θ:

$$w_i^{*s} = \Theta^{-1}(y_i^{*(j)}) \tag{2.32}$$

$$w_{i+1}^{*s} = \Theta^{-1}(y_{i+1}^{*(j)}) \tag{2.33}$$

Calculated with (2.32) and (2.33) new wind speed values are $W_t^{s(j)} :=$ (w_i^{*s}, w_{i+1}^{*s}) with their average equals

$$\overline{W_t^{s(j)}} := \frac{w_i^{*s} + w_{i+1}^{*s}}{2}$$

where $\overline{W_t^{s(j)}}$ is the average wind speed corresponding to the generated values $(y_i^{*(j)}, y_{i+1}^{*(j)})$.

The generated point $(y_i^{*(j)}, y_{i+1}^{*(j)})$ is tested. If $\overline{W_t^{s(j)}}$ equals $\overline{W_t^s}$ within a specified tolerance, the point (w_i^{*s}, w_{i+1}^{*s}) is accepted, otherwise $(y_i^{*(j)}, y_{i+1}^{*(j)})$ is shifted in order to satisfy $\overline{W_t^s}$ as explained in steps 3 and 4 of this algorithm.

3. We assumed λ to vary in the interval between -10 and 10, that are sufficiently large to find Y in (2.23). By advancing λ from one border of the interval to another with a step 0.001, we search along the line

$$Y_t^{(j)} = -\lambda \mathbf{1}^T \varphi + Y_t^{*(j)}, \tag{2.34}$$

where $Y_t^{*(j)}$ is the point A sampled in step 1 of this algorithm, φ is a covariance matrix of distribution $[Y_t]$ and $\mathbf{1}$ is a vector of the same size as Y_t and consists of scalars 1 only. Points Y^C and Y^D (C and D in Figure 2.8) are found during the search.

Definition Let us denote Y^B (B in Figure 2.8) as the point on the curve $f(Y_t) = \overline{W_t^s}$ that acquires the shortest distance to the center of the distribution $[Y]$.

Definition Let us denote Y^C as the intersection of the line (2.34) with the tangent to the curve $f(Y_t) = \overline{W_t^s}$ at the point Y^B, i.e. a line $\mathbf{1}^T Y_t = \overline{Y}$ defined in the Section 2.2.5 of this work. A scalar $\overline{Y}$ is calculated as in the Section 2.2.5:

$$\text{If } \mathbf{1}^T Y^B \leq \mathbf{1}^T \mu, \qquad \overline{Y} = \mathbf{1}^T Y^B, \text{ and}$$
$$\text{if } \mathbf{1}^T Y^B > \mathbf{1}^T \mu, \qquad \text{we assume } \overline{Y} = b_3,$$

37

where b_3 is a parameter of the quadratic function in (2.18). By modifying the value of λ, Y^C (and a corresponding λ^C) are found so that $\mathbf{1}^T Y^C$ and $\overline{Y}$ match to small given tolerance.

Definition Let us denote Y^D as the point on the line (2.34) that satisfies the condition of two adjacent one-minute wind speeds being equal a given average value $f(Y^D) = \overline{W_t^s}$. By modifying the value of λ, Y^D (and a corresponding λ^D) are found so that $f(Y^D)$ and $\overline{W_t^s}$ match to small given tolerance.

4. The probabilities of the points Y^D and Y^C are further compared:

$$\text{If } \frac{\phi(Y^D)}{\phi(Y^C)} > \rho \qquad \text{accept } Y_t^{(j)} = Y^C$$

$$\text{Else} \qquad \text{reject } Y^C \text{ and Go to step 1,}$$

where $\phi(*)$ is the probability distribution function for truncated normal distribution used for sampling normalised wind speed. We assumed ρ to be a fixed number 0.95. Glabey et al. in [17] suggested to take ρ as a random number from the uniform $[0, 1]$ distribution in order to add random character to the test.

5. Take $i = i + 1$. If $i \leq T$ Go to step 1, Else Finish j-th iteration of Gibbs sampling algorithm.

Steps 1 to 5 are repeated until j reaches a specified number of iterations j^*. We determine j^* so that a stochastic process of the resulting sample is weakly stationary.

2.3.3 Multivariate sampling

The two-variable algorithm was described in order to illustrate wind speed generation when the average value of adjacent values is given. We wish to apply the demonstrated method to the sampling of ten minutes of wind speed when their average value is given.

In [16], Glasbey et al. generate hourly rainfall with a given daily value by repeated sampling from the multivariate normal distribution until the data total fell within a certain margin of the target. To sample hourly rainfall values it required an average of 170 simulations per day (sometimes considerably larger

numbers for wet days) for one iteration of the Gibbs sampling. This means that many samples were rejected.

On the interval $[0, 1, \ldots, qT]$ we wish to generate wind speeds w_i^s subject to the measured ten-minute average wind speed $\overline{W_t^s}$:

$$\frac{1}{q}(w_i^s + w_{i+1}^s + \ldots + w_{i+q-1}^s) = \overline{W_t^s},$$

where $q = 10$ and $t = 1, \ldots, T$. This can be achieved through a sequence of steps similar to that described for two-variable sampling in Section 2.3.2. The algorithm starts with normalising a given average wind speed by transforming it to the truncated normal variable:

$$Y_t^{(0)} := (y_i^{(0)}, y_{i+1}^{(0)}, \ldots, y_{i+q-1}^{(0)}) := (\Theta(\overline{W_t^s}), \Theta(\overline{W_t^s}), \ldots, \Theta(\overline{W_t^s}))$$

This gives us an initial set of variables for Gibbs sampling. The repeated sub-problem when using Gibbs sampling to generating samples with given means, is to sample from one group of variables conditional on achieving a given average wind speed. Here are the main steps of j-th iteration:

1. We wish to generate a multivariate $Y_t^{(j)} \sim N_q(\mu, \phi)$, where

$$\mu = \begin{pmatrix} \mu_1 \\ \vdots \\ \mu_q \end{pmatrix}$$

and

$$\varphi = \begin{pmatrix} \varphi_{11} \ldots \varphi_{1j} \ldots \varphi_{1q} \\ \ldots \ldots \ldots \ldots \ldots \ldots \\ \varphi_{i1} \ldots \varphi_{ij} \ldots \varphi_{iq} \\ \ldots \ldots \ldots \ldots \ldots \ldots \\ \varphi_{q1} \ldots \varphi_{qj} \ldots \varphi_{qq} \end{pmatrix}$$

are given (see below). We are interested in generating ten minutes of wind speed at any single time, hence $q = 10$.

A covariance matrix for a set of one-minute wind speed data recorded with MST Radar near Aberystwyth is first calculated for a lag $L = 1440$ minutes. For sampling of a multivariate variable of size $q = 10$ we use a covariance matrix of size (10×10) and mean of size (10×1). Both can be found as a conditional covariance $\varphi_{qq|(L-q)}$ and a conditional mean $\mu_{q|(L-q)}$ as was shown in section 2.3.1. The calculated conditional covariance φ does not

depend on the values of adjacent normalised wind speeds and has the same values for any sample.

Table 2.1: Covariance matrix φ calculated for the normal variables transformed from the minute-by-minute wind speed data

0.076	0.031	0.017	0.011	0.009	0.008	0.007	0.006	0.005	0.003
0.031	0.089	0.038	0.021	0.015	0.012	0.010	0.009	0.007	0.005
0.017	0.038	0.092	0.040	0.023	0.016	0.013	0.011	0.009	0.006
0.011	0.021	0.040	0.094	0.041	0.023	0.016	0.013	0.010	0.007
0.009	0.015	0.023	0.041	0.094	0.041	0.023	0.016	0.012	0.008
0.008	0.012	0.016	0.023	0.041	0.094	0.041	0.023	0.015	0.009
0.007	0.010	0.013	0.016	0.023	0.041	0.094	0.040	0.021	0.011
0.006	0.009	0.011	0.013	0.016	0.023	0.040	0.092	0.038	0.017
0.005	0.007	0.009	0.010	0.012	0.015	0.021	0.038	0.089	0.031
0.003	0.005	0.006	0.007	0.008	0.009	0.011	0.017	0.031	0.076

Conditional covariance for our illustrative example is presented in the Table 2.1. The calculated conditional mean, however, is defined by the normalised wind speed values of the partition $(L - q)$. It is calculated for every sample separately.

Assume a point $U_t^{*(j)} = (u_i^{*(j)}, \ldots, u_{i+q-1}^{*(j)}) \sim N_q(0, I_q)$ is generated. It is then transferred to the required conditional normal probability distribution $N_q(\mu, \varphi)$.

$$Y_t^{*(j)} = \mu + M U_t^{*(j)}$$

where μ is a conditional mean and a conditional covariance matrix $\varphi = MM^T$. Matrix M can be found using the algorithm demonstrated in Section 2.3.1. For the covariance matrix φ presented in Table 2.1, matrix M can be found as in Table 2.2.

Table 2.2: M-matrix such that $MM^T = \varphi$

0.276	0.000	0.000	0.000	0.000	0.000	0.000	0.000	0.000	0.000
0.113	0.276	0.000	0.000	0.000	0.000	0.000	0.000	0.000	0.000
0.061	0.112	0.276	0.000	0.000	0.000	0.000	0.000	0.000	0.000
0.041	0.060	0.111	0.276	0.000	0.000	0.000	0.000	0.000	0.000
0.033	0.040	0.059	0.111	0.275	0.000	0.000	0.000	0.000	0.000
0.028	0.032	0.039	0.057	0.110	0.275	0.000	0.000	0.000	0.000
0.025	0.027	0.030	0.038	0.056	0.108	0.274	0.000	0.000	0.000
0.022	0.023	0.025	0.028	0.036	0.054	0.106	0.273	0.000	0.000
0.018	0.019	0.020	0.022	0.025	0.032	0.050	0.102	0.270	0.000
0.012	0.013	0.014	0.015	0.016	0.019	0.025	0.041	0.088	0.255

2. Generated normalised wind speed is transformed further using the inverse of function Θ:

$$W_t^{s(j)} = \Theta^{-1}(Y_t^{*(j)}) \tag{2.35}$$

Calculated with (2.35) new values of wind speed are $W_t^{s(j)} := (w_i^{*s}, \ldots, w_{i+q-1}^{*s})$ with ten-minute average wind speed equals

$$\overline{W_t^{s(j)}} = \frac{1}{q}(w_i^{*s} + \ldots + w_{i+q-1}^{*s})$$

where $\overline{W_t^{s(j)}}$ is an average wind speed corresponding to the generated earlier values of the normalised wind speed $(y_i^{*(j)}, \ldots, y_{i+q-1}^{*(j)})$.

The generated point $Y_t^{*(j)} := (y_i^{*(j)}, \ldots, y_{i+q-1}^{*(j)})$ is tested. If $\overline{W_t^{s(j)}}$ matches $\overline{W_t^s}$ within a specified tolerance, the point $(w_i^{*s}, \ldots, w_{i+q-1}^{*s})$ is accepted. Otherwise $(y_i^{*(j)}, \ldots, y_{i+q-1}^{*(j)})$ is shifted in order to satisfy $\overline{W_t^s}$ as explained in steps 3 and 4 of this algorithm.

3. As in the case of two variables a shifted point $(y_i^{*(j)}, \ldots, y_{i+q-1}^{*(j)})$ acquires a value from the vector of maximum probabilities of the truncated normal probability distribution, so the following applies. We assumed again λ to vary in the interval between -10 and 10, that are sufficiently large to find Y in (2.23). By advancing λ from one border of the interval to another with a step 0.001, we search along the line

$$Y_t^{(j)} = -\lambda \mathbf{1}^T \varphi + Y_t^{*(j)}, \tag{2.36}$$

where $Y_t^{*(j)}$ is a point sampled in step 1 of this algorithm, φ is a covariance matrix of distribution $[Y_t]$ and $\mathbf{1}$ is a vector of the same size as Y_t and consists of scalars 1 only. Points Y^C and Y^D are found during the search.

Direction in which point $Y_t^{*(j)}$ is shifted is defined by the covariance matrix φ and evaluates how much information each of ten variables contributes to the average wind speed $\overline{W_t^s}$. Information carried by each of the ten generated variables is calculated as a sum of elements in every column of the covariance matrix:

$$\eta = (\eta_1, \eta_2, \ldots, \eta_q)$$

where

$$\eta_j = \sum_{i=1}^{q} \varphi_{ij}$$

41

Figure 2.9 plots the amount of information carried by each of the ten generated points in the total sum.
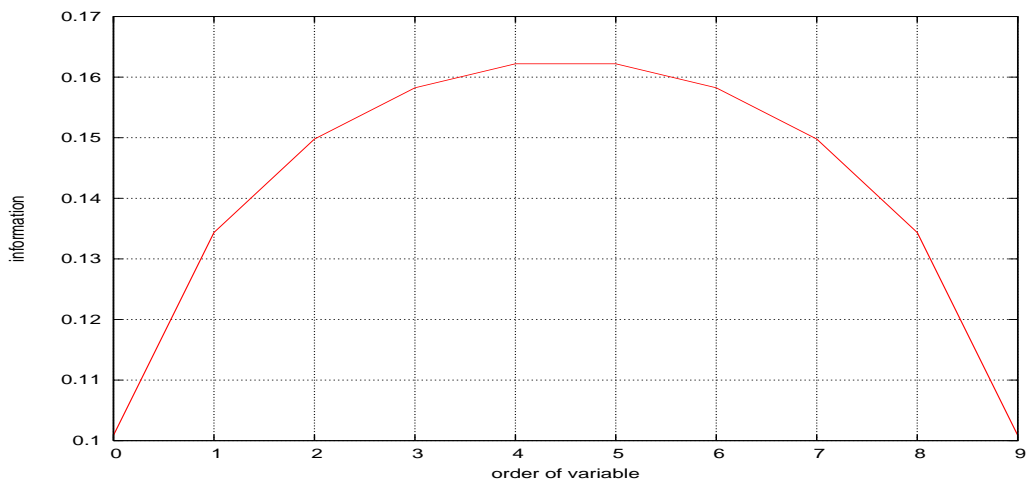
Figure 2.9: Amount of the information carried by each of the ten variables

Point $Y_t^{*(j)}$ is shifted in the specified above direction η towards a curve that presents a required sum of q wind speed values in terms of a normal variable, i.e. $f(Y_t) = \overline{W_t^s}$.

Definition Let us denote Y^B as a vector that satisfies the equation $f(Y_t) = \overline{W_t^s}$ and acquires the shortest distance to the center of the distribution Y_t.

Definition Let us denote Y^C as a vector on the intersection of the line (2.36) and the tangent to the curve $f(Y_t) = \overline{W_t^s}$, i.e. a line of the form $\mathbf{1}^T Y_t = \overline{Y}$ as defined in the Section 2.2.5 of this work. A scalar $\overline{Y}$ is calculated as in the section 2.2.5:

$$\text{If } \mathbf{1}^T Y^B \le \mathbf{1}^T \mu, \qquad \overline{Y} = \mathbf{1}^T Y^B, \text{ and}$$
$$\text{if } \mathbf{1}^T Y^B > \mathbf{1}^T \mu, \qquad \text{we assume } \overline{Y} = b_3,$$

where b_3 is a parameter of the quadratic function in (2.18). By modifying the value of λ, Y^C (and a corresponding λ^C) are found so that $\mathbf{1}^T Y^C$ and $\overline{Y}$ match to a small given tolerance.

Definition Let us denote Y^D as the point on the line (2.36) that satisfies the condition of ten one-minute wind speeds being equal a given average

value $f(Y_t) = \overline{W_t^s}$. By modifying the value of λ, Y^D (and a corresponding λ^D) are found so that $f(Y^D)$ and and $\overline{W_t^s}$ match within a small given tolerance.

4. The probabilities of the points Y^D and Y^C are further compared:

   If $\dfrac{\phi(Y^D)}{\phi(Y^C)} > \rho$ $\qquad\qquad$ accept $Y_t^{(j)} = Y^C$

   Else $\qquad\qquad\qquad\qquad$ reject Y^C and Go to step 1,

   where $\phi(*)$ is the probability distribution function for truncated normal distribution used for sampling wind speed. As in the case of two-variable sampling, we assumed ρ to be a fixed number 0.95.

5. Take $i = i + 1$. If $i \leq T$ Go to step 1, Else Finish j-th iteration of Gibbs sampling algorithm.

Steps 1 to 5 are repeated until j reaches a specified number of iterations j^*. We determine j^* so that a stochastic process of the resulting sample is weakly stationary. For an interval of 5 years when the average wind speed is given, there are $j^* = 12$ Gibbs sampling iterations being performed.

Out of five years of ten-minute average wind speed data records there were between 34 to 87 rejects reported for a single iteration. Therefore, shifting a generated point is an improvement to the method used by Allcroft and Glasbey in [17], even with high wind speeds it rejects very view trial points.

2.3.4 Testing the results of wind speed sampling

On Figure 2.10 there is one hour of generated wind speed plotted along with original wind speed. However good the generated sample can look on Figure 2.10 it necessary to evaluate it statistically. Let us begin by defining a second-order stationary process. A process is called **second-order stationary** (or weakly stationary) if its mean is constant and its autocovariance function depends only on the lag [43], so that

$$E[Y^{(j^*)}] = \mu$$

and

$$Cov[Y^{(j^*)}, Y_l^{(j^*)}] = \varphi(l)$$

No requirements are placed on moments higher than second order. By letting $l = 0$, we note that the form of a stationary autocovariance function implies that

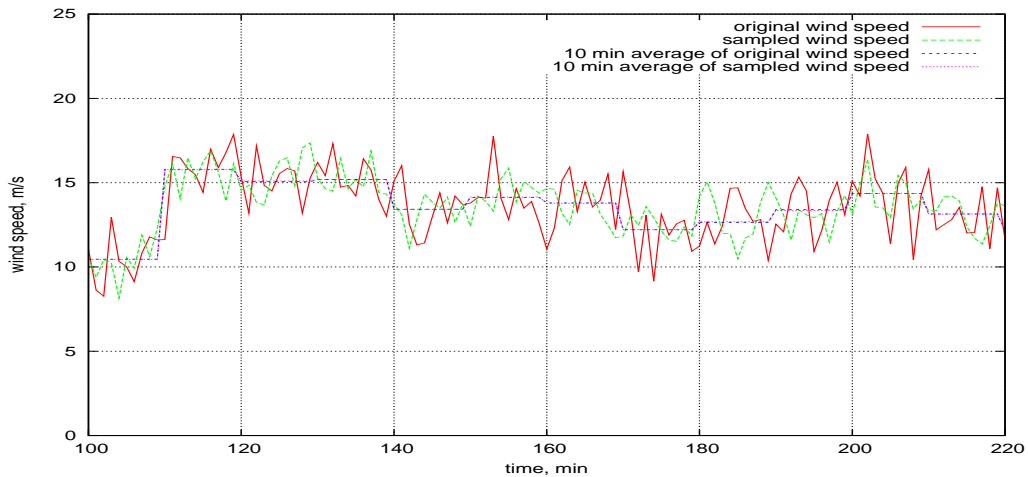the variance, as well as the mean, is constant.

Figure 2.10: An example of the sampled and the original values of 1-minute wind speed plotted along with the ten minute average wind speed

The chains encountered in Monte Carlo Markov Chain settings satisfy a stability property, namely a stationary probability distribution that exists by construction. This means, if there exists a distribution $[Y]$ such that $Y_i^{(j^*)} \sim [Y]$, then $Y_{i+1}^{(j^*)} \sim [Y]$.

Let us analyse the first two moments of the probability distribution for the original and sampled data sets. The **first moment** of the probability distribution is calculated as an expected value for the sampled normalised wind speed, it reflects the mean of truncated normal distribution described in the section 2.2.4:

$$E[Y^{(j^*)}] = 0.2412079 \quad \text{while} \quad \mu = 0.2419591$$

where $Y^{(j^*)}$ is the j^*-th sample of the Gibbs sampling method.

The **second moment** of the probability distribution is calculated with the autocovariance coefficients of the sampled normal variables. Let us take 5 years of the recorded one-minute wind speed for the analysis, which is 2592000 points in the data set. Figure 2.11 plots the autocovariance functions of the original and sampled normalised wind speeds.

We see that the difference between the mean of the i-th sample and the original data is insignificant, $\mu - E(Y^{(j^*)}) < 10^{-3}$. One day is chosen as a significant test interval to compare the autocovariance of the sampled and the original datasets where they are very close to each other.

44
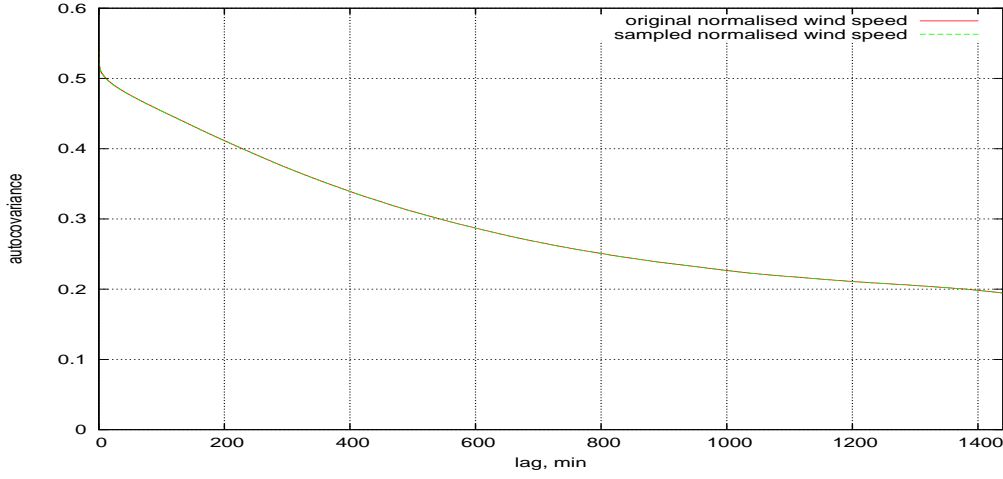
Figure 2.11: Autocovariance of the sampled and the original normalised 1-minute wind speed

For the next test we calculate **variance** of one-minute wind speeds inside ten-minute time sections. The variance is calculated for all consecutive groups of ten minute wind speeds.

$$var(Y^{j^*}) = \frac{1}{Tq} \sum_{t=1}^{Tq} (y_t^{j^*} - \overline{Y_i^{j^*}})^2 \tag{2.37}$$

where $y_t^{j^*}$ are the sampled normalised wind speeds from the ten-minute interval i with the average $\overline{Y_i^{j^*}}$. As data was sampled for ten-minute sections it is important to ensure that there is no boundary effect appearing in the results. To test this, variance (2.37) is calculated for shifted ten-minute intervals.

Table 2.3: Variance of the original and the sampled normalised wind speed

shift	original data	sampled data
0	0.027672	0.025126
1	0.027672	0.025126
2	0.027672	0.025126
3	0.027672	0.025126
4	0.027672	0.025126
5	0.027672	0.025126
6	0.027672	0.025126
7	0.027672	0.025126
8	0.027672	0.025126
9	0.027672	0.025126

45

Table 2.3 shows that independent of the start point for the grouping of the interval $1 \ldots Tq$ cumulative variance has the same value 0.025126. This supports a statement that there are no boundary effect appearing in the sampled data.

2.4 Diversification of wind energy

As it was stated at the beginning of this chapter, we require a dataset of geographically distributed one-minute wind speed in order to model short-term electricity generation. Utah Geological Survey publishes ten-minute wind speed ([21]) recorded in different sites of the Utah state of the United States of America. Section 2.2 of this work introduced Gibbs sampling algorithm and in Section 2.3 we originally adapted this algorithm so that one-minute wind speed is sampled when the average value of ten-minute wind speed is given. We applied further the modified Gibbs sampling to generation of one-minute wind speed using ten-minute wind speed provided by the Utah Geological Survey. Statistical characteristics of one-minute wind speed were based on the data received with the MST Radar located at the Frongoch farm in Wales ([20]) that allowed us to study short-term wind electricity generation with wind energy in Great Britain.
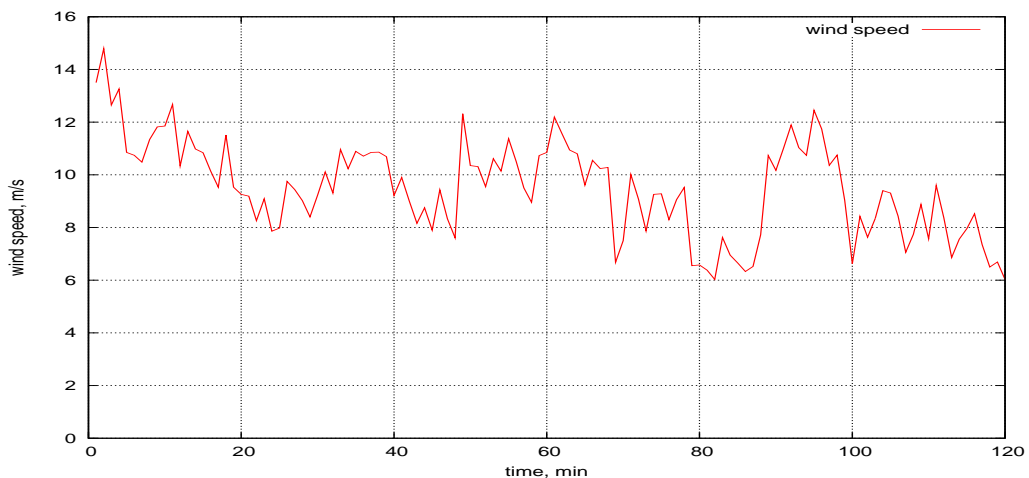

Figure 2.12: An example of wind speed sampled for one of the Utah sites

We chose 22 different sites from the Utah state where ten-minute wind speed was recorded by Utah Geological Survey. They are distributed around the state that introduces an effect of the geographical diversity into the accumulated wind energy curve. For every site we generated a valid sample of one-minute wind

speed using the modified Gibbs sampling algorithm explained in Section 2.3.3, so that a given value of ten-minute wind speed is achieved. Figure 2.12 plots an example of wind speed sampled for one of the sites in Utah.
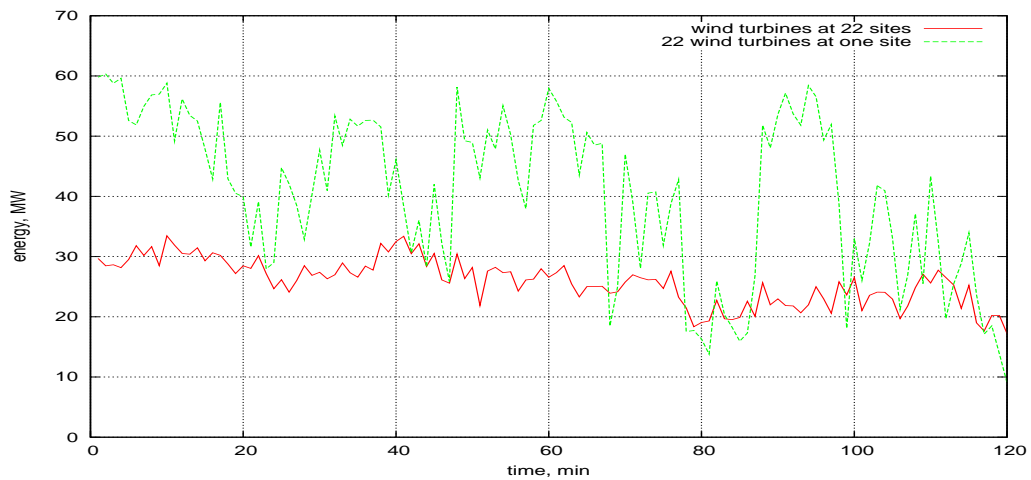
Figure 2.13: An example of geographically distributed wind energy output

We sampled 22 sets of one-minute wind speed for different sites in Utah that were further transfered into energy using the wind power curve plotted in Figure 2.1. Notice, variability of the combined wind energy from 22 sites in Utah varies less than the same amount of energy produced at one site. To demonstrate this, Figure 2.13 plots the combined wind energy that could have been generated from 22 sites in Utah against wind energy that could have been generated by 22 wind turbines using a single wind speed sample plotted in Figure 2.12.

Considering a geographical diversity of wind farms in Great Britain we wish to use the combined wind energy from 22 sites in the Utah state for the optimization modelling of the electricity generation further in this work.

Chapter 3

Modelling Electricity Generation with Wind Energy

Scheduling electricity generation is a complex engineering problem that takes into account various parameters of generation, demand, transmission and distribution. This chapter specifies the details of the electricity demand and generation in the United Kingdom and formulates a mathematical programming problem of scheduling the operating reserve so that the supply and demand match within the target range. We use the formulated optimization model to investigate the costs involved in incorporating different levels of wind energy into the electricity generation system of Great Britain.

We assume in this chapter that wind speed is forecast with certainty. Therefore, the formulated optimization model is deterministic and includes some of the common constraints of power generation. The uniqueness of the model developed in this chapter consists in the data representing the power system of the UK and the application of the optimization model to estimating the system balancing cost of the variable wind energy.

3.1 Elements of the British power system and simplifying assumptions

Section 3.1 introduces the electricity generation system of the United Kingdom and how it can be adapted for the optimization modelling. In Chapter 2 we developed an algorithm that would produce one-minute wind energy data, therefore, this section focuses on the parameters of thermal generation and its fuel cost. We assume that the electricity load only slowly changes, leaving the matter of

interaction between the demand and wind power for further research.

3.1.1 Electricity generation

Currently electricity generation in the United Kingdom includes a diversity of generating units. The amount of generation provided by different types of generating units vary depending on the time of the year and the size of the load. For the purpose of this work we use Plant/Demand Balance of the "Seven Year Statement" published by the National Grid Electricity Transmission in 2008 [35]. Table 3.1 shows the percent of power from the various plant types in the total generation.

According to the figures in Table 3.1 two types of plants that cover more than 70% of the total British electricity generation are Gas and Coal turbines. Various nuclear generators contribute to another 14% of the total generating capacity. Coal, gas and nuclear units have common characteristics with other units of the same type that we wish to incorporate in the model. Parameters describing a certain type of the generator are available through the Balancing Mechanism (BM) reporting system ([5]). This website publishes on a daily basis Physical and Dynamic parameters (as defined in Appendix A) of the units participating in the balancing mechanism. We wish to incorporate some of the characteristics into the mathematical programming model, in particular the available capacity and the maximum rates of change in the power output.

The first characteristic that the System Operator takes into account while planning an output of a thermal generator, like gas, coal or nuclear, is a **capacity limit**. Capacity limit is specified in the BM reporting system as the Export Limits parameter (defined in Appendix A) and describes a maximum level at which the generating unit may be exporting power to the transmission system. The capacity limit of any type of the generator depends on the size of the unit and can vary within the same type of generators. However, for the modelling purpose we wish to use a single value as a capacity limit for every type of a same plant. Let us use a capacity limit for a typical gas generator as 500MW and 600MW for typical coal and nuclear types of generating units.

The output levels of thermal plants are not constant and can vary following the changes in the electricity load. The maximum rate at which units change their production can be described by **Run-Up** and **Run-Down** export rates (defined in Appendix A). These rates depend on the current output of the generator and are used by the System Operator in scheduling the operating Reserve when balancing the supply and demand in real-time.

Table 3.1: Plant/Demand balance for SYS Background (2007/2008)

hline Plant type	Capacity (MW)	%
biomass	45	0.06
CCGT	25532	32.58
CHP	1725	2.20
Hydro	1028	1.31
Interconnector	1988	2.54
Large coal	4413	5.63
Large coal+AGT	21462	27.39
Medium coal	1152	1.47
Medium coal+AGT	1102	1.41
Small coal	783	1.00
Nuclear AGR	8365	10.68
Nuclear Magnox	1450	1.85
Nuclear PWR	1190	1.52
OCGT	589	0.75
Offshore wind	140	0.18
Oil+AGT	3496	4.46
Pumped storage	2300	2.94
Wind	1597	2.04

The Run-Up and Run-Down export rates specified in the BM reporting system are further adjusted to be used in the model. Maximum Run-Up and Run-Down rates are published in the form of a table with three different values for each of the rates that depend on a production level. The rates for different power output can cause a non-convex constraint in the optimization model. Let us consider the following example:

Table 3.2: An example of the Run-Up and Run-Down export rates for a typical coal plant

Export rate	r_1	e_1	r_2	e_2	r_3
Run-Up	5.0	177	0.2	180	5.0
Run-Down	5.0	240	0.4	234	58.5

Table 3.2 gives an example of the Run-Up and Run-Down export rates published for a typical coal plant by the Balancing Mechanism reporting system. There are usually three Run-Up and Run-Down export rates, r_1, r_2 and r_3 submitted by the generating unit before the Gate Closure. Every rate is applied to a different output level specified by the "elbows", e_1 and e_2. So, Run-Up rate $r_1 = 5.0$ MW per minute is applied to the production level from 0 to 177 MW. And a maximum Run-Down export rate $r_3 = 58.5$ MW per minute can be applied when a coal generator cools down between 234 MW and 0.

The specified sequence of maximum Run-Down and Run-Up export rates leads to the non-convex constraint describing the power output rate of change between the current and the following minute. Hence, we wish to simplify the rates presented in Table 3.2. First, the rate r_2 can be dropped as it is likely to be an internal work taking place in the generating unit and is not important for our work. Later in this chapter we modify the values of the remaining rates r_1 and r_3 so that they form a convex feasible set. The resulting constraints will be formulated in Section 3.2.2.

Short time scale water reservoir limits are often not building and a hydro generator can be modelled in the same way as a thermal generator except that the "fuel" is water. Table 3.1 also shows that the hydro and pumped storage contribute no more than 5% to the total electricity generation. Considering a limit of water resources in United Kingdom and capital cost of pumped storage generation we wish to avoid modelling hydro generation in this work.

According to the "Seven Year Statement" published in the beginning of 2008 wind contributes only 2% to the total electricity generation, however, the installed wind energy capacity have doubled during the last year and is expected further to increase. We wish to introduce the wind energy output into the electricity generation system based on the wind speed data provided by the Utah Geological Survey. Every site is assumed to contribute an equal number of wind turbines to the total wind energy curve. This curve is further scaled so that wind contributes a required amount of energy to the total electricity generation.

3.1.2 Cost of generation

Due to the fact that the electricity generation is scheduled minute by minute during the real time, there is not enough time to make a decision about switching additional thermal plants. For some coal generators it takes up to 2 hours to be warm and ready to respond. Therefore, we assume that only generators that are currently onstream can be used to meet the load. Short term scheduling determines a cost of the electricity generation as the fuel cost for all types of generators. Following this, generating cost of wind and nuclear energy is zero and cost of gas and coal is defined by the fuel prices.

In the report "Keeping the lights on: Nuclear Renewables and Climate Change" Milborrow [41] discusses current cost of the electricity generation and the way it can be calculated. Also governmental organisation "Department for Business Enterprise and Regulatory Reform" (BERR) regularly publishes the average prices of fuels purchased by the major UK producers. We wish to use the quarterly

energy prices reported by BERR for year 2008 [7]. An average price of coal for power stations was increasing since 2007 and amounted to 0.72 p/KWh. The price of gas has increased by more than 50% up to 1.5 p/KWh.

In order to apply these prices to the electricity generation in one-minute frequency we recalculate the given prices in £/MW*min.

$$c_{coal} = 0.72\text{p/KWh} \qquad\qquad = 0.12£/\text{MW*min}$$
$$c_{gas} = 1.5\text{p/KWh} \qquad\qquad = 0.25£/\text{MW*min}$$

Note, there is no capital cost included in the cost of the electricity generation, we are interested in minimizing the fuel cost later in this work.

3.1.3 Electricity demand

We wish to model the electricity demand with the same time frequency as the generation, i.e. on a minute by minute basis. However, a most frequent electricity demand reported through the Balancing Mechanism reporting system is the historic and real-time records of the national demand.
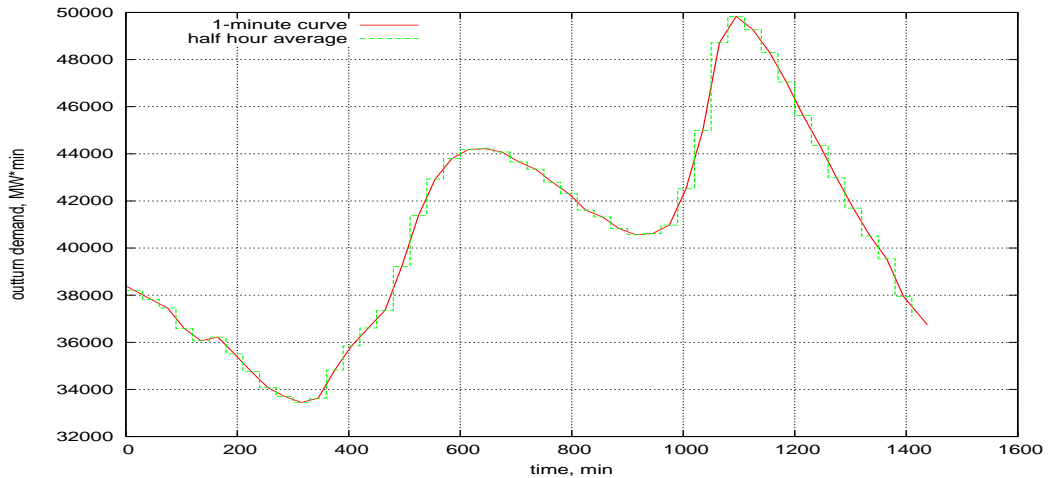
Figure 3.1: Half-an-hour average of the daily electricity demand in the United Kingdom and its piecewise linear approximation with 1-minute frequency

As the electricity demand is available in half-an-hour average estimates we wish to transfer it into a continuous piecewise linear function with one minute frequency. Figure 3.1 shows an example of the winter electricity demand used later for the deterministic and stochastic models.

52

3.1.4   Cost of demand-and-supply mismatch

In reality it is very hard to generate exactly the value of the national electricity demand at any moment. Considering the uncertainty of consumer's behaviour and a probability of losing a generating capacity in the system, it is important to have a flexibility of meeting the demand. As it was stated in Chapter 1 the transmission system of the United Kingdom operates at the frequency 50Hz with a range of 1% variation above and below 50Hz.

We wish to incorporate an option of the mismatch between the electricity generation and demand in the model. The transformation function that calculates the deviation in power, based on a given deviation in frequency is complex: it depends on the system parameters and the load level. Transmission system is not modelled in this work, therefore, a mismatch between the generation and the electricity demand that corresponds to the variations in the frequency is assumed to be a function of the electricity demand. Further, the generation is allowed to vary 2% above or below the electricity load which corresponds to the 1% variation in frequency.

Although it is possible for the generation to deviate from the demand it is not a good practise to get close to the upper and lower limits. This can get the transmission system into zones of too high or too low frequency. As a result of modelling minimization of the electricity generating costs, the solution tends to produce an output of the electricity generation 2% below the electricity demand. To prevent this happening let us introduce a penalty of mismatch between the demand and generation.
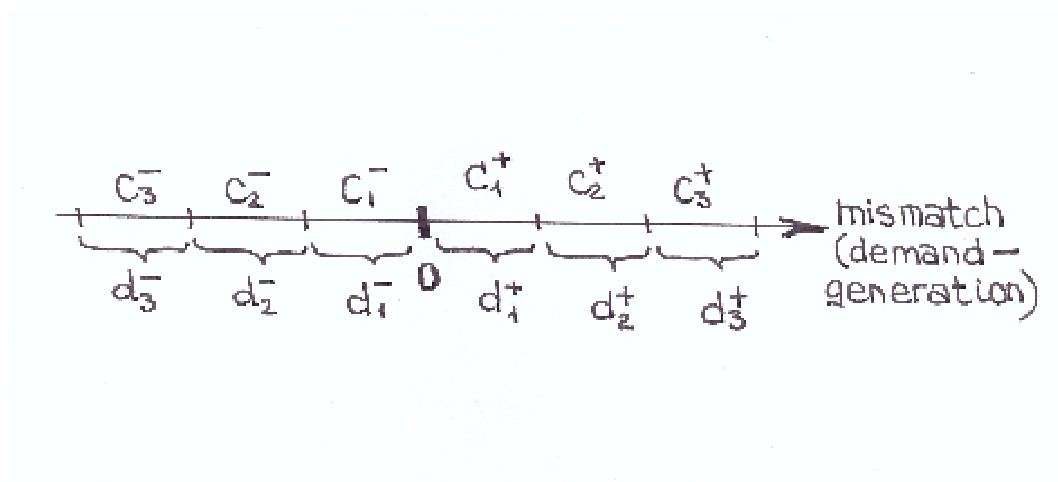

Figure 3.2: A mismatch between the electricity demand and the generation with the cost attached

Let us divide the allowed mismatch between the electricity demand and generation into several intervals so that the cost of a mismatch increases with the higher deviation between the demand and generation.

Gas generating units are assumed to be a marginal type of the electricity generation. Gas turbines have the highest fuel cost among the thermal plants but the Run-Up and Run-Down rates are also higher than that of the coal and nuclear generators. Determined as the marginal generator, gas turbines are used first to respond to the mismatch between the electricity demand and generation, so that a cost of the mismatch is estimated according to the fuel cost of the gas generator. In Figure 3.2 the cost c_1^+ corresponding to the mismatch between the electricity demand and the generation d_1^+ is marginally higher than the fuel cost of the gas generator. If gas turbines are able to cope with the load fluctuations, higher cost of mismatch encourages the generation to meet the demand exactly. However, it is rather allowed for the generation to deviate from the demand than to modify the power output of the coal or gas turbines. The cost c_3^+ is significantly higher than the cost of the marginal generator so that the mismatch between the electricity demand and generation exceeds $d_1^+ + d_2^+$ only if no other feasible solution exists.

3.1.5 Summary

Let us summarise the above points in order to formulate a deterministic problem of the electricity generation. To estimate the system balancing cost when variable wind energy is incorporated into the electricity generation system we assume:

a. there is no transmission cost;

b. there are three types of thermal generators (gas, coal and nuclear) included in the model. They are characterised by the limited capacity and the Run-Up and Run-Down rates;

c. there is only generating (fuel) cost considered in the problem. Time scale is short so there is no start-up costs of thermal generation;

d. wind power generation is determined by the incoming data and is perfectly forecast for the deterministic problem;

e. there is no hydro energy included in the model;

f. the electricity demand is deterministic;

g. there is a cost of mismatch between the electricity demand and generation.

3.2 Deterministic model for the electricity generation with wind energy

This section formulates a linear programming (LP) mathematical optimization model for the electricity generation scheduling problem specified in Section 3.1.

3.2.1 Decision variables

Let T denote the number of time intervals obtained by discretising the planning horizon. This discretisation may be chosen uniformly or non-uniformly. For the current problem we use one-minute uniform discretization of the planning horizon.

Let G denote the set of all the generators and consist of the union of C, the set of the conventional generators, and W, the set of the wind generators. The set of conventional generators also consists of Coal, Nuclear and Gas generating plants. The decision variables in the model correspond to the outputs of each thermal unit, i.e. the electric power generated by the Coal, Gas and Nuclear generators. The decision variables are denoted by

$$x_{tg}, \quad t = 1, 2, \ldots, T; g \in C$$

where x_{tg} is the production level of thermal unit g during time period t. We assume a constant power output during 1 minute and measure it in MW*min.

Wind power generation is determined by the wind speed and equals to the power w_t^e at time t:

$$x_{tg} = w_t^e, \quad t = 1, 2, \ldots, T, g \in W \tag{3.1}$$

3.2.2 Constraints

The electricity generation system is complex so it is possible to include different constraints in its optimization model (capacity, emission limits, system security and others). The model described in this section would contain only those constraints that allow us studying a problem of incorporating the wind energy into the electricity generation system. Decision variables corresponding to the thermal generation mentioned above have finite upper and lower bounds representing

unit capacity limits of the generation system:

$$\underline{x_g} \le x_{tg} \le \overline{x_g}, \qquad t = 1, 2, \ldots, T, g \in C \qquad (3.2)$$

The constants $\underline{x_g}$ and $\overline{x_g}$ denote minimal and maximal possible outputs of the thermal units respectively.
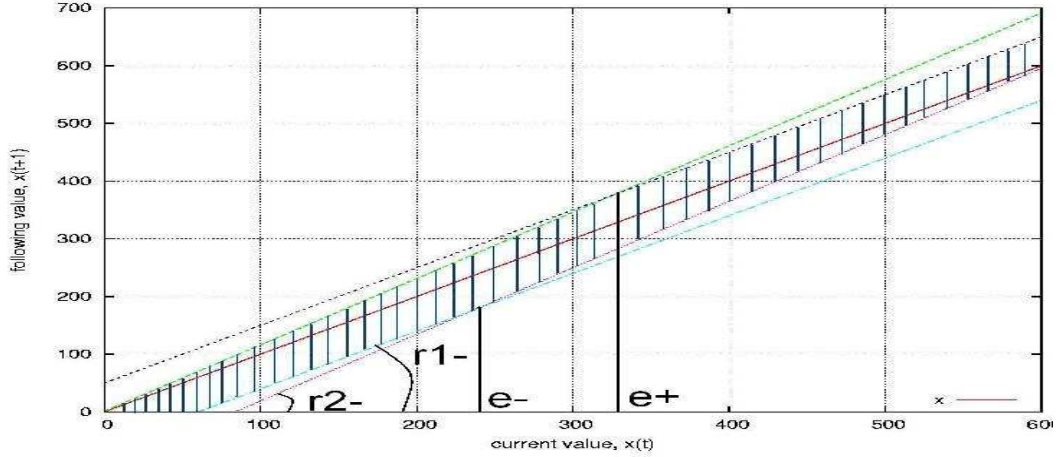

Figure 3.3: Area formed by Run-Up and Run-Down constraints for thermal generators

Further single-unit constraints describe maximum Run-Up and Run-Down export rates introduced in Section 3.1.1. An example of Run-Up and Run-Down export rates that a generating plant provides to the System operator before the "Gate closure" is given in Table 3.2. As it was stated then, these export rates cause a non-convex constraint. Hence, let us modify the limits of maximum Run-Up and Run-Down rates in a way that they form a convex set $(x_{tg}, x_{(t+1)g}), t = 1, 2, \ldots, (T-1), g \in C$ of the decision variables.

As mentioned in Section 3.1.1 we use only two Run-Up and two Run-Down rates that are connected in a piecewise linear function and form a convex set. The piecewise linear function can be chosen in a way that tighten or relax the maximum export rate limits. Constraints $(3.3) - (3.6)$ formulated below relax the limits of Run-Up and Run-Down rates of generating plants. Let r^{1+} and r^{2+} denote two Run Up rates separated by the "elbow" e^+, while r^{1-} and r^{2-} - denote two Run Down rates separated by the "elbow" e^-. The corresponding constraints of the change in the power output are described by inequalities:

$$x_{t+1,g} \le \frac{e^+ + r^{2+} - r^{1+}}{e^+} x_{t,g} + r^{1+}, \qquad t = 1, 2, \ldots, T, g \in C \qquad (3.3)$$

$$x_{t+1,g} \leq x_{t,g} + r^{2+}, \qquad t = 1, 2, \ldots, T, g \in C \qquad (3.4)$$

and

$$x_{t+1,g} \geq \frac{\overline{x_g} - e^- + r^{2-} - r^{1-}}{\overline{x_g} - e^-} x_{tg} - \frac{r^{2-}\overline{x_g} - r^{1-}e^-}{\overline{x_g} - e^-}, \qquad t = 1, 2, \ldots, T, g \in C$$

$$(3.5)$$

$$x_{t+1,g} \geq x_{t,g} - r^{2-}, \qquad t = 1, 2, \ldots, T, g \in C \qquad (3.6)$$

Figure 3.3 plots a convex set $(x_{tg}, x_{(t+1)g}), t = 1, 2, \ldots, (T-1), g \in C$ with new Run-Up and Run-Down export rates in a form of the shaded area bordered by two lines from the above and two lines from the below. Every line on the graph states a maximum rate of change between the output at the current minute and the following minute. The two lines from the above in Figure 3.3 intersect in a point of the "elbow" e^+ and are described by the inequalities $(3.3) - (3.4)$. The two lines from the below intersect in a point of the "elbow" e^-, their gradients are r^{1-} and r^{2-} respectively. Run-Down rates are described by the inequalities $(3.5) - (3.6)$.
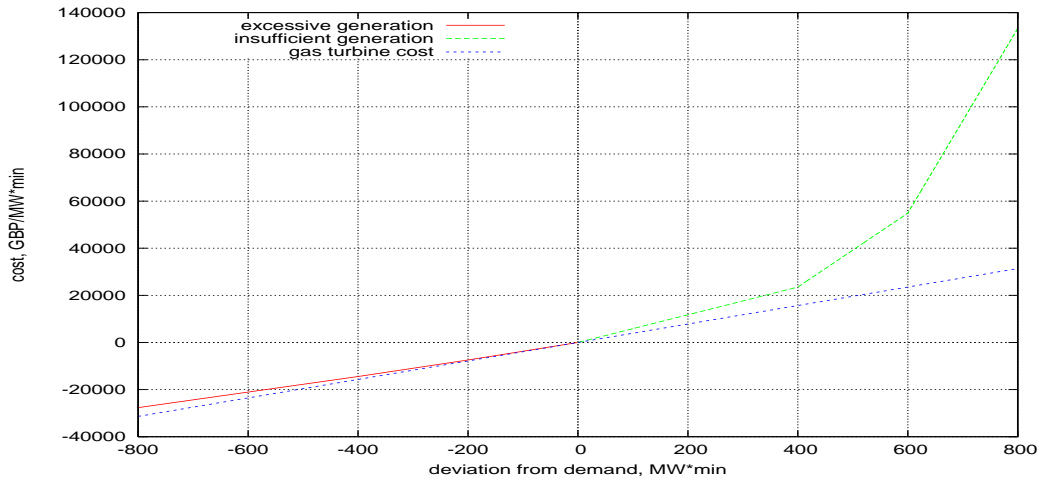
Figure 3.4: Load mismatch costs: the difference between the curves gives the penalty for generation deviating from demand.

The loading constraint couples across all the generating units. It is essential for the operation of the power system and means that the difference between the total power generation and the load demand does not exceed the allowed (by the transmission system) limit at any time. Denoting by D_t the electricity demand during a time period t and by Δ_D a percent mismatch allowed between the electricity load and the generation, the loading constraint is described by the

inequalities:

$$(1 - \Delta_D)D_t \leq \sum_{g \in G} x_{tg} \leq (1 + \Delta_D)D_t \qquad t = 1, 2, \dots, T \qquad (3.7)$$

In (3.7) a parameter Δ_D is taken as 2% that corresponds to 1% variation in the system frequency.

In Section 3.1.1 we discussed a cost of the mismatch between the electricity supply and demand. Logically the generators should produce close to the demand and as far away from the lower and upper bounds as possible. To achieve this result in the model we introduce a piecewise linear cost for the load imbalance $\{\zeta_v^+; \zeta_v^+\}, v = 1, 2, \dots, V$ where V denotes a number of bands in the penalty cost. To avoid giving an incentive to violate the load constraint, this piecewise linear load imbalance cost should be above the cost of the marginal generator at that time. Figure 3.4 plots the fuel cost of the marginal generator (gas in our case) and three different cost bands for the generation exceeding the demand and the demand exceeding the generation. The higher mismatch between the electricity demand and generation the higher the cost of coping with it.

Let us denote a mismatch between the electricity generation and the load by a set of variables d_{tv}^+ and d_{tv}^-, $t = 1, 2, \dots, T, v = 1, 2, \dots, V$ such that

$$\sum_{g \in G} x_{tg} - D_t = \sum_{v \in 1..V} (d_{tv}^+ - d_{tv}^-) \qquad t = 1, 2, \dots, T \qquad (3.8)$$

In (3.8) T denotes the planning horizon while V is a number of the cost bands in the accepted mismatch between the supply and demand $[(1 - \Delta_d)D_t; D_t]$ and $[D_t; ((1 + \Delta_d)D_t)]$. Size of every interval $v = 1, 2, ; dots, V$ is measured in MW and defined by the inequalities:

$$0 \leq d_{tv}^+ \leq \overline{d_{tv}^+} \qquad (3.9)$$

$$0 \leq d_{tv}^- \leq \overline{d_{tv}^-} \qquad (3.10)$$

where $\overline{d_{tv}^+}$ is an upper bound of interval v when the electricity demand exceeds the generation at time t, $\sum_{g \in G} x_{tg} < D_t$. $\overline{d_{tv}^-}$ is an upper bound of interval v when the generation exceeds the demand at time t, $\sum_{g \in G} x_{tg} > D_t$.

Set of parameters $[\overline{d_{tv}^+}, \overline{d_{tv}^-}]$ is time dependent and defined by the changing value of demand. It can be calculated in the following way

$$\overline{d_{tv}^+} = \Delta_d * D_t * \beta_v^+ \qquad (3.11)$$

where β_v determines a part of the demand envelope $\Delta_d * D_t$ that corresponds to the cost band $v = 1, 2, \ldots, V$.

3.2.3 Objective function

The constraints described above form a feasible set of solutions for our optimization problem of scheduling the electricity generation. To complete our LP model, let us introduce the operational cost of the electricity generation for different types of plant. Let c_g denote the fuel cost for each thermal generator $g \in C$. Fuel cost of the coal and gas generation was introduced in the section 3.1.2. Then $\sum_{g \in C} c_g \sum_{t=1}^{T} x_{tg}$ is the operational cost paid by the Supplier to generate $\sum_{g \in C} \sum_{t=1}^{T} x_{tg}$ amount of electricity.

In order to decrease a mismatch between the electricity generation and demand we wish to include the cumulative cost of the mismatch into the objective. If parameters ζ_v^+ and ζ_v^- denote the cost of the excessive and insufficient generation respectively, we wish to minimize the total cost of the electricity demand and generation mismatch:

$$\sum_{v=1}^{V} \zeta_v^+ \sum_{t=1}^{T} (\sum_{g \in G} x_{tg} - D_t) \qquad + \qquad \sum_{v=1}^{V} \zeta_v^- \sum_{t=1}^{T} (D_t - \sum_{g \in G} x_{tg})$$

If we define $d_{tv}^+ := \sum_{t=1}^{T} (\sum_{g \in G} x_{tg} - D_t)$ and $d_{tv}^- := \sum_{t=1}^{T} (D_t - \sum_{g \in G} x_{tg})$ this can equivalently be rewritten as:

$$\sum_{v=1}^{V} \zeta_v^+ \sum_{t=1}^{T} d_{tv}^+ \qquad + \qquad \sum_{v=1}^{V} \zeta_v^- \sum_{t=1}^{T} d_{tv}^-$$

Taking into consideration the fuel cost and the cost of the load imbalance, the objective of the mathematical programming model is to minimize the cumulative operational cost of the electricity for the planning horizon T:

$$\min_{x} \sum_{g \in C} c_g \sum_{t=1}^{T} x_{tg} + \sum_{v=1}^{V} \zeta_v^+ \sum_{t=1}^{T} d_{tv}^+ + \sum_{v=1}^{V} \zeta_v^- \sum_{t=1}^{T} d_{tv}^- \qquad (3.12)$$

In the objective function (3.12) $\sum_{g \in C} c_g \sum_{t=1}^{T} x_{tg}$ denotes the fuel cost of the thermal generators $g \in C$ and $\sum_{v=1}^{V} \zeta_v^+ \sum_{t=1}^{T} d_{tv}^+ + \sum_{v=1}^{V} \zeta_v^- \sum_{t=1}^{T} d_{tv}^-$ denotes the cost of mismatch between the electricity supply and demand.

3.2.4 Formulation of the LP deterministic optimization model

The constraints and and the objective described in Section 3.2.2 and Section 3.2.3 are combined below:

Objective (minimize cost):

$$\min_x \sum_{g \in C} c_g \sum_{t=1}^{T} x_{tg} + + \sum_{v=1}^{V} \zeta_v^+ \sum_{t=1}^{T} d_{tv}^+ + \sum_{v=1}^{V} \zeta_v^- \sum_{t=1}^{T} d_{tv}^-$$

Subject to:

$$x_{tg} = w_{tg} \qquad \forall g \in W$$

$$\underline{x_g} \leq x_{tg} \leq \overline{x_g} \qquad \forall g \in C$$

$$x_{(t+1),g} \leq \frac{e^+ + r^{2+} - r^{1+}}{e^+} x_{t,g} + r^{1+} \qquad \forall g \in C$$

$$x_{(t+1),g} \leq x_{t,g} + r^{2+} \qquad \forall g \in C$$

$$x_{(t+1),g} \geq \frac{\overline{x_g} - e^- + r^{2-} - r^{1-}}{\overline{x_g} - e^-} x_{tg} - \frac{r^{2-}\overline{x_g} - r^{1-}e^-}{\overline{x_g} - e^-} \qquad \forall g \in C$$

$$x_{(t+1),g} \geq x_{t,g} - r^{2-} \qquad \forall g \in C$$

$$(1 - \Delta_D)D_t \leq \sum_{g \in G} x_{tg} \leq (1 + \Delta_D)D_t$$

$$\sum_{g \in G} x_{tg} - D_t = \sum_{v=1}^{V}(d_{tv}^+ - d_{tv}^-)$$

$$0 \leq d_{tv}^+ \leq \overline{d_{tv}^+} \qquad \forall v = 1, 2, \ldots, V$$

$$0 \leq d_{tv}^- \leq \overline{d_{tv}^-} \qquad \forall v = 1, 2, \ldots, V$$

$$\overline{d_{tv}^+} = \Delta_d * D_t * \beta_v^+ \qquad \forall v = 1, 2, \ldots, V$$

$$\overline{d_{tv}^-} = \Delta_d * D_t * \beta_v^- \qquad \forall v = 1, 2, \ldots, V$$

where $t = 1, 2, \ldots, T$.

3.3 Calculating cost of wind energy variability

An output of the mathematical optimization model $(3.1) - (3.12)$ formulated in Section 3.2 represents a series of one-minute electricity generation level for every thermal generator $g \in C$ over a time period of T minutes. The optimal solution is chosen according to the minimization function that includes fuel cost of the

thermal generators and the cost of a mismatch between the electricity supply and demand.

The deterministic LP optimization model formulated in Section 3.2.4 includes two sets of variables $\{x_{tg}\}$ and $\{d_{tv}\}$, where $g \in C$, $t = 1, 2, \ldots, T$ and $v = 1, 2, \ldots, V$. If we denote κ as a number of thermal generators in the set C, a total number of decision variables in the model equals $\kappa*T+V*T$. To reduce a number of variables we wish to group thermal generators so that there are only three generators included in the set C: nuclear, gas and coal. Each of these thermal generators represent a big number of plants with similar fuel costs and capacity limits. Then, taking $V = 6$ there are 12960 decision variables in the deterministic optimization problem of daily (T=1440) electricity generation. Assuming further one accumulated wind energy curve in the set of wind generators, a number of constraints results in 60480 for a daily electricity generation problem.

Formulated deterministic optimization problem is linear so that it can be efficiently solved with a CPLEX solver. We used version 10.00 of the CPLEX solver that resulted in CPU time $<$ 1s.

Formulated deterministic model can be used now to estimate the system balancing cost that appears as a result of wind energy variability. In order to estimate this cost we compare the results of two different cases. The power system benefits initially from the wind energy being present in the system as there is no fuel cost associated with the generation of wind energy. But this advantage of wind energy is challenged by its variability. If a significant amount of the wind energy fluctuates, thermal generators must frequently modify their production level in order to balance these fluctuations in the power system. Fluctuations of the wind energy result not only in the additional fuel cost but also the cost of a mismatch between the electricity generation and the load.

3.3.1 Case of constant wind energy that reduces the operational cost

First let us consider a case when a wind energy profile if flat, i.e. there are no fluctuations in the wind output. There are three types of thermal generators used to meet the electricity load: nuclear, coal and gas generators. These generating units can be ordered by the fuel cost and the output flexibility, i.e. a size of the maximum Run-Up and Run-Down export rates.
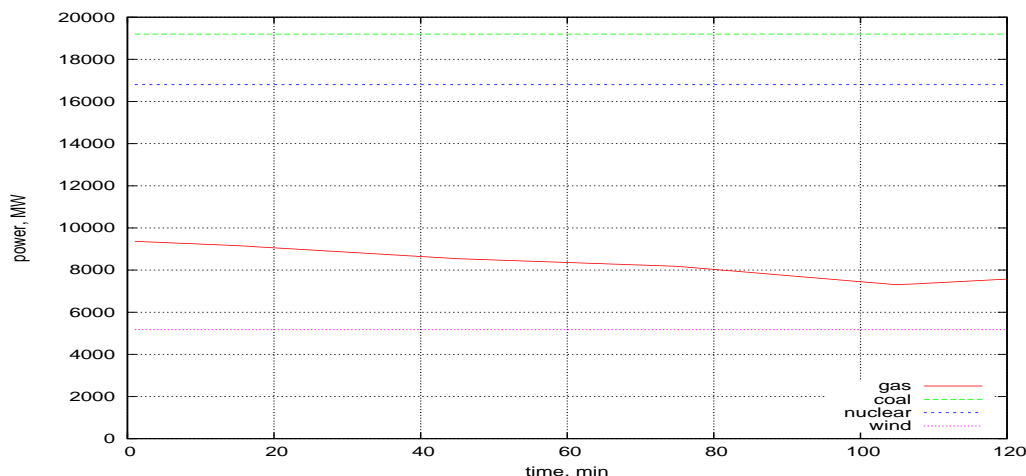
Figure 3.5: Electricity generation when 11% of wind energy with flat profile is introduced to the system

Figure 3.5 plots an example of the optimization model output, which is a generation level for the thermal plants as well as the available wind energy with the flat profile. Nuclear generators are the cheapest, we price the fuel cost as zero in the model. It is also the least flexible type of generation as it has the lowest Run-Up and Run-Down rates. Gas turbines are the most expensive type of generation in the model but they are the most flexible generators. As a result the model output shows the nuclear and coal generation at the maximum available capacity and gas generators produce the remaining electricity to meet the load.

Definition Let us denote a flexible generation producing electricity away from its upper and lower boundaries as the *marginal generation* with the fuel cost equals c_m. Marginal generators are the first to react on changes in the electricity load.

Wind energy is constant for this solution with the output of 5173 MW*min that makes up to 11% of the load in two hours.

The cumulative fuel cost corresponding to this problem of scheduling the generation is reduced by the fuel cost of the marginal generator that would be used if there was no wind present in the system.

Definition Let us denote F_w^{flat} as the *cumulative fuel cost* of the mathematical optimization problem *with flat wind energy profile* and f_w^+ as *the saving in fuel cost* by the Supplier of the electricity when it uses the wind energy in the total generation.

62

Cumulative fuel cost F_w^{flat} is related to the problem with no wind energy in the system in the following way:

$$F_w^{flat} = F_0 - f_w^+ \tag{3.13}$$

In (3.13), F_0 is the fuel cost related to the optimization problem with no wind energy available. The cost of the mismatch between the electricity demand and the generation equals zero in the current case as the load can be met exactly.

3.3.2 Case of variable wind energy that increases operational cost

For the next case a profile of the wind energy curve is variable. It is balanced by the group of thermal generators: nuclear, coal and gas. As in the previous case they are ordered by the fuel cost and maximum Run-Up and Run-Down export rates.
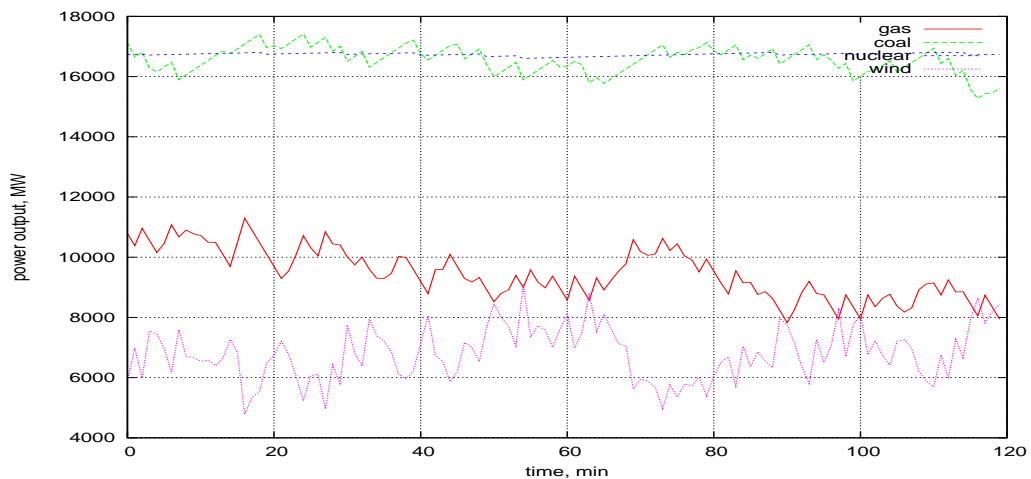
Figure 3.6: Electricity generation when 11% of variable wind energy is introduced to the system

Figure 3.6 plots an example of the optimization model output, which is a generation level for the thermal plants as well as the available wind energy. Unlike the case presented in the Section 3.3.1, wind energy for the current problem fluctuates. Let the fluctuations of the wind energy curve be proportional to the amount introduced to the power system. Figure 3.6 plots 11% of the wind energy in total electricity generation of 1 day. In order to balance the variable

63

wind energy the thermal generators have to modify their production profile. Gas turbines have the highest Run-Up and Run-Down exports rates so it reflects most of the variation in the wind energy. However, gas generation is not able to cover some of the steep changes in wind energy from minute to minute. Then the coal generators modify the power output so that the supply and the electricity demand are within the target range. The nuclear plants have the lowest Run-Up and Run-Down rates which results in the output profile being flat at almost all the time $t = 1, 2, \ldots, T$.

Figure 3.6 shows that it is hard to meet the electricity demand exactly when variable wind energy is introduced into the power system. In the reality coal generators can not modify the power output as often. Therefore, we wish to allow the total generation to deviate from the electricity demand within a certain range. This can be achieved by setting the penalty cost of the first band $v = 1$ marginally higher than the fuel cost of the gas turbine that acts most of the time as the marginal generator. If the gas turbines are able to cope with the variation of the wind energy it is cheaper for the total generation not to deviate from the electricity demand. However, a small mismatch between the supply and the electricity demand is preferable to the modification of the coal power output as it is shown in Figure 3.7.

The cumulative fuel cost corresponding to the problem of scheduling the electricity generation with the variable wind energy is affected not only by the fuel cost of the marginal generator but also by the fuel cost of the generators that modify the output profiles in order to balance the fluctuations of the wind energy.

Definition Let us denote F_w^{var} as the *cumulative fuel cost* of the optimization problem *with variable wind energy profile* and f_w^- as the *additional fuel cost* of the generators that modify the output profiles in order to balance the fluctuations of the wind energy.

Cumulative fuel cost F_w^{var} is related to the problem with no wind energy in the system in the following way:

$$
\begin{aligned}
F_w^{var} = \quad & F_0 - f_w^+ + f_w^- \\
& F_w^{flat} + f_w^-,
\end{aligned}
$$

where F_0 is the fuel cumulative cost related to the optimization problem with no wind energy available and F_w^{flat} was calculated in (3.14) as the accumulated fuel cost of the problem with the flat wind energy profile.
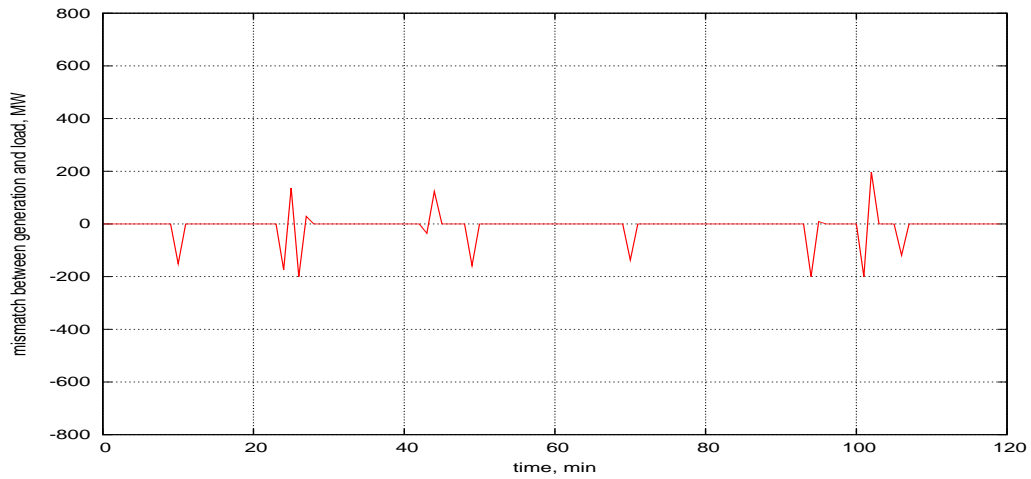
Figure 3.7: Electricity generation and load mismatch when 5% of variable wind energy is introduced to the system

Figure 3.8 plots the cumulative fuel cost of a daily electricity generation weighted by the total amount of the produced power. The highest cost is the fuel cost calculated for a problem when there is no wind energy in the power system. The fuel cost from the bottom reflects a problem with the variable wind energy that can be balanced by the marginal generator. So the weighted fuel cost is a piecewise linear function with the gradient of the marginal generator.
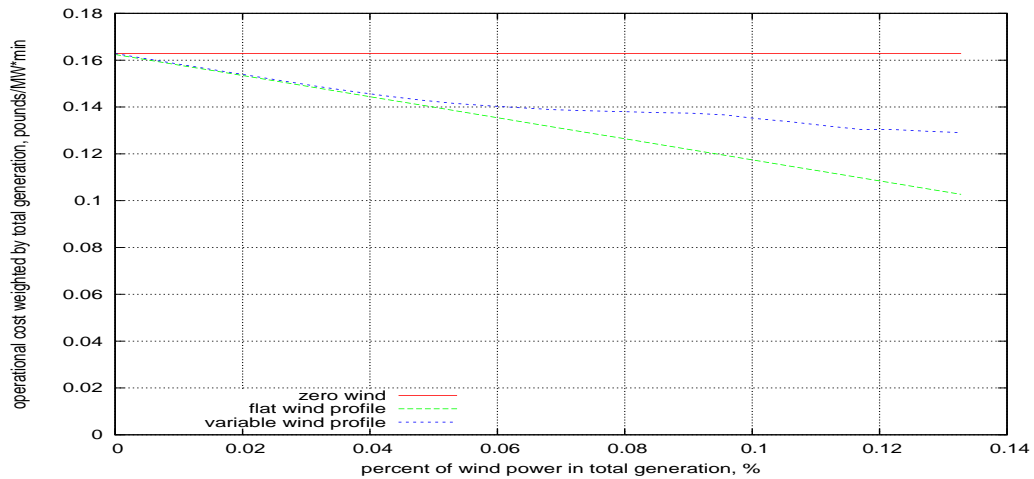
Figure 3.8: The fuel cost of the wind energy variability shown for different levels of it introduced into the electricity system

The system balancing cost that appears when variable wind energy is introduced into the power system can be estimated as the difference between the fuel cost

calculated for the problem with variable wind energy that can be balanced with a combination of different thermal generators and the fuel cost calculated for a problem with variable wind energy that can be balanced by the marginal generator.

Chapter 4

Statistical analysis of operational cost

In the previous chapter we introduced the deterministic optimization LP model of the electricity generation system. This model was used to estimate the system balancing cost that appears when variable wind energy was incorporated into the generation system. We assume further that the saving in fuel cost and the additional fuel cost (as defined in Section 3.3.1 and Section 3.3.2) can be determined as a function of the statistical parameters of the wind energy and develop a unique model that estimates the parameters of such a model.

4.1 Formulation of the problem

To evaluate how well the statistical model estimates the system balancing cost, the optimal value of the cumulative fuel cost is found using the deterministic optimization model described in Chapter 3. Again we assume that the wind speed can be forecast exactly over the planning horizon and there is no uncertainty about the electricity load. For the purpose of this chapter we wish to make the following modifications to the optimization model:

- The electricity demand is constant so that variability in wind energy is clearly presented in the output. However, the general conclusions can be applicable for the case of slowly changing load.

- The electricity load has to be met exactly by the generating units, which means that there is no cost of mismatch between the electricity supply and demand. The objective function of the optimization models in this chapter is presented only by the accumulated fuel cost.

- There is hydro generation included in the optimization model, however, it is small and does not affect the solution.

Let us consider a small electricity generation system where the set of the conventional generators C consists of 15 thermal units. Thermal generators are not differentiated by the available capacity and every plant has the following upper and lower bounds:

$$\underline{x_g} = 0MW \qquad\qquad \text{and}$$
$$\overline{x_g} = 30MW, \qquad\qquad g \in C.$$

Hydro generation is small for all the models in this chapter and has a constant output of 20 MW. Maximum Run-Up and Run-Down export rates (introduced in Section 3.1.1) of thermal generating units are the same for all the range of the electricity output, $\underline{x_g} \leq x_{t,g} \leq \overline{x_g}$, therefore, inequalities $(3.3) - (3.6)$ are simplified as

$$x_{t+1,g} \leq x_{t,g} + r^+$$
$$x_{t+1,g} \geq x_{t,g} - r^- \qquad\qquad t = 1, 2, \ldots, T, g \in C,$$

where r^+ equals 0.125 MW*min and r^- equals 0.125 MW*min for all the models in this chapter.

The thermal generators are differentiated by the fuel cost chosen in a certain merit order so that cheaper thermal plants are used first. Let us take a merit order of the fuel costs to be a piecewise linear function, so that the cost of the first unit $c_1 = 1\pounds/MW$*min increasing by $0.1\pounds/MW$*min for every next unit so that the 15th thermal plant is priced at $c_{15} = 2.4\pounds/MW$*min. There is no cost associated with hydro generation.

Definition Let us denote F_A as the *actual accumulated fuel cost* calculated using the deterministic optimization model.

Further in this chapter we will consider different statistical models of the accumulated fuel cost and compare these with the actual accumulated fuel cost. Every next model is chosen so that the error between the actual and calculated accumulated fuel cost decreases. We assume the accumulated fuel cost of the electricity generation to be a piecewise linear function. The value of F_A is calculated per unit time (per minute in the current case), therefore all the statistical models in this chapter are independent of the planning horizon T.

4.2 Case of marginal generator following a profile of the wind energy curve

Let us begin with a simplified situation of the electricity generation when the wind energy is constant and equals zero. In this case the accumulated fuel cost can be calculated accurately with an error $\epsilon = 0$ by:

$$F_A = F_0 \tag{4.1}$$

where F_0 is the generated cost when there is no wind energy available and can be found from the merit order fuel costs of the thermal generators.

The model described by (4.1) is not, however, suitable for calculating the accumulated fuel cost if there is wind energy incorporated into the power system. In this case error of the calculation $\epsilon = F_A - F_0$ can be significantly higher than zero. To improve the model we take into account another simplified situation of electricity generation, when a marginal thermal generator (as defined in Section 3.3.1) has the Run-Up and Run-Down export rates big enough to cope with variability of wind energy curve.
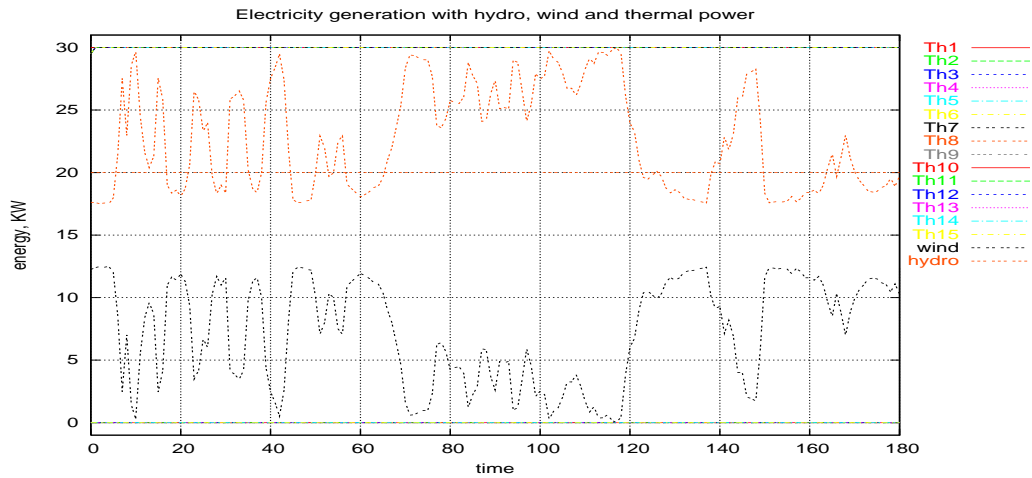

Figure 4.1: Electricity generation with only the marginal generator modifying the power output

Figure 4.1 plots an example of the solution for this simplified case of electricity generation. On this graph thermal plant with the index "Th8" is the marginal generator. It frequently changes the production plan in order to balance the

wind energy output and meet the electricity load exactly. The first seven generators have the lowest fuel cost so that they produce at full capacity. The last seven generators with fuel cost higher than that of the marginal generator do not produce.

This case improves the model that estimates the operational cost of the electricity generation:

$$F_A = F_0 - c_m \overline{x_w} - \epsilon. \tag{4.2}$$

In (4.2) c_m denotes the fuel cost of the marginal thermal generator and $\overline{x_w}$ is an average wind energy over the modelled period of time T.

For both simplified cases considered in this section, the operational cost can be calculated with (4.2) with an error $\epsilon = 0$. However, for a situation when the rates of change of the wind energy curve are higher than that of the marginal generator, there can be an error calculating the operational cost from the right-hand side of formula (4.2). The error term in (4.2) is non-zero and can be significant. Thus, we wish to find a better model in order to improve accuracy of the operational cost calculation.

4.3 Case of wind energy curve having a zigzag profile

Assume, the other elements of the model that estimates the operational cost also depend on the statistical parameters of the wind energy curve.
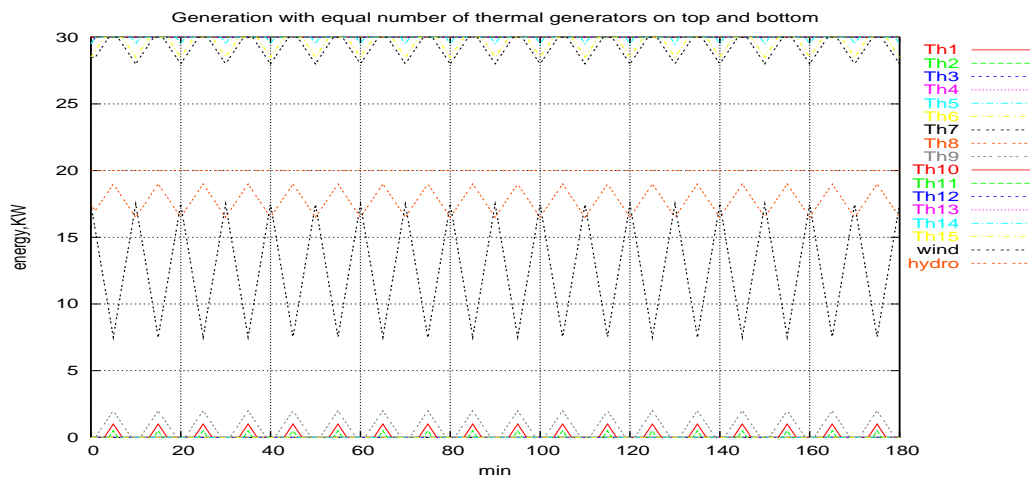

Figure 4.2: Electricity generation with the wind energy profile as a zigzag

70

To evaluate them we construct another simplified case when the marginal generator has the Run-Up and Run-Down export rates smaller than those of the wind energy curve, however, the wind energy itself is periodic and has a form of a zigzag. Figure 4.2 shows that the solution is also periodic and makes it possible to calculate the accumulated fuel cost exactly as it is found using the deterministic optimization model.

Further in this section there is a number of tests performed with one V-shaped drop in wind energy that is plotted in Figure 4.3. Because the solution shown in Figure 4.2 is periodic, calculations for one V-shaped drop are applicable to the whole zigzag curve.

4.3.1 Analytical calculation of the accumulated fuel cost

Definition Let us denote a *height of wind energy curve* as h_w that represents the difference between the highest and the lowest value of wind energy in the time horizon $1, 2, \ldots, T$.

A first test investigates how the accumulated fuel cost changes depending on the modification of the height of every V-shaped wind energy curve defined in Figure 4.3 while a length of the planning period of time T remains the same.
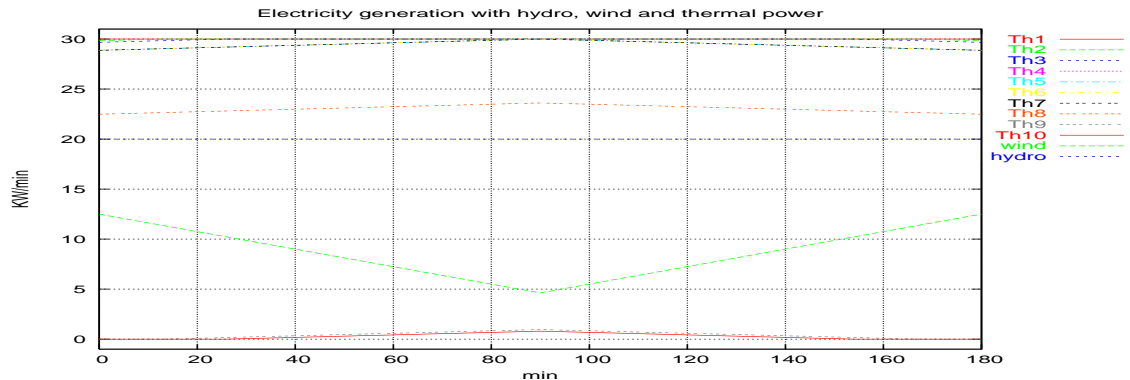
Figure 4.3: Electricity generation for a wind energy curve as one zigzag and the thermal plants increasing and decreasing their output in a symmetric Λ-shape

Definition We denote γ_w as the *average of the absolute value of the gradients* calculated for the wind energy curve.

Modification of the wind energy height h_w is performed in a way that the absolute value of the gradient of the drop in the symmetric V-shaped wind energy curve

71

changes proportionally to the height while the average of wind energy $\overline{x_w}$ remains the same.

Definition Let γ_g denote the *average of the absolute value of the gradients* of a thermal plant $g \in C$; then $\overline{\gamma_g}$ denotes the *maximum of the absolute gradients* of the thermal plant and is defined by the Run-Up and Run-Down export rates.

In Section 4.1, $\overline{\gamma_g}$ was assumed to be the same for all $\kappa = 15$ thermal generators. Then, for every γ_w such that $\gamma_w \leq \kappa\overline{\gamma_g}$ there exist situations where the output from thermal plants decreases or increases in a symmetric Λ-shape. Note, that for the case where generation has to meet the electricity load exactly:

$$\gamma_w = \sum_{g \in C} \gamma_g \tag{4.3}$$

i.e. the absolute value of the average gradient of the wind energy equals a sum of the absolute values of the gradient of κ thermal plants.

We wish to find a formula that calculates the accumulated fuel cost of the electricity generation where a V-shaped wind energy curve is given. To do this, let us look into the output of the thermal generators for a series of problems with the absolute value of gradient of the wind energy curve increasing. After finding a way every thermal plant responds to the increase of the variability in wind energy, we can calculate its total generated energy and, hence, the accumulated fuel cost.

Besides the cases where the output of the thermal generators increases or decreases in a symmetric Λ-shape, there are also transition cases between the two adjacent Λ-shapes where the the output of the thermal generators increases or decreases in a symmetric broken-Λ-shape. Figures 4.5 and 4.6 plot an example of a symmetric broken-Λ-shape for the generators "Th6" and "Th10" respectively.

Definition Let us denote the *active thermal generators* as generators that run away from the upper and lower capacity limits so that an increase or decrease in their output has a broken-Λ-shape. For an odd number of the thermal plants there always exists a pair of *matching active thermal generators*, one of which increases the output and the other decreases it.

Figure 4.4 plots an example of the solution with the broken-Λ-shapes; Figure 4.5 emphasizes this solution for the thermal generators running close to the upper capacity limit and Figure 4.6 - for the thermal generators running close to the lower capacity limit. Thermal generators "Th6" and "Th10" are matching ther-

mal generators and change the gradient of the Λ-shape at the same time intervals $t = 30$ and $t = 150$.
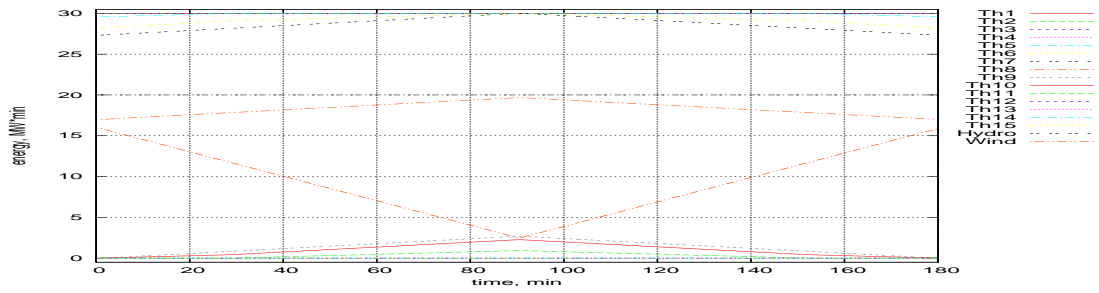

Figure 4.4: An example of the solution with the thermal plants increasing and decreasing their output in symmetric shapes
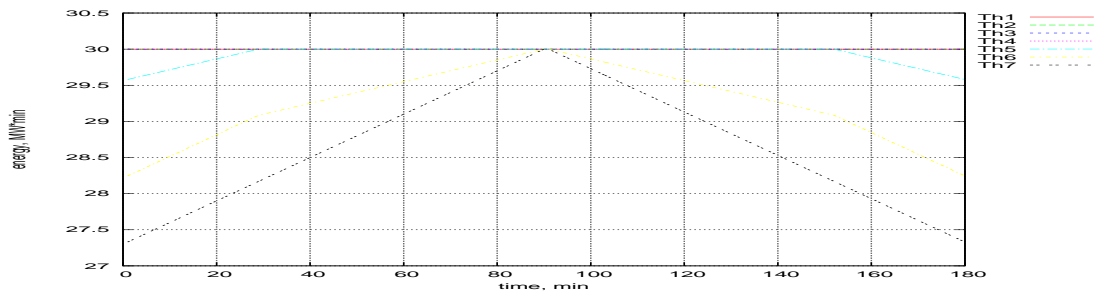

Figure 4.5: Seven cheapest thermal plants increasing and decreasing their output in symmetric shapes
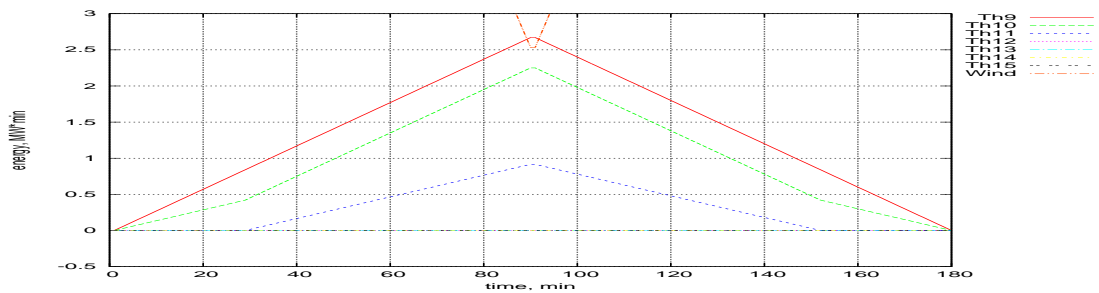

Figure 4.6: Seven most expensive thermal plants increasing and decreasing their output in symmetric shapes

A point in time t where a pair of two matching active thermal generators running at the maximum and minimum production levels modify a gradient of the Λ-shape is determined by a proportion between their fuel costs and the fuel cost of the marginal generator:

$$\frac{c_{m+i} - c_m}{c_{m+i} - c_{m-j}}$$

where c_{m+i} is the fuel cost of a thermal generator, higher than that of the fuel cost of the marginal generator, c_m, and c_{m-j} is the fuel cost of a matching thermal generator, lower than that of the marginal generator.

Using information on the shapes of the thermal generation, increase or decrease in the produced energy can be calculated as the volume of an isosceles triangle. Then, the accumulated fuel cost, F_A, for the planning horizon T can be estimated using Formula (4.4) below. In order to simplify visually further analysis, the right-hand side of Formula (4.4) is divided into three parts: $(I), (II)$ and (III).

$$F_A(\gamma_w, T) = F_0 - c_m \overline{x_w} + \tag{I}$$
$$c_m \gamma_w \frac{T}{4} + \tag{II}$$
$$\frac{\gamma^*}{T} \sum_{i=1}^{\kappa-1} \sum_{g \in C} \left((\Delta_g^{i+1} - \Delta_g^i) T c_m \frac{1 - s_g}{4} + ((\Delta_g^{i+1})^2 - (\Delta_g^i)^2) c_g \frac{s_g}{4} \right) \tag{III}$$

where

$$\Delta_g^i := \begin{cases} \frac{\tilde{c}_g^i - c_m}{\tilde{c}_g^i - c_g^i} T, & c_g < c_m \\ T, & c_g = c_m \\ T(1 - \frac{c_g^i - c_m}{c_g^i - \tilde{c}_g^i}) = \frac{c_m - \tilde{c}_g^i}{c_g^i - \tilde{c}_g^i} T, & c_g > c_m; \end{cases} \tag{4.4}$$

F_0, c_m and $\overline{x_w}$ are defined as in the previous model (4.2);

T denotes a planning horizon with one-minute discrete intervals;

c_g^i and $\tilde{c}_g^i$ are the fuel costs of the paired active thermal generators;

γ^* denotes the sum of the absolute values of the average gradient of the thermal generators $g \in C$ as in (4.3);

κ represents a number of thermal generators;

s_g is a parameter that equals 1 for the active generators $g \in C$ running at the minimum capacity, equals -1 for the active generators $g \in C$ running at the maximum capacity and equals 0 for the marginal generator.

The actual accumulated fuel cost F_A is significantly close to that calculated with the right-hand side of (4.4) and weighted by the planning horizon T with

respect to the gradient of a V-shaped drop of the wind energy curve. To find how close the LP-modelled and the calculated accumulated fuel costs are, we wish to estimate the marginal fuel cost for each of them.

Let us take a discrete interval of the absolute values of the gradient for the wind energy curve with a discretisation step j.

Definition Let us denote the *marginal fuel cost* as F_m. It is calculated as the difference between the accumulated fuel cost for the adjacent values of the absolute value of the gradient of the wind energy curve weighted by the difference in the height of the wind energy h_w.

Then, for every γ_w, the marginal fuel cost can be estimated by (4.5):

$$F_m = \frac{F_A(\gamma_w, T) - F_A^T(\gamma_w - j, T)}{h_w(\gamma_w) - h_w(\gamma_w - j)} \tag{4.5}$$

where $(\gamma_w - j)$ is the average of the absolute value of the gradients of the wind energy preceding the current value γ_w.

Proposition 4.3.1 *The marginal fuel cost does not depend on the planning horizon T and is constant for every transition case where the active thermal generators increase or decrease the output in the broken-Λ-shape.*

Proof Let us consider, first, a simple case where $\gamma_w \leq \overline{\gamma_g}$ for the planning horizon $t = 1, 2, \ldots, T$, i.e. the variability of the wind energy can be balanced with the marginal generator. We wish to calculate the marginal fuel cost by analysing parts $(I) - (III)$ of Formula 4.4. By construction of the case on the modification of a height of wind energy curve (introduced at the beginning of Section 4.3.1), the average wind energy $\overline{x_w}$ remains the same through the series of tests. Therefore, a part (I) of (4.4), calculated for $F_A(\gamma_w, T)$ and $F_A(\gamma_w - j, T)$ has the same value; part (I) of (4.4) is set to zero in the numerator of (4.5). A part (III) of (4.4) consists of the fuel costs for the active generators, however, there are no thermal plants deviating from the capacity limits when $\gamma_w \leq \overline{\gamma_g}$, thus, a part (III) of (4.4) equals zero for $F_A(\gamma_w, T)$ and $F_A(\gamma_w - j, T)$. As parts (I) and (III) are not used, the numerator of (4.6) is calculated as the difference in parts (II) of (4.4) for $F_A^T(\gamma_w)$ and $F_A^T(\gamma_w - j)$. Taking into account a V-shape of the wind energy, the marginal fuel cost F_m equals the fuel cost of the marginal generator:

$$F_m = \frac{c_m \gamma_w \frac{T}{4} - c_m(\gamma_w - j)\frac{T}{4}}{h_w(\gamma_w) - h_w(\gamma_w - j)} = \frac{c_m j \frac{T}{4}}{j \frac{T}{4}} = c_m \tag{4.6}$$

Next, we wish to look at the general case of (4.5), again by analysing parts $(I) - (III)$ of Formula (4.4). As for the simple case, a part (I) of (4.4), calculated for $F_A(\gamma_w, T)$ and $F_A(\gamma_w - j, T)$ has the same value, therefore, part (I) of (4.4) is set to zero in the numerator of (4.5). For every transition case pairs of the active generators are the same when calculating the accumulated fuel cost, thus, a part (III) of (4.4) calculated for $F_A^T(\gamma_w)$ and $F_A^T(\gamma_w - j)$ has the same value. Then applying the results of (4.6) the marginal fuel cost for a transition case can be calculated in the following way:

$$
F_m = c_m + \frac{\frac{\gamma^*}{T} \sum_{i=1}^{\kappa-1} \sum_{g \in C} \left((\Delta_g^{i+1} - \Delta_g^i) T c_m \frac{1-s_g}{4} + ((\Delta_g^{i+1})^2 - (\Delta_g^i)^2) c_g \frac{s_g}{4} \right)}{h_w(\gamma_w) - h_w(\gamma_w - j)}
$$

$$
- \frac{\frac{\gamma^* - j}{T} \sum_{i=1}^{\kappa-1} \sum_{g \in C} \left((\Delta_g^{i+1} - \Delta_g^i) T c_m \frac{1-s_g}{4} + ((\Delta_g^{i+1})^2 - (\Delta_g^i)^2) c_g \frac{s_g}{4} \right)}{h_w(\gamma_w) - h_w(\gamma_w - j)}
$$

$$
= c_m + \frac{\frac{j}{T} \sum_{i=1}^{\kappa-1} \sum_{g \in C} \left((\Delta_g^{i+1} - \Delta_g^i) T c_m \frac{1-s_g}{4} + ((\Delta_g^{i+1})^2 - (\Delta_g^i)^2) c_g \frac{s_g}{4} \right)}{j \frac{T}{4}}
$$

$$
= c_m + \frac{\sum_{i=1}^{\kappa-1} \sum_{g \in C} \left((\Delta_g^{i+1} - \Delta_g^i) T c_m (1 - s_g) + ((\Delta_g^{i+1})^2 - (\Delta_g^i)^2) c_g s_g \right)}{T^2}
$$

Using the definition for Δ_g^i in (4.4) the marginal operational cost is further calculated as

$$
F_m = c_m + \frac{\sum_{g \in C} \left((\frac{c_g^{i+1} - c_m}{c_g^{i+1} - \tilde{c}_g^{i+1}} T - \frac{c_g^i - c_m}{c_g^i - \tilde{c}_g^i} T) T c_m (1 - s_g) + ((\frac{c_m - \tilde{c}_g^{i+1}}{c_g^{i+1} - \tilde{c}_g^{i+1}} T)^2 - (\frac{c_m - \tilde{c}_g^i}{c_g^i - \tilde{c}_g^i} T)^2) c_g s_g \right)}{T^2}
$$

$$
= c_m + \sum_{g \in C} \left((\frac{c_g^{i+1} - c_m}{c_g^{i+1} - \tilde{c}_g^{i+1}} - \frac{c_g^i - c_m}{c_g^i - \tilde{c}_g^i}) c_m (1 - s_g) + ((\frac{c_m - \tilde{c}_g^{i+1}}{c_g^{i+1} - \tilde{c}_g^{i+1}})^2 - (\frac{c_m - \tilde{c}_g^i}{c_g^i - \tilde{c}_g^i})^2) c_g s_g \right)
$$

where $i = 1, 2, \ldots, (\kappa - 1)$. This shows that an additional unit of the calculated accumulated fuel cost depends only on the combination of the fuel costs of the thermal generators $g \in C$.

Figure 4.7 demonstrates that the marginal fuel cost is constant for every transition case where the active thermal generators increase or decrease the output in the broken-Λ-shape. A length of the interval where the marginal fuel cost is constant equals to the Maximum Run-Up and Run-Down Export Rates of the thermal plants, $r^+ = r^- = 0.125$ for our small electricity generation system. Notice, that for the first interval, $0 \leq \gamma_w \leq 0.125$, marginal fuel cost equals to the fuel cost of the marginal generator, $c_m = 1.7$.

The calculated marginal fuel cost acquires the same value as the LP-modelled, which is shown in Figure 4.7. This provides an insight into the next element of

the statistical model calculating the accumulated fuel cost that would reduce the error ϵ. We assume further in Section 4.3.2 that another element of the statistical model includes the height and the average of the absolute value of the gradient of the wind energy curve and test it through a series of cases.
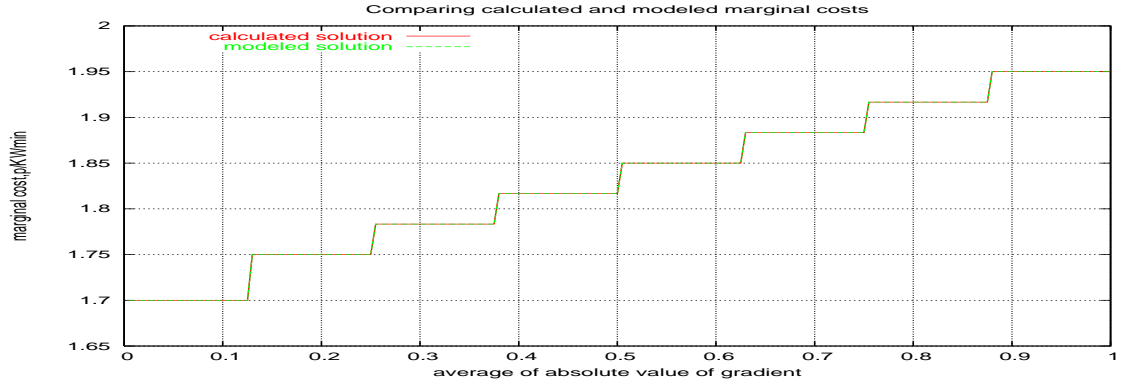
Figure 4.7: Comparing the calculated and the LP-modelled marginal fuel costs

4.3.2 Improving the estimation of the accumulated fuel cost

Analysis provided in the section 4.3.1 helps us improving the model (4.2) that evaluates the accumulated fuel cost of the electricity generation. Section 4.3.1 showed that the accumulated fuel cost depends on the absolute value of the gradient of the wind energy curve, hence, we wish to perform two tests with the wind energy curves having various profiles similar to the tests performed for the wind energy curve with a zigzag profile.

a. For a first test the average of the absolute value of gradients of the wind energy curve γ_w remains the same while the height and planning horizon T are modified linearly. This can be achieved by the scaling of the wind energy curve.

b. For another test the average of the absolute value of gradients of the wind energy curve γ_w and the height of the wind energy curve h_w are changing while the planning horizon T remains the same.

For the calculation later in this chapter we chose a set of 30 wind energy curves so that they provide a variety of the statistical parameters such as the mean, the absolute value of the gradient, the standard deviation and the height.

It was noticed that the height of the wind energy and the average of the absolute value of gradients are linearly dependent and a remaining error of the model (4.2) plotted against γ_w has a quadratic form. Figure 4.8 demonstrates the results of the tests a) and b) performed for the different values of h_w. In the test a) only the height of the wind energy drop changes while the average of the absolute value of the gradients remains constant. So the error ϵ in the model (4.2) is linear with respect to the changing height h_w. Test b) is more complex as two variables: the height and the average value of the absolute gradients of the wind energy curve are changing. Error ϵ can be plotted as quadratic function as long as the height and the absolute value of the gradient are modified linearly.
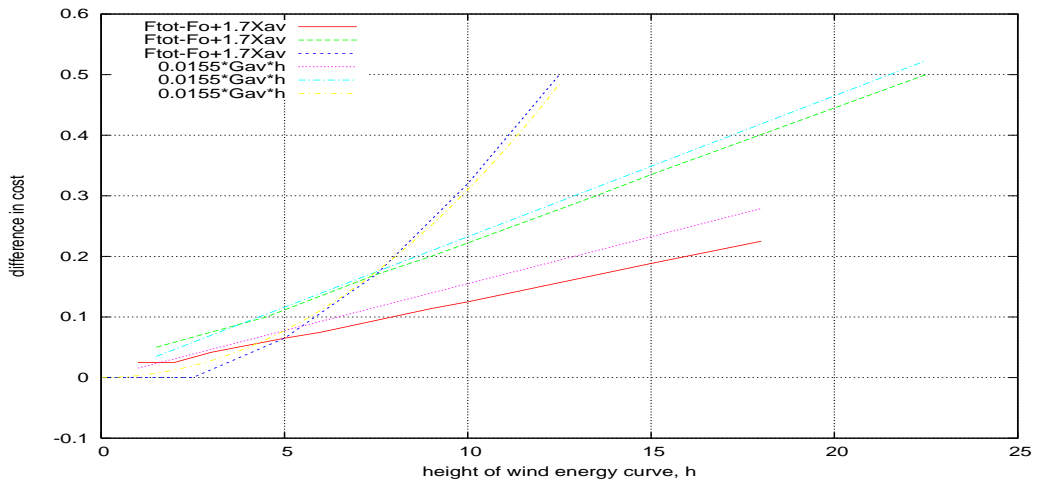
Figure 4.8: Fitting a quadratic term into the model that estimates the accumulated fuel cost of electricity generation

Tests a) and b) support a statement that an error in the model (4.2) depends on a quadratic term containing the average of the absolute value of gradients γ_w and the height of the wind energy curve h_w. In Figure 4.8 three functions from the below use the same quadratic $0.0155\overline{\gamma}_w h_w$ to approximate another term included in the model that estimates the accumulated fuel cost. Hence, an improved model estimating the accumulated fuel cost of the electricity generation is formulated further as (4.7).

$$F_A = F_0 - c_m \overline{x_w} + k_1 \overline{\gamma}_w h_w + \epsilon \qquad (4.7)$$

In (4.7) $k_1 \approx 0.0155$ is a parameter that can be estimated with the fuel costs of the thermal plants, it is independent of the wind energy curve.

Let us find how good the model (4.7) is for the estimation of the accumulated fuel cost of the electricity generation. Figure 4.10 plots the error term of the

model (4.2) and compares it to the quadratic term $0.0155\overline{\gamma_w}h_w$ calculated for a set of 30 wind energy curves.

Figure 4.9: Comparison of the error term for the LP-modelled and the calculated accumulated fuel cost with the model (4.2) for a set of 30 wind energy curves

Figure 4.9 shows that within a range of the wind energy curves with low variability (represented by a low $\overline{\gamma_w}$) the model (4.7) can be considered a good estimate of the accumulated fuel cost of the electricity generation. However, for the more variable wind energy we wish further to improve the model (4.7).

4.4 Case of the wind energy curve with changing standard deviation

Let us estimate the error term in the model (4.7) to decide on the elements that would improve it. We wish to calculate the error for two different cases: for all the planning horizon T and an accumulated error if calculated for the ten-minute intervals that a planning horizon T is divided into.

Figure 4.10 plots the error of estimating the accumulated fuel cost calculated for all the planning horizon T and an accumulated error calculated for $\frac{T}{10}$ intervals of the planning horizon. For both curves in Figure 4.10 the error is relatively high. However, an accumulated error for $\frac{T}{10}$ intervals of the planning horizon is convenient for further improvement as all the values are positive. An error calculated for all the planning horizon T has positive and negative values for the different wind energy curves so that it is hardly possible to improve the result.
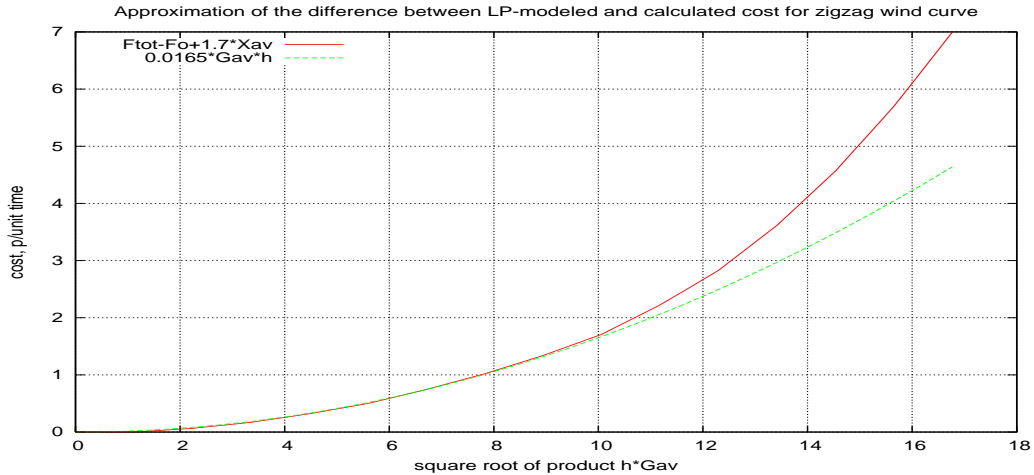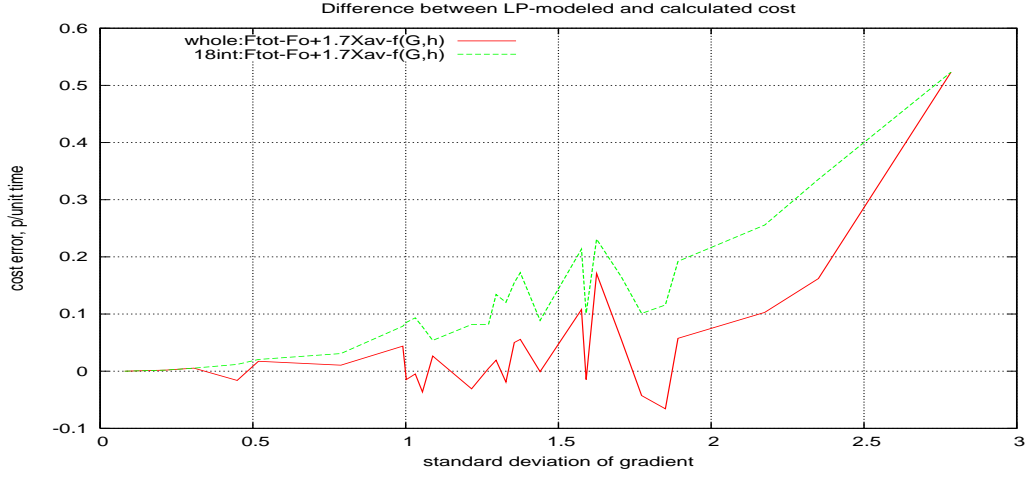
Figure 4.10: Comparison of the error term for the LP-modelled and the calculated accumulated fuel cost with the model (4.7) for a set of 30 wind energy curves

When plotted along the axis of the standard deviation of the absolute value of the gradient of the wind energy curve, an accumulated error for $\frac{T}{10}$ intervals of the planning horizon has a trend of a power function. Thus, we wish to use a standard deviation of the wind energy and a standard deviation of the absolute value of the gradients of the wind energy to formulate another element in the model estimating the accumulated fuel cost of the electricity generation. Again we are looking at two different ways of calculating both values of the standard deviation: over the whole planning horizon T and accumulated for $\frac{T}{10}$ intervals of the planning horizon T.

An improved model estimating the accumulated fuel cost of the electricity generation is formulated as follows:

$$F_A = F_0 - c_m \overline{x}_w + k_1 \overline{\gamma}_w h_w + k_2 \sigma_x \sigma_\gamma^\alpha + \epsilon \tag{4.8}$$

where σ_x denotes the standard deviation of the wind energy and σ_γ is the standard deviation of absolute value of gradient in a power $\alpha = 1.28$ for our case. Parameter k_2 equals 0.05 for our case.

Figure 4.11 plots a comparison of the error term in three models estimating the accumulated fuel cost of the electricity generation, (4.2), (4.7) and (4.8), calculated for a set of 30 wind energy curves. The figure shows that the error, found as the difference between the LP-modelled and the calculated accumulated fuel cost, decreases with the additional statistical parameters being added to the model. This is an expected result as the latter models are richer and include the

80

former when setting parameters $k_1 := 0$ and/or $k2 := 0$.
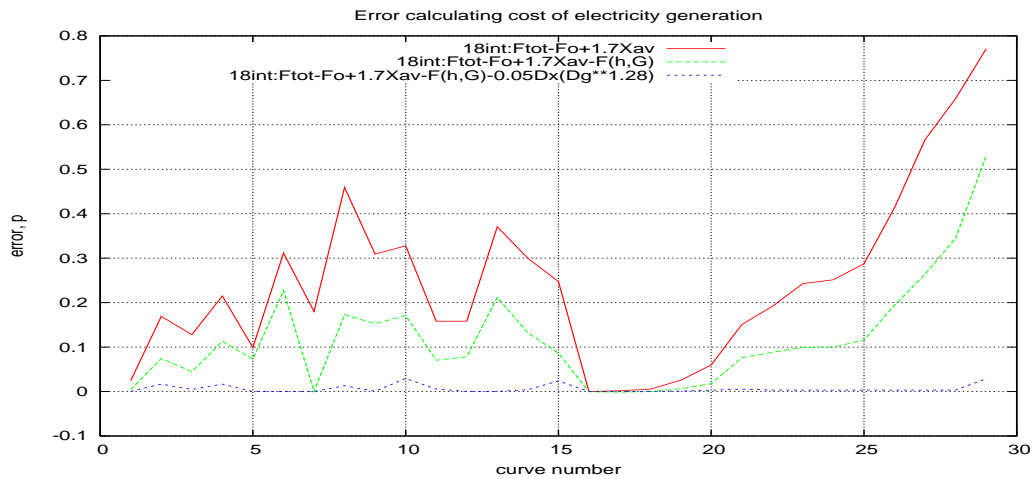
Figure 4.11: Comparing an error of calculating the accumulated fuel cost of the electricity generation with the models (4.2), (4.7) and (4.8)

A small error of estimating the accumulated fuel cost when calculated with the statistical model (4.8) shows that the saving in fuel cost and the additional fuel cost (introduced in Section 3.3.1 and Section 3.3.2) are determined by the statistical parameters of the wind energy curve. When wind energy is incorporated into the electricity generation system, the accumulated fuel cost is reduced by the amount of wind energy present in the system, however, one-minute fluctuations of the wind speed, described by the absolute value of gradients and the standard deviation, cause an increase in the accumulated fuel cost.

Chapter 5

Stochastic Modelling

Chapters 3 and 4 use deterministic modelling for scheduling the electricity generation assuming the electricity load is known and all the generating units are strictly following the operating plan. However, this is a strong assumption in real-life situations, so this chapter introduces an uncertainty of the electricity generation. We wish to use stochastic programming as a method of structuring possible future scenarios and estimating the system balancing cost that appears when wind energy is not forecast for certain.

The System Operator of the United Kingdom balances the electricity generation and consumption in the power system every moment of the real time and is responsible for keeping the system frequency within a target range. In order to cope with an unexpected mismatch between the electricity supply and demand the System Operator uses the available Response and Reserve provided by the generators. As it was specified in Chapter 1, Response and Reserve are being used on different time scales. Response is an automatic process provided by the large generating plants that keeps the power system within the target frequency in a time range from 0 seconds to several minutes. By that time operating Reserve is expected to increase or decrease the output and support the power system in minutes or hours.

Response is an automatic process provided by the generators while a decision about the amount of operating Reserve is made by the System Operator and depends on possible losses or fluctuations of the load that can happen in the future. For example, 1GW of Reserve means that some generators run away from their maximum export limits so that they can increase the power output by 1GW if required by the System Operator. The aim of the stochastic programming is to formulate an operating plan that keeps feasible possible scenarios of wind energy output and minimizes the system balancing cost.

The stochastic optimization model is formulated using the deterministic model introduced in Chapter 3 and includes common constraints of the electricity generation. Our original contribution consists in developing a scenario tree that reflects two uncertainties: uncertainty in the available capacity of the thermal plants and uncertainty in wind energy output. We use the formulated stochastic optimization model to achieve the aim of this thesis by calculating the system balancing cost when unpredictable wind energy is introduced into the electricity generation system.

5.1 Uncertainty of the wind energy

A motivation to model the uncertainty of the wind energy comes from the fact that wind speed is hard to forecast. Mathematical techniques of forecasting an average wind speed for the next hour or half an hour have improved significantly during last 30 years ([36, 37, 38, 39, 40]), however, one minute variations as well as sub-hourly capacity of wind energy are still calculated with possible errors. Until the short-term prediction of the wind speed is further improved, the available wind energy creates an additional uncertainty in the electricity generation system. Currently the installed wind capacity does not exceed 4% of the total electricity generation, so that the matter of wind speed low predictability can be resolved without an increase in the operating Reserve. However, if the wind energy production amounts to 15% and higher, as it is planned by the Renewables Obligation, then the system balancing cost would significantly increase.

Assuming the uncertainty of the wind energy output, planning the electricity generation can be described as a sequence of random realisations and decisions of the System Operator on the modification of the operating plan for the thermal plants. In its simplest form the discrete stochastic process can be represented as a scenario tree describing the unfolding of uncertainty over the planning horizon [28].

A scenario tree consists of nodes and arcs as in the example pictured in Figure 5.1. For our case the **nodes** represent the states when the information about the wind energy output is revealed and the operating plan of the thermal generators is determined to match the electricity load. The **arcs** do not have a physical meaning and are used to structure the nodes and form possible scenarios. For every two nodes connected by an arc the preceding node is named a **parent** and the following node is named a **child**. The current state is taken as the first node of every scenario, it is named the **root** of the tree while the last node of a scenario

is named a **leaf**. A path, from the root to a leaf of the scenario tree, represents a **scenario**. Thus, node 1 on Figure 5.1 is parent of three nodes-children, $2, 3$ and 4, while node 2 is parent of only two nodes, 5 and 6 that are considered leaves as they do not have any children. An example of a scenario is the set of nodes $\{1, 3, 7\}$.
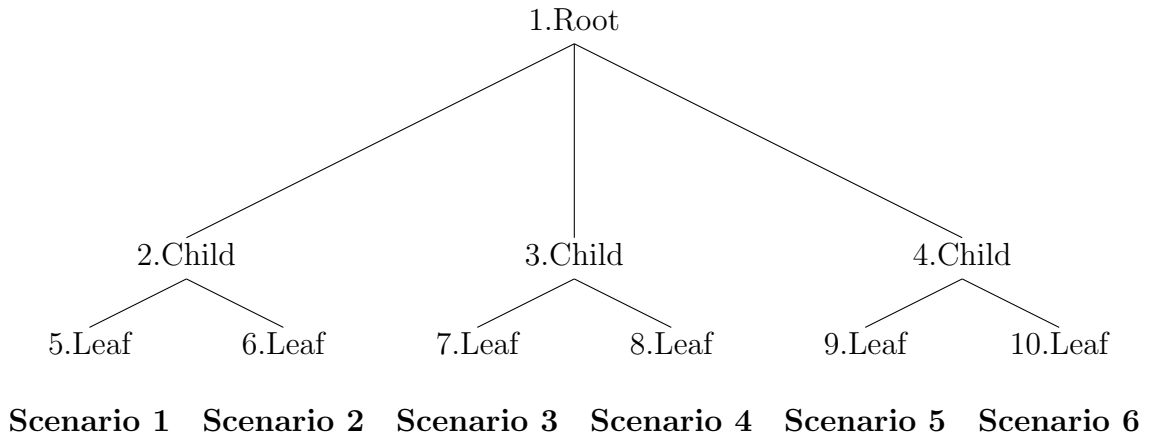
Figure 5.1: An example of a scenario tree

It is important to capture the nonanticipativity property with the structure of the scenario tree. Nonanticipativity property can be explained in the following way. At each state the System Operator makes a decision about the operating Reserve under the uncertainty of the future realisations of the wind energy. This uncertainty is gradually reduced, since the decision process is being accompanied by a flow of information, however, at the moment of making a decision, the System Operator does not have a preference for any of the scenarios so that the decision is nonanticipative [34]. For example, node 1 of the tree presented in Figure 5.1 corresponds to the first stage, and the associated decisions at this node are identical for all six scenarios.

Let us specify further the parameters of the scenario tree. The System Operator balances the electricity generation and demand every moment of the time, however, in Chapter 3 we used the discrete time with the smallest interval of 1 minute. The aim of the modelling is to schedule the operating Reserve of gas and coal plants whose production level can not be modified too frequently. At the same time, the Reserve has to respond to the changes in the electricity load as soon as possible, hence one minute is considered the most appropriate frequency for short-term scheduling. We wish to use the discrete time further for the stochastic programming as well, and incorporate it in the scenario tree so that a decision about the electricity generation is made every other minute. A

length of the Settlement Period (as it was defined in Chapter 1) is 30 minutes. Denote further a length of the **modelling horizon** as T^S, and for the current problem $T^S = 30$.

Let us define an **event** as an output of the available wind farms in MW every minute $t = 1, 2, \ldots, T$ where $T \geq T^S$ is a certain **planning horizon**. Assume that wind speed and, therefore, the wind energy output are known at the current state $t = 1$ when decision about the generating plan for the conventional plants is made. It is unknown whether at the minute $t + 1, t + 2, \ldots, T^S$ the wind speed remains as it was forecast or a wind speed profile deviates from the forecast or shifts in time. This means that a number of possible scenarios for the wind energy profile can be significantly large.

Assume further multistage stochastic programming so that the wind energy branches several times during the modelling horizon T^S. Let us branch the scenario tree every 10 minutes so that there are 4 stages in this multistage stochastic program. Accumulated length of all the stages equals the length of the modelling interval T^S so that for every stage $s \in S := \{1, 2, 3, 4\}$ we set:

$$T^1 = 1, T^2 = 9, T^3 = 10, T^4 = 10 : \qquad \sum_{s=1}^{4} T^s = T^S = 30$$

Branching the scenario tree every 10 minutes reflects the uncertainty of the wind energy and keeps a limit on the number of nodes that can grow dramatically when branching the scenario tree every minute of the modelling time period.
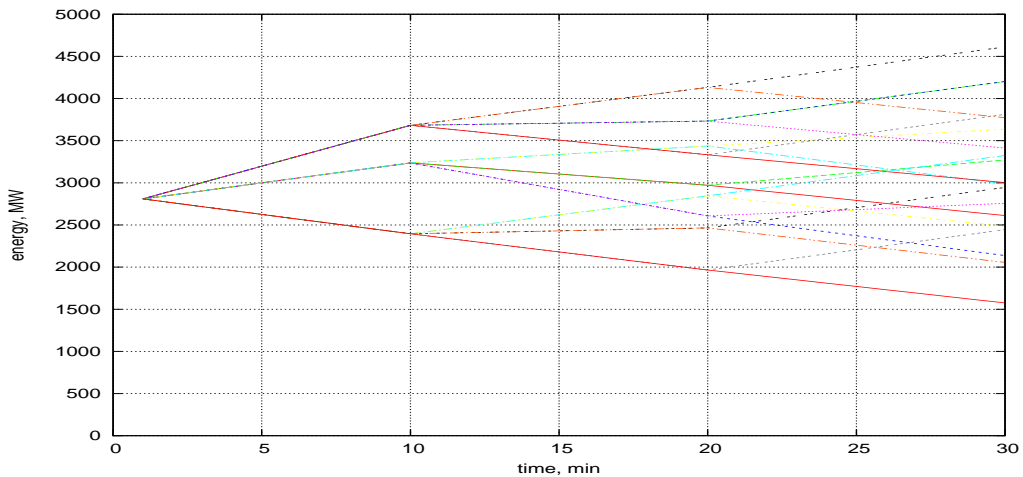

Figure 5.2: Tree of scenarios that represent possible changes in wind speed

Branching of the scenario tree is an individual process and depends on the characteristics of the underlying events. Although variability and capacity of the wind energy turbines depend on the geographical and weather characteristics of the site, we wish to outline further some general directives for building a scenario tree for the wind energy output. Assume there are four main elements of the available wind energy taken into account when building a scenario tree, namely:

1. the current output from the wind energy turbines;

2. an average wind energy predicted for the next hour;

3. a heuristic distribution of the wind energy; and

4. the preceding values of the wind energy;

The transformation function that allows us calculating the wind power from the wind speed, provides a useful information for building a scenario tree. Figure 2.1 plots a typical transformation function and shows that the wind energy output has upper as well as lower bounds. Besides, when the wind speed exceeds 15m/s the power output flattens at the maximum capacity. Hence, we wish to build a scenario tree of the wind power rather than the wind speed as it can reduce a number of nodes in the tree and increase the speed of solving a problem.

We wish a scenario tree to capture the unpredictable nature of the wind power, however, it does not reflect the variability of the wind power that was estimated in Chapter 3. Every possible scenario of the wind power output is a piecewise linear function so that the slope of a linear segment of this function remains the same for every node.

When calculating the probability distribution of the wind power, bullet points 3 and 4 of the above list can be combined so that the distribution of the wind energy output is conditional to the preceding values.

$$P(w_{t+1}^e) = P(w_{t+1}^e | w_t^e, w_{t-1}^e) \tag{5.1}$$

The conditional probability distribution (5.1) provides the information on the variability of the wind power from a given value w_t^e. While building a scenario tree we consider three ways of branching, such as two extreme outcomes; two extreme outcomes balanced by the mean wind power; and five or more branches.

- **two extreme outcomes**. In this case a wind power value of the parent node branches into two child nodes so that two new nodes are represented

86

by the highest positive and negative deviation of the wind power from the current value:

$$w_{t+1}^{e+} : max(w_{t+1}^e - w_t^e) \text{ and } w_{t+1}^{e-} : min(w_{t+1}^e - w_t^e) \qquad (5.2)$$

where w_{t+1}^e is found with the probability distribution (5.1).

The probability for each of the two child nodes is calculated so that the stochastic process of the wind power output is preserved. In the case of two nodes it requires the expectation of the probability distribution (5.1) to remain the same. If w_{t+1}^{e+} and w_{t+1}^{e-} are new child nodes acquired by respectively the highest positive and negative deviation of the wind power then the probability of their outcome can be calculated as follows:

$$p(w_{t+1}^{e-}) = \frac{w_{t+1}^{e+} - \overline{w_{t+1}^e}}{w_{t+1}^{e+} - w_{t+1}^{e-}}$$

$$p(w_{t+1}^{e+}) = 1 - p(w_{t+1}^{e-})$$

where $\overline{w_{t+1}^e}$ is the expected value of the conditional probability distribution (5.1).

- **two extreme outcomes balanced by the mean wind power**. In this case a wind power value of the parent node branches into three child nodes two of which are represented by the highest positive and negative deviation of the wind power from the current value (as in (5.2)) and the third child node is the expected value of the conditional distribution (5.1).

The probability for each of the three child nodes is calculated so that the stochastic process of the wind power output is preserved. In the case of three nodes it requires that the expectation and the variance of the probability distribution (5.1) remain the same. If σ_{t+1}^w denotes the variance of the probability distribution (5.1) then the probability of the outcomes w_{t+1}^{e+}, w_{t+1}^{e-} and $\overline{w_{t+1}^e}$ are as follows:

$$p(w_{t+1}^{e+}) \qquad = \frac{\sigma_{t+1}^w}{(w_{t+1}^{e+} - \overline{w_{t+1}^e})^2 - (w_{t+1}^{e+} - \overline{w_{t+1}^e})(w_{t+1}^{e-} - \overline{w_{t+1}^e})}$$

$$p(w_{t+1}^{e-}) \qquad = \frac{\sigma_{t+1}^w}{(w_{t+1}^{e-} - \overline{w_{t+1}^e})^2 - (w_{t+1}^{e+} - \overline{w_{t+1}^e})(w_{t+1}^{e-} - \overline{w_{t+1}^e})}$$

$$p(\overline{w_{t+1}^e}) \qquad = 1 - p(w_{t+1}^{e+}) - p(w_{t+1}^{e-})$$

- **five or more branches**. In this case a wind power value of the parent node

branches into five or more child nodes two of which are represented by the highest positive and negative deviation of the wind power from the current value (as in (5.2)) and the remaining possible outcomes are the mean values of the equally spaced segments.

A scenario tree can be built by combining different branching methods. For example, a scenario tree in Figure 5.2 was built with the combination of $(T^1 : T^2 : T^3 : T^4) := (1 : 5 : 3 : 2)$. This combination means that at stage $s = 1$ there is only one node that branches into 5 nodes at stage $s = 2$. Each of these 5 nodes branches into 3 nodes resulting in 15 nodes at stage $s = 3$, each of which branches further into 2 nodes resulting in 30 nodes at stage $s = 4$.

We tested different combinations of branching methods for building a four-stage scenario tree by finding a solution of the stochastic linear optimization model, described further in Section 5.3.1. All the branching methods result in a feasible solution, hence, we determined the best branching combination with the accumulated fuel cost over the planning horizon of 5 days. Table 5.1 compares the accumulated fuel cost weighted by the generated power and calculated for different branching methods.

Table 5.1: Accumulated fuel cost weighted by the generated power and calculated for different branching combinations, £/(MW*day)

$(T^1 : T^2 : T^3 : T^4)$	day 1	day 2	day 3	day 4	day 5	total
$(1 : 2 : 2 : 2)$	15.28	17.43	16.10	16.81	17.71	83.33
$(1 : 3 : 2 : 2)$	14.21	15.12	14.55	14.85	15.17	73.90
$(1 : 3 : 3 : 2)$	13.44	14.36	13.72	13.88	14.43	69.83
$(1 : 3 : 3 : 3)$	12.66	13.13	12.87	12.36	12.98	64.00
$(1 : 5 : 2 : 2)$	11.67	11.95	11.20	11.77	12.03	58.62
$(1 : 5 : 3 : 2)$	11.12	11.51	10.82	10.96	11.84	56.25
$(1 : 5 : 5 : 2)$	11.56	12.07	11.15	11.65	12.16	58.59

Table 5.1 shows that the accumulated fuel cost calculated for the branching combination $(1 : 5 : 3 : 2)$ is the lowest, therefore, we wish to use this branching method further in this chapter for the stochastic optimization modelling. Figure 5.2 plots an example of scenario tree where every scenario represents a possible output of the wind turbines. This scenario tree is used to solve a single stochastic programming problem of scheduling the electricity generation at the current minute t of the planning horizon $1, 2, \ldots, T$ such that the resulting generation prepares the system for a variety of wind power outcomes. After the solution is obtained, the electricity generation of the root of the scenario tree is fixed at its optimal value that establishes the final schedule for this minute of the time

horizon.

For the next minute $t = 1, 2, \ldots, T$ the modelling horizon $1, 2, \ldots, T^S$ is rolled forward in time and a new scenario tree is built based on a new value of the wind power w_t^e. The next stochastic programming problem is solved using a new scenario tree and the optimal electricity generation for the root is fixed for the current minute t. This process of the **rolling modelling horizon** is repeated so that the optimal values obtained from each iteration yield the final solution for every minute of the planning time horizon $1, 2, \ldots, (T - T^S)$.

5.2   Uncertainty of lost generating capacity

Another uncertainty that the System Operator of the United Kingdom has to take into account while balancing the electricity demand and generation involves a loss of the generating capacity. An example of an event captured by this uncertainty could be a conventional plant tripped and taken out of service. A probability of such an event is low, however it can happen at any moment and effect the target frequency with a significant mismatch between the electricity supply and demand.

As it was specified in Chapter 1, the System Operator can use the automatic Response and the planned operating Reserve to increase or decrease an active power in the system and preserve the integrity of the GB Transmission System. An impact of the generating capacity loss on the power system increases when there is also the uncertainty of the wind energy output taken into consideration. Therefore, we wish to build a scenario tree that describes a possible loss of the capacity and estimate the system balancing cost when resolving both uncertainties by the System operator, loss of the generating capacity and the wind energy output.

A scenario tree that captures a possible loss of the capacity is built so that it is compatible with the wind power scenario tree. Every **node** represents a state when the information about the available capacity of the conventional plants enters the system and the System Operator determines whether their operating plan should be modified. The **arcs** connect the nodes forming a path from the root to the leaves of the scenario tree. Modelling time horizon T^S is discretized for the scenario tree of the possible capacity loss and, similar to the wind power scenario tree, equals 30 minutes.

In order to introduce a possible capacity loss of any type of conventional plant in one scenario tree, we define an **event** as a size of the electricity load

in MW every minute $t = 1, 2, \ldots, T^S$. The fact that the electricity demand is a deterministic value in this work allows us interpreting a loss of the capacity as an increase in the electricity load. Assume that the available generating capacity and, therefore, the electricity load are known at the current state $t = 1$ when a decision is made whether to modify an operating plan of the conventional plants or not. It is unknown whether the onstream generating capacity is available at minutes $t + 1, t + 2, \ldots, T^S$ or there is an importing or exporting capacity lost. On the event tree it can be pictured as a linear change in the forecast demand for a minute $t + 1, t + 2, \ldots, T^S$ comparing to the previous state. Figure 5.3 plots a scenario tree of the electricity load values where every minute there is an expected loss of the exporting or importing capacity. Every scenario suggests a loss of 600MW in the generating capacity and a loss of 100MW in the importing capacity at a certain minute t.
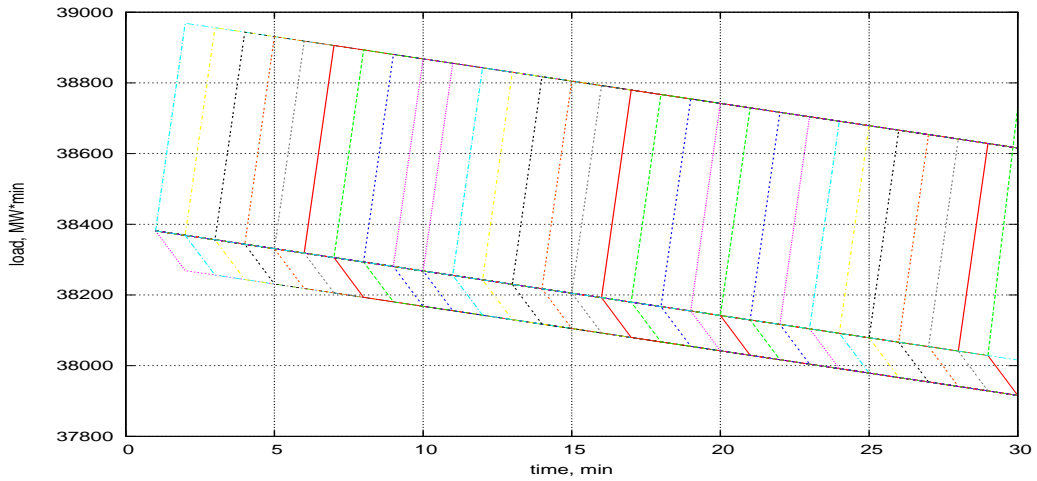
Figure 5.3: A scenario tree of the changes in the electricity load equivalent to the loss of the capacity

A scenario tree plotted on Figure 5.3 presents three possible outcomes every minute t of the modelling horizon $2, 3, \ldots, T^S$: all the planned generating capacity is available; there is a loss of the generating capacity; there is a loss of the importing capacity. For every scenario we assume that once the capacity is lost, the remaining generating units are available until the end of the modelling horizon T^S.

We wish to capture the expectation of a loss in the generating capacity every minute of the modelling horizon. In this case, however, the number of stages when a new information becomes available is $T^S - 1$, which is higher than that for the

scenario tree of the changes in the wind power where $S = 4$. In order to formulate a mathematical model for both uncertainties, a loss of the generating capacity and the change in the wind power, we assume there are four stages in the scenario tree of the changes in the electricity load rather than T^S. This assumption leads to the situations where parent and child belong to the same stage, they are formulated in the next section so that the nonanticipativity property is preserved.

The optimal solution at the root of the scenario tree ensures that the electricity generating system is prepared for a capacity loss at any minute t of the modelling horizon. This solution is fixed and the modelling horizon is rolled forward so that the optimal solution can be found for the next minute $t = 1, 2, \ldots, T$. The optimal solution for the root of the scenario tree which is now a new minute t, is fixed again. The **rolling horizon** method is applied until the optimal solution is found for every minute t of the planning horizon $1, 2, \ldots, (T - T^S)$.

5.3 Solving a problem with the uncertainty

The uncertainties presented in sections 5.1 and 5.2 are formulated in the stochastic programming problem later in this section. The output of a number of tests performed with the stochastic model result in the estimate of the system balancing cost when the wind power and the available capacity are uncertain.

5.3.1 Decision variables and constraints of the LP stochastic optimization model

To formulate the deterministic equivalent of the multistage stochastic programming problem, let us combine the wind power and the electricity load scenario trees described in sections 5.1 and 5.2, and enumerate all nodes of the combined scenario tree. We use a breadth-first search order [28], i.e. start from a root node corresponding to the first stage.

Definition Let n denote a *node* of the scenario tree and a_n denote the direct *ancestor* of a node n to capture the dynamics in the stochastic optimization model.

The root of the scenario tree has index $n = 1$, so the stage 2 nodes start from index 2. The numbers of children for each node in the event tree may differ, as they depend on a probability distribution of the appropriate stochastic process and a choice of the branching. However, the "parent-child" structure of the scenario tree preserves the nonanticipativity property of the stochastic problem.

Let N denote the last node at the stage 4 so that each scenario goes through a certain number of nodes $n \in \{1, 2, \ldots, N\}$. A number of time intervals associated with every node n is denoted by $T_n > 0$. For the root node, a number of intervals $T_1 = 1$ shows that there is only the current minute information available at the moment of the decision making. Depending on a choice of the branching method (as described in Section 5.1) nodes of the scenario tree can be grouped by stages of the scenario tree. Then, for the scenario tree that captures the uncertainty of the wind power output, T_n equals a length of the stage s corresponding to node n. However, the scenario tree of the changes in the electricity load branches every minute, so a number of intervals T_n for a node n of this tree varies depending on a minute when the generating capacity is lost, and ancestor a_n sometimes corresponds to the same stage as node n.

Definition Let the index τ denote *a minute of node n*, such that $\tau = 0, 1, \ldots, T_n$. If a certain event describes a loss of the generating capacity at time $\tau = \tau^* < T^s$ of node a_n then $T_{a_n} = \tau^*$ and $T_n = T^s - \tau^*$, where s is a stage of node a_n.

Let G denote the set of all the generators and consist of the union of C, the set of the conventional generators, with W, the set of the wind generators. The set of the conventional generators also consists of Coal, Nuclear and Gas generating plants. The decision variables in the model correspond to the output of each generating unit in the power system. The decision variables are denoted by

$$x_{n\tau g} \quad \forall n = 1, 2, \ldots, N, \tau = 0, 1, \ldots, T_n, g \in C \tag{5.3}$$

where $x_{n\tau g}$ is a production level of the thermal unit g during time interval τ of node n. The wind power generation is determined by the wind power scenario tree.

$$x_{n\tau g} = w_{n\tau g} \quad \forall n = 1, 2, \ldots, N, \tau = 1, 2, \ldots, T_n, g \in W \tag{5.4}$$

There are two groups of constraints that can be formulated for the stochastic model: the constraints applied to every node $n = 1, 2, \ldots, N$ and the constraints that reflect the stochastic properties of the model. First let us formulate the constraints that connect the nodes into the scenarios and show the "parent-child" relationship between the nodes.

$$x_{n0g} = x_{a_n T_n g} \quad \forall n = 2, 3, \ldots, N, g \in G \tag{5.5}$$

These inter-nodal constraints state that for every generator g the first value of an output in a node n has to be the same as the last value of its ancestor a_n. The

first value of a node n is described with an index 0, it is fixed by the ancestor while decisions are made beginning with $\tau = 1$. The last value of a node n is determined by an index T_n.

Further there are constraints that are applied to every node n, they are equivalent to the constraints formulated for the deterministic model in Chapter 3. Planning the production level of the electricity generation units is bounded by the available resources and technology. Decision variables introduced above have finite upper and lower bounds representing unit capacity limits of the generation system.

$$\underline{x_g} \leq x_{n\tau g} \leq \overline{x_g} \quad \forall n = 1, 2, \ldots, N, \tau = 1, 2, \ldots, T_n, g \in C \qquad (5.6)$$

The parameters $\underline{x_g}$ and $\overline{x_g}$ denote the lowest and the highest possible output of unit g respectively.

Further, Run-Up and the Run-Down constraints also applied to the thermal generation. Following the notation of Chapter 3, let r^{1+} and r^{2+} denote two Run-Up rates separated by the "elbow" output level e^+ and r^{1-} and r^{2-} denote two Run-Down rates separated by the "elbow" e^- output level. Then the corresponding constraints of the possible change in the output of the thermal plants are formulated as the inequalities:

$$x_{n(\tau+1)g} \leq \frac{e^+ + r^{2+} - r^{1+}}{e^+} x_{n\tau g} + r^{1+} \qquad (5.7)$$

$$x_{n(\tau+1)g} \leq x_{n\tau g} + r^{2+} \qquad (5.8)$$

and

$$x_{n(\tau+1)g} \geq \frac{\overline{x_g} - e^- + r^{2-} - r^{1-}}{\overline{x_g} - e^-} x_{n\tau g} - \frac{r^{2-}\overline{x_g} - r^{1-}e^-}{\overline{x_g} - e^-} \qquad (5.9)$$

$$x_{n(\tau+1)g} \geq x_{n\tau g} - r^{2-} \qquad (5.10)$$

where $n = 1, 2, \ldots, N, \tau = 0, 1, \ldots, T_n, g \in C$.

The loading constraint combines different generating units and applied for every node separately. Denoting by $D_{n\tau}$ the load demand during interval τ of node n and by Δ_D a percent mismatch allowed between the electricity load and the generation, the loading constraint is formulated with the inequalities:

$$D_{n\tau}(1 - \Delta_D) \leq \sum_{g \in G} x_{n\tau g} \leq D_{n\tau}(1 + \Delta_D) \qquad (5.11)$$

where $n = 1, 2, \ldots, N, \tau = 1, 2, \ldots, T_n$.

Similarly to the case of the deterministic problem, the minimization of the accumulated fuel cost affects the stochastic solution by setting the generation of the thermal units close to the lower bound of the allowed mismatch between the electricity generation and the demand $D_{\tau n}(1 - \Delta_D)$. This fact increases the risk of operating at a frequency below the target level. To avoid this we reintroduce a cost of mismatch between the electricity demand and the generation $\{\zeta_v^+; \zeta_v^-\}$ as it was described in Chapter 3.

Let us introduce further another set of variables:

$$\{d_{n\tau v}^+, d_{n\tau v}^-\} \tag{5.12}$$

where $n = 1, 2, \ldots, N, \tau = 1, 2, \ldots, T_n, v = 1, 2, \ldots, V$. These variables denote the difference between the electricity demand and the generation formulated in the following way:

$$\sum_{g \in G} x_{n\tau g} - D_{n\tau} = \sum_{v=1}^{V} (d_{n\tau v}^+ - d_{n\tau v}^-) \tag{5.13}$$

where $n = 1, 2, \ldots, N, \tau = 1, 2, \ldots, T_n$ and V is a number of the penalty cost bands in the allowed mismatch between the electricity demand and the generation $[(1 - \Delta_d)D_{n\tau}; (1 + \Delta_d)D_{n\tau}]$.

The size of every penalty cost band $v = 1, 2, \ldots, V$ is formulated with the inequalities:

$$0 \leq d_{n\tau v}^+ \leq \overline{d_{n\tau v}^+} \tag{5.14}$$

$$0 \leq d_{n\tau v}^- \leq \overline{d_{n\tau v}^-} \tag{5.15}$$

where $\overline{d_{n\tau v}^+}$ is an upper bound of the band v when the generation exceeds the electricity demand and $\overline{d_{n\tau v}^-}$ is an upper bound of the band v when the electricity demand exceeds the generation.

The set of parameters $[\overline{d_{n\tau v}^+}, \overline{d_{n\tau v}^-}]$ depends on the scenario tree of the electricity load and can be calculated in the following way

$$\overline{d_{n\tau v}^+} = \Delta_d * D_{n\tau} * \beta_v^+ \tag{5.16}$$

$$\overline{d_{n\tau v}^-} = \Delta_d * D_{n\tau} * \beta_v^- \tag{5.17}$$

where $\beta_v^{\pm}$ is the part of the allowed mismatch between the electricity demand and the generation $\Delta_d * D_{n\tau}$ that corresponds to the penalty band $v = 1, 2, \ldots, V$.

As distinct from the deterministic case there are four penalty cost bands for the stochastic programming problems. Because of the uncertainty that the System Operator has to deal with, the amount of the wind power in the electricity generation system that produced a feasible solution for the deterministic problem maybe give an infeasible result for the stochastic model. First, three penalty cost bands are associated with the costs $\{\zeta_v^+; \zeta_v^-\}$ and the size $\{\overline{d_{n\tau v}^+}; \overline{d_{n\tau v}^-}\}$ as in the deterministic case. The fourth price band has a very high cost and big enough size associated with it so that the variables $(d_{n\tau 4}^+; d_{n\tau 4}^-)$ are nonzero only in the exceptional cases where there is no other way to avoid infeasible solution.

The objective of the stochastic problem is to find a feasible solution $\{x_{n\tau g}\}$ such that it satisfies all the constraints $(5.2) - (5.17)$ at the minimal operational cost, i.e.:

$$\min_x \sum_{n=1}^{N} p_n \Big(\sum_{g \in C} c_g \sum_{\tau=1}^{T_n} x_{n\tau g} + \sum_{v=1}^{V} \zeta_v^+ \sum_{\tau=1}^{T_n} d_{n\tau v}^+ + \sum_{v=1}^{V} \zeta_v^- \sum_{\tau=1}^{T_n} d_{n\tau v}^- \Big) \qquad (5.18)$$

In the objective function (5.18) the operational cost is calculated for every node n and includes the fuel cost $\sum_{g \in C} c_g \sum_{\tau=1}^{T_n} x_{n\tau g}$ and the cost of a mismatch between the electricity generation and the load $\sum_{v=1}^{V} \zeta_v^+ \sum_{\tau=1}^{T_n} d_{n\tau v}^+ + \sum_{v=1}^{V} \zeta_v^- \sum_{\tau=1}^{T_n} d_{n\tau v}^-$. It is uncertain if a node $n = 1, 2, \ldots, N$ will realise in the future, however, there is a probability p_n associated with node n. The probabilities in the objective function are not those that were formulated for the scenario tree but **path probabilities**

$$p_n = P(n) * P(a_n) * P(a_{a_n}) * \cdots * P(1)$$

where $P(n)$ is a probability formulated for a node n in the scenario tree. This probability is multiplied by the probabilities of its ancestors to get the path probability p_n. Therefore, the objective function (5.18) estimates the **expected operational cost** of the electricity generation.

The stochastic LP optimization model formulated in this section includes two sets of variables $\{x_{n\tau g}\}$ and $\{d_{n\tau v}\}$, where $g \in C$, $v = 1, 2, \ldots, V$ $n = 1, 2, \ldots, N$ and , $\tau = 1, 2, \ldots, T_n$. We take κ again as a number of thermal generators in the set C so that a total number of decision variables in the model equals $\kappa \sum_{n=1}^{N} T_n + V \sum_{n=1}^{N} T_n$. Similarly to the case of the deterministic optimization model, we wish to reduce a number of variables by grouping thermal generators: one nuclear, one gas and one coal generators in the set C. Number of nodes N in the stochastic optimization problem depends on a chosen scenario tree. For the problem formulated in this section we combine two scenario trees plotted in

Figure 5.2 and Figure 5.3. The aggregated tree results in $N = 1000$ nodes. Then, taking $V = 6$ there are $72,882$ decision variables in the stochastic optimization problem for a single t of the rolling horizon $1, 2, \ldots, T$. We assume again one accumulated wind energy curve in the set of wind generators, thus, number of constraints result in $344,112$ for a single t of the rolling horizon $1, 2, \ldots, T$.

5.3.2 Formulation of the LP stochastic optimization model

The constraints and the objective function described in Section 5.3.1 are combined below:

Objective (minimize cost):

$$\min_{x} \sum_{n=1}^{N} p_n \left(\sum_{g \in C} c_g \sum_{\tau=1}^{T_n} x_{n\tau g} + \sum_{v=1}^{V} \zeta_v^+ \sum_{\tau=1}^{T_n} d_{n\tau v}^+ + \sum_{v=1}^{V} \zeta_v^- \sum_{\tau=1}^{T_n} d_{n\tau v}^- \right)$$

Subject to:

$$x_{n\tau g} = w_{n\tau g} \quad \forall g \in W$$

$$\underline{x_g} \leq x_{n\tau g} \leq \overline{x_g} \quad \forall g \in C$$

$$x_{n(\tau+1)g} \leq \frac{e^+ + r^{2+} - r^{1+}}{e^+} x_{n\tau g} + r^{1+} \quad \forall g \in C$$

$$x_{n(\tau+1)g} \leq x_{n\tau g} + r^{2+} \quad \forall g \in C$$

$$x_{n(\tau+1)g} \geq \frac{\overline{x_g} - e^- + r^{2-} - r^{1-}}{\overline{x_g} - e^-} x_{n\tau g} - \frac{r^{2-}\overline{x_g} - r^{1-}e^-}{\overline{x_g} - e^-} \quad \forall g \in C$$

$$x_{n(\tau+1)g} \geq x_{n\tau g} - r^{2-} \quad \forall g \in C$$

$$\sum_{g \in G} x_{n\tau g} \leq D_{n\tau}(1 + \Delta_D)$$

$$\sum_{g \in G} x_{n\tau g} \geq D_{n\tau}(1 - \Delta_D)$$

$$\sum_{g \in G} x_{n\tau g} - D_{n\tau} = \sum_{v=1}^{V}(d_{n\tau v}^+ - d_{n\tau v}^-)$$

$$0 \leq d_{n\tau v}^+ \leq \overline{d_{n\tau v}^+} \quad \forall v = 1, 2, \ldots, V$$

$$0 \leq d_{n\tau v}^- \leq \overline{d_{n\tau v}^-} \quad \forall v = 1, 2, \ldots, V$$

$$\overline{d_{n\tau v}^+} = \Delta_d * D_{n\tau} * \beta_v^+ \quad \forall v = 1, 2, \ldots, V$$

$$\overline{d_{n\tau v}^-} = \Delta_d * D_{n\tau} * \beta_v^- \quad \forall v = 1, 2, \ldots, V$$

$$x_{n0g} = x_{a(n)T_n g} \quad \forall n = 2, 3, \ldots, N, g \in G$$

where $\quad n = 1, 2, \ldots, N, \quad \tau = 1, 2, \ldots, T_n.$

Formulated stochastic optimization problem is linear and, although a number of decision variables and constraints is high, it can be efficiently solved with a CPLEX solver. Using version 10.00 of the CPLEX solver CPU time of solving the optimization problem was 0.54s for a single t of the rolling horizon $1, 2, \ldots, T$. However, there is 2.36s of CPU time spent for calculating a new scenario tree for the stochastic optimization problem. This adds-up to CPU time of 2.8s for a single iteration or 67.2min for a daily electricity generation problem, or $T = 1440$.

5.3.3 Output of the stochastic model with the uncertainty of the wind power and the capacity loss

The decision on the power output of the thermal plants at the current minute t is based on the expected operational cost of the stochastic problem. The expected cost depends on the heuristic probability distribution of the wind power illustrated with the scenario tree. We wish the System Operator to be ready and respond to the highest fluctuations recorded historically which means that the fluctuations may be stronger than that happening in real time. To evaluate the operational cost of the electricity generation during the real time rather than the expected cost based on the chosen scenario tree we use the decision variables recorded at the root of the scenario tree while solving the rolling horizon problems.

Let $(x_{1g}, x_{2g}, \ldots, x_{T-T^S,g})$ be a vector of the real-time decisions after solving a sequence of T stochastic problems:

$$x_{tg} := x_{1,1,g}^{(t)}, t = 1, 2, \ldots, (T - T^S)$$

where $x_{1,1,g}^{(t)}$ is the power output at the root of the stochastic tree for the t-th problem of the rolling horizon.

In a similar way a mismatch between the electricity generation and the load is recorded.

$$d_{tv}^+ := d_{1,1,v}^{+(t)}, v = 1, 2, \ldots, V$$
$$d_{tv}^- := d_{1,1,v}^{-(t)}, v = 1, 2, \ldots, V$$

where $d_{1,1,v}^{+(t)}$ and $d_{1,1,v}^{-(t)}$ are the positive and the negative mismatch between the electricity generation and the load respectively at the root of the scenario tree for the t-th problem of the rolling horizon.

Knowing the fuel cost c_g of each generating plant $g \in C$ and the cost of the

mismatch between the electricity generation and the load (ζ_v^+, ζ_v^-), the operational cost can be calculated for the planning horizon $t = 1, 2, \ldots (T - T^S)$ as follows.

$$F_{stoch} = \sum_{g \in C} c_g \sum_{t=1}^{T-T^S} x_{tg} + \sum_{v=1}^{V} \zeta_v^+ \sum_{t=1}^{T-T^S} d_{tv}^+ + \sum_{v=1}^{V} \zeta_v^- \sum_{t=1}^{T-T^S} d_{tv}^- \qquad (5.19)$$

where $\{x_{tg}, d_{tv}^+, d_{tv}^-\}$ is a set of real-time decision variables recorded for $(T - T^S)$ stochastic problems.
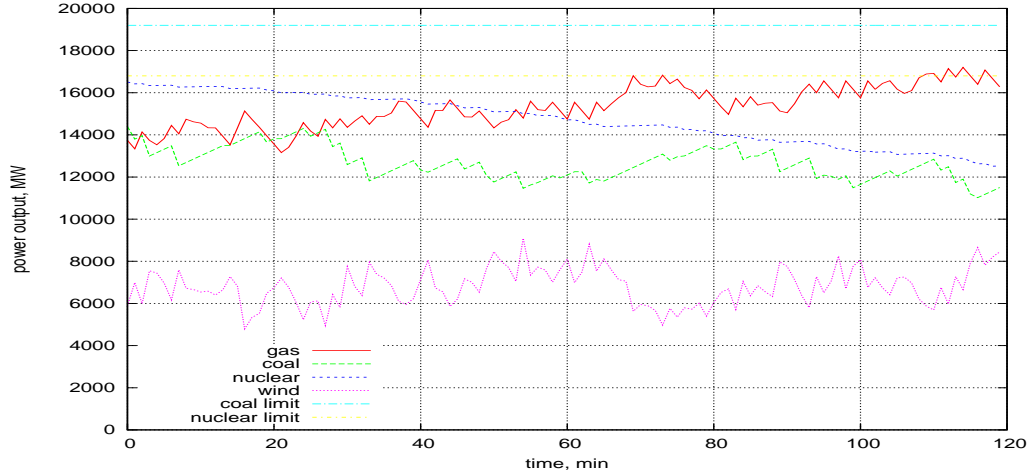

Figure 5.4: An example of the rolling horizon stochastic programming solution with the uncertainty of the capacity loss when 11% of the wind power is incorporated in the total generation

To evaluate the system balancing cost that appears when the wind power is incorporated into the electricity generation system let us find the operational cost in (5.19) for two cases:

Case A: there is uncertainty in the available capacity of the thermal plants but wind energy output is known for the planning horizon T. A scenario tree for this stochastic problem is illustrated in Figure 5.3.

Case B: there is uncertainty in the available capacity of the thermal plants and uncertainty in wind energy output is represented with the scenario tree. A scenario tree for this stochastic problem is a combination of two scenario trees illustrated in Figure 5.2 and Figure 5.3.

Figure 5.4 shows an example of the solution for Case A when there is uncertainty of a possible capacity loss but the wind speed is forecast for certain. Problem with 11% of wind energy in the total generation is feasible but the operational cost is high because the Coal and Nuclear generators are taken down from the maximum capacity levels and the cheaper power is replaced by the more expensive gas power output. Such a scheduling of the thermal plants ensures that in the event of capacity loss, the power system remains within the target frequency until the end of the modelling horizon.

To calculate the operational cost for the Case A there are decision variables recorded for the solution at the root of the scenario tree:

$$(x_{1g}^{(a)}, x_{2g}^{(a)}, \ldots, x_{T-T^S,g}^{(a)})$$
$$(d_{1v}^{+(a)}, d_{2v}^{+(a)}, \ldots, x_{T-T^S,v}^{+(a)})$$
$$(d_{1v}^{-(a)}, d_{2v}^{-(a)}, \ldots, x_{T-T^S,v}^{-(a)})$$

The above variables are used to calculate the operational cost by applying them into the right-hand side of (5.19). The operational cost of the electricity generation when there is only uncertainty in the available thermal capacity but the wind power output is known, is then the following:

$$F_{stoch}^{(a)} = \sum_{g \in C} c_g \sum_{t=1}^{T-T^S} x_{tg}^{(a)} + \sum_{v=1}^{V} \zeta_v^+ \sum_{t=1}^{T-T^S} d_{tv}^{+(a)} + \sum_{v=1}^{V} \zeta_v^- \sum_{t=1}^{T-T^S} d_{tv}^{-(a)}$$

If compared with the operational cost F_{var} calculated in Section 3.3.2, the cost of the stochastic problem $F_{stoch}^{(a)}$ is higher because of the thermal generation running at the level that would allow them responding to a sudden increase or decrease in load. The scheme of having a number of thermal generators away from the output limits to secure feasibility of solution is currently being applied in practise. It is also illustrated with the solution of the stochastic programming problem. The system balancing cost that appears with the uncertainty of the available capacity of the thermal generation can be estimated as follows:

$$f^{(a)} = F_{stoch}^{(a)} - F_{var}$$

We wish to compare further the results of Case A with that calculated for Case B when there is also the uncertainty about wind power output added to the uncertainty of the load. Similarly to Case A, there are decision variables recorded

for a rolling horizon stochastic problem of Case B:

$$(x_{1g}^{(b)}, x_{2g}^{(b)}, \ldots, x_{T-T^S,g}^{(b)})$$
$$(d_{1v}^{+(b)}, d_{2v}^{+(b)}, \ldots, x_{T-T^S,v}^{+(b)})$$
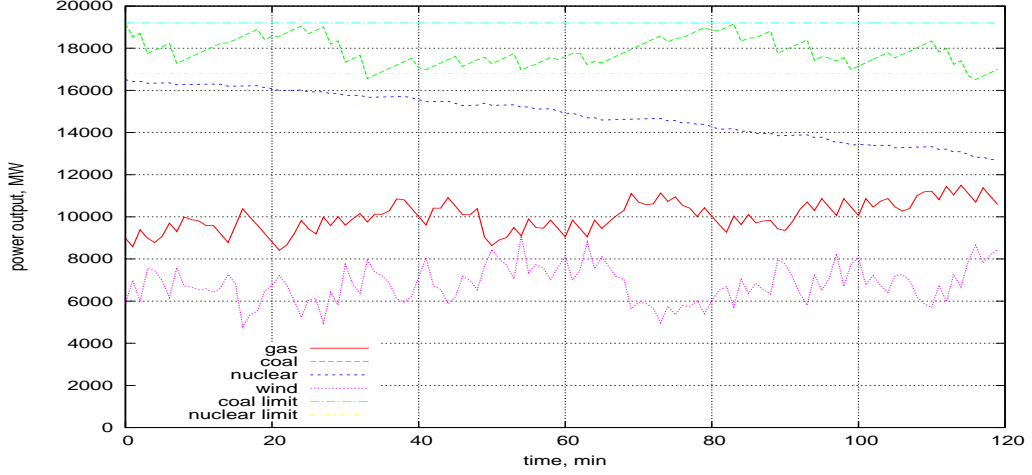$$(d_{1v}^{-(b)}, d_{2v}^{-(b)}, \ldots, x_{T-T^S,v}^{-(b)})$$

Figure 5.5: An example of the rolling horizon stochastic programming solution with the uncertainty of the wind power output and the capacity loss when 7% of the wind energy is incorporated in the total generation

The above variables are further used to calculate the operational cost of the electricity generation when there are two uncertainties that the System Operator faces: uncertainty of capacity loss and uncertainty of wind power output.

$$F_{stoch}^{(b)} = \sum_{g \in C} c_g \sum_{t=1}^{T-T^S} x_{tg}^{(b)} + \sum_{v=1}^{V} \zeta_v^+ \sum_{t=1}^{T-T^S} d_{tv}^{+(b)} + \sum_{v=1}^{V} \zeta_v^- \sum_{t=1}^{T-T^S} d_{tv}^{-(b)}$$

In Case B the System Operator does not have the information about the variability of future wind power output as it is not reflected in the scenario tree. The solution of the stochastic programming problem for Case B is found with the expectation that wind power output is slowly changing over the modelling horizon. Therefore, the cost of the uncertainty in the wind power is calculated as follows:

$$f^{(b)} = F_{stoch}^{(b)} - F_{stoch}^{(a)} + f_w^+ \tag{5.20}$$

where f_w^+ is the additional cost of wind power fluctuations.

100

Figure 5.5 plots an example of the rolling horizon stochastic programming solution when 7% of the wind power is incorporated in the total generation. This is the highest possible amount of wind energy that can be incorporated into the electricity generation system. With wind power higher than 7% in the total generation, the variables of the fourth penalty cost band $(d_{t4}^+; d_{t4}^-)$ are given non-zero values, which means that the mismatch between the electricity generation and the load is so high that it affects the target frequency.

5.4 The system balancing cost when there is the uncertainty of the wind power in the electricity generation system

In order to calculate the system balancing cost of the uncertainty in the wind and thermal generation, the operational cost of Case A and Case B are estimated for a day (or 1440 minutes) of electricity generation for different levels of wind power in the total generation.
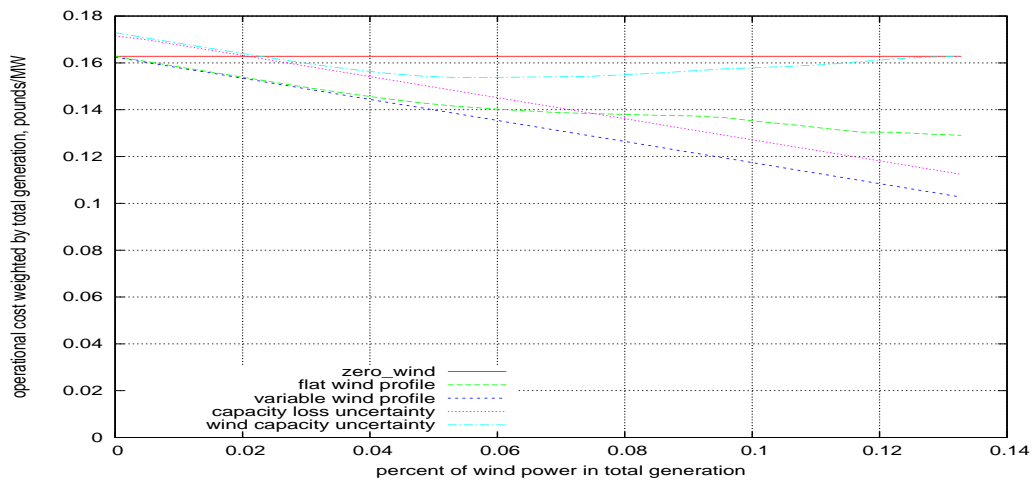
Figure 5.6: The fuel cost of the uncertainty in wind power output and the available thermal capacity, shown for different levels of the wind introduced into the electricity system

Figure 5.6 plots the fuel costs of a daily electricity generation weighted by the total amount of the produced power. For up to 13.3% of wind energy in the total generation, the highest cost is the fuel cost calculated for a problem when there is no wind energy in the power system. However, when the amount of wind exceeds

13.3% in the total generation, the balancing cost of the uncertainty in the wind power output combined with the uncertainty of the available thermal capacity is so high that the power system does not benefit from the incorporation of extra wind into the electricity generation system.

Two optimization models that we developed in this work, deterministic and stochastic, interact when estimating the system balancing cost of variable and unpredictable wind energy incorporated into the electricity generation system. Each of the models covers only one aspect of the wind speed: variability or uncertainty. In case variable wind energy is also uncertain the system balancing cost can be estimated as in (5.20). Even at 0% of wind energy integration the balancing cost of variability is complemented by the cost of uncertainty in loss of thermal generating capacity.

Even though it is possible to estimate the system balancing cost of variable and unpredictable wind energy using the results of deterministic and stochastic optimization models, we wish to emphasize the importance of developing a model that captures both characteristics of wind. Building a scenario tree that includes both, variability and uncertainty of wind energy can be suggested as a future project.

Chapter 6

Conclusion

This thesis presented a study of the statistical characteristics of one-minute wind speed and estimated the system balancing costs when the wind power is incorporated into the electricity generation system. The problem of the increase in the system balancing cost arises as a result of variable and unpredictable nature of the wind speed that transferred into the wind power output. National Grid has to balance the electricity supply and demand every moment, which leads to different problems formulated on time scales of a year, hour, one minute or one second. In this work we were focusing on one-minute electricity generation when the System Operator makes a decision on the output of the available thermal generators. This area was not well-researched before but has an important application in the industry.

We wish to use optimization modelling to estimate the system balancing cost that requires the appropriate data with one-minute resolution. However, there is no one-minute wind speed available on the country level. Least frequent data was presented by ten-minute wind speed published by the Utah Geological Survey, therefore, we wish to generate unbiased samples from the wind stochastic process conditional on each consecutive group of wind speeds having a given average value. To do this, we developed a unique algorithm based on one of the Monte Carlo Markov Chain methods, Gibbs sampling algorithm. It ensures that as the number of iterations of sampling from a known distribution increases, the density of a resulting set of variables converges to the required one.

We originally adapted an algorithm that transfers one-minute wind speed into the deseasonalised and normalised wind speed, first used by Glasbey et al. ([16, 17]), so that the modified Gibbs sampling algorithm is described as follows:

step A: generate normalised wind speed that further transfered into original wind speed;

step B:	if the average of the generated one-minute wind speed does not equal a given average ten-minute wind speed, it is shifted along the vector of the maximum probabilities of the probability distribution;
step C:	a new value of the shifted normalised wind speed is found within a specified tolerance interval of the probability space;
Iterations:	steps A to C are repeated a big number of times that ensures the probability distribution of the resulting set is second-order stationary process.

Generated samples of one-minute wind speed were further used in deterministic and stochastic optimization modelling of the electricity generation system. Both optimization models include common constraints of the electricity generation while our original contribution consists in reflecting the characteristics of the UK power system and developing algorithms that estimate the system balancing costs of variable and unpredictable wind energy.

The system balancing costs appear when the System Operator uses or keeps on stand-by flexible but expensive generating units in order to deal with an unexpected mismatch between the electricity supply and demand. The levels of the operating reserve required at any given time depend partly on the uncertainties in the electricity load but also in the available generating capacity.

Electricity supply and demand in the transmission and distribution power systems need to be balanced every single moment of time. This thesis investigated the electricity generation on one-minute basis and, therefore, the **variability** of the wind energy and the electricity generation with one-minute frequency. The system balancing cost caused by the fluctuations of the wind energy was estimated through a series of cases. The power system benefits from the fact that wind power does not include fuel costs but the operational cost is increased when the thermal plants modify the power output in order to balance the electricity generation and the load.

We assumed in this work that the saving in fuel cost and the additional fuel cost appearing when wind energy is incorporated into the electricity generation system, can be determined as a function of the statistical parameters of the wind energy. To demonstrate this, we developed a unique model of the actual accumulated fuel cost, depending on the mean, absolute value of gradients and standard deviation of the wind energy curve.

In reality the System Operator does not have the information about the variability or the capacity of the future wind power output. The system balancing cost of this **uncertainty** was evaluated using stochastic programming when the flow of the information and a sequence of the decisions by the System Operator were illustrated with a scenario tree. Our original contribution consisted in developing a scenario tree that reflected two uncertainties: uncertainty in the available capacity and uncertainty in wind energy output. The fact that the deterministic and the stochastic optimization models cover only one aspect of wind speed, variability or uncertainty, means that they have to interact in order to estimate the system balancing cost. We wish to suggest exploring different scenario trees in future work that would allow us to estimate the system balancing cost of variable and unpredictable wind speed in one model. We also leave the matter of interaction between the electricity demand and wind speed for future research.

In summary, the statistical characteristics of the wind speed have been explored and the system balancing costs of wind speed variability and unpredictability have been estimated. The results showed that depending on the statistical parameters and the geographic distribution of the wind speed the system balancing cost of the electricity generation can be significant. However, the recent developments in construction of wind turbines as well as introduction of smart metering into the global energy market could open a new area of application for the results of this work.

Appendices

Appendix A. Definitions by the National Grid

NGET is National Grid Electricity Transmission plc (NO: 2366977) whose registered office is at $1 - 3$ Strand, London, $WC2N5EH$.

Supplier is

- (a) A person supplying electricity under an Electricity Supply Licence; or

- (b) A person supplying electricity under exemption under the Act; in each case acting in its capacity as a supplier of electricity to Customers in Great Britain.

Customer is a person to whom electrical power is provided (whether or not he is the same person as the person who provides the electrical power).

Generator is a person who generates electricity under licence or exemption under the Act acting in its capacity as a generator in Great Britain.

Network operator is a person with a User System directly connected to the GB Transmission System to which Customers and/or Power Stations (not forming part of the User System) are connected, acting in its capacity as an operator of the User System, but shall not include a person acting in the capacity of an Externally Interconnected System Operator.

Settlement Period is a period of 30 minutes ending on the hour and half-hour in each hour during a day.

Gate Closure means, in relation to a Settlement Period, the spot time 1 hour before the spot time at the start of that Settlement Period.

Operational Day is the the period from $05:00$ hours on one day to $05:00$ on the following day.

Balancing Mechanism (BM) is a period of time which allows the System Operator to call upon additional generation/consumption or reduce generation/consumption in order to balance the System minute by minute. From July this period of time will be one hour before each trading period.

BM Unit means a unit established and registered (or to be established and registered) by a Party in accordance with Section K3 or, where the context so requires, the Plant and/or Apparatus treated as comprised in or assigned to such unit for the purposes of the Code.

Physical Notification means, in respect of a Settlement Period and a BM Unit, a notification made by (or on behalf of) the Lead Party to the Transmission Company under the Grid Code as to the expected level of Export or Import, as at the Transmission System Boundary, in the absence of any Acceptances, at all times during that Settlement Period.

Quiescent Physical Notification is the data that describes the MW levels to be deducted from the Physical Notification of a BM Unit to determine a resultant operating level to which the Dynamic Parameters associated with that BM Unit apply, and the associated times for such MW levels. The MW level of the QPN must always be set to zero.

Export (Import) Limits is a series of MW figures and associated times, making up a profile of the maximum level at which the BM Unit may be exporting (importing) in MW to the GB Transmission System at the Grid Entry Point or Grid Supply Point, as appropriate.

Dynamic Parameters comprise

- Up to three **Run-Up Rate**(s) and up to three Run-Down Rate(s), expressed in MW/minute and associated Run-Up Elbow(s) and Run-Down Elbow(s), expressed in MW for output and the same for input. It should be noted that Run-Up Rate(s) are applicable to a MW figure becoming more positive;

- **Notice to Deviate from Zero** (NDZ) output or input, being the notification time required for a BM Unit to start importing or exporting energy, from a zero Physical Notification level as a result of a Bid-Offer Acceptance, expressed in minutes;

- **Notice to Deliver Offers** (NTO) and Notice to Deliver Bids (NTB), expressed in minutes, indicating the notification time required for a BM Unit to start delivering Offers and Bids respectively from the time that the Bid-Offer Acceptance is issued. In the case of a BM Unit comprising a Genset, NTO and NTB will be set to a maximum period of two minutes;

- **Minimum Zero Time** (MZT), being either the minimum time that a BM Unit which has been exporting must operate at zero or be importing,

before returning to exporting or the minimum time that a BM Unit which has been importing must operate at zero or be exporting before returning to importing, as a result of a Bid-Offer Acceptance, expressed in minutes;

- **Minimum Non-Zero Time** (MNZT), expressed in minutes, being the minimum time that a BM Unit can operate at a non-zero level as a result of a Bid-Offer Acceptance;

- **Stable Export Limit** (SEL) expressed in MW at the Grid Entry Point or Grid Supply Point, as appropriate, being the minimum value at which the BM Unit can, under stable conditions, export to the GB Transmission System;

- **Stable Import Limit** (SIL) expressed in MW at the Grid Entry Point or Grid Supply Point, as appropriate, being the minimum value at which the BM Unit can, under stable conditions, import from the GB Transmission System;

- **Maximum Delivery Volume** (MDV), expressed in MWh, being the maximum number of MWhr of Offer (or Bid if MDV is negative) that a particular BM Unit may deliver within the associated Maximum Delivery Period (MDP), expressed in minutes, being the maximum period over which the MDV applies.

Target Frequency is that Frequency determined by NGET, in its reasonable opinion, as the desired operating Frequency of the Total System. This will normally be 50.00Hz plus or minus 0.05Hz, except in exceptional circumstances as determined by NGET, in its reasonable opinion when this may be 49.90 or 50.10Hz. An example of exceptional circumstances may be difficulties caused in operating the System during disputes affecting fuel supplies.

High Frequency response is an automatic *reduction* in Active Power output in response to an increase in System Frequency above the Target Frequency (or such other level of Frequency as may have been agreed in an Ancillary Services Agreement). This reduction in Active Power output must be in accordance with the provisions of the relevant Ancillary Services Agreement which will provide that it will be released increasingly with time over the period 0 to 10 seconds from the time of the Frequency increase on the basis set out in the Ancillary Services Agreement and fully achieved within 10 seconds of the time of the start of the Frequency increase and it must be sustained at no lesser reduction thereafter.

Primary Response is the automatic *increase* in Active Power output of a

Genset or, as the case may be, the decrease in Active Power Demand in response to a System Frequency fall. This increase in Active Power output or, as the case may be, the decrease in Active Power Demand must be in accordance with the provisions of the relevant Ancillary Services Agreement which will provide that it will be released increasingly with time over the period 0 to 10 seconds from the time of the start of the Frequency fall on the basis set out in the Ancillary Services Agreement and fully available by the latter, and sustainable for at least a further 20 seconds.

Secondary Response is the automatic *increase* in Active Power output of a Genset or, as the case may be, the decrease in Active Power Demand in response to a System Frequency fall. This increase in Active Power output or, as the case may be, the decrease in Active Power Demand must be in accordance with the provisions of the relevant Ancillary Services Agreement which will provide that it will be fully available by 30 seconds from the time of the start of the Frequency fall and be sustainable for at least a further 30 minutes.

Operating Reserve is the additional output from Large Power Stations or the reduction in Demand, which must be realisable in real-time operation to respond in order to contribute to containing and correcting any System Frequency fall to an acceptable level in the event of a loss of generation or a loss of import from an External Interconnection or mismatch between generation and Demand.

Good Industry Practice is the exercise of that degree of skill, diligence, prudence and foresight which would reasonably and ordinarily be expected from a skilled and experienced operator engaged in the same type of undertaking under the same or similar circumstances.

Bibliography

[1] Government of United Kingdom. *White paper on energy.* UK, May 2007.

[2] Government of United Kingdom. *Renewables Obligation.* UK, 2002.

[3] National Grid Code *http://www.nationalgrid.com/uk/Electricity* Issue 3 Revision 32, 8 December 2008

[4] Balancing and Settlement Code *http://www.elexon.co.uk* V1.1 Designated 21st March 2001

[5] Balancing Mechanism Reporting System *http://www.bmreports.com/* supported by ELEXON Ltd.

[6] Wind Power in the UK. A guide to the key issues surrounding onshore power development in the UK. *Report of the Sustainable Development Comission* UK, 2005

[7] Quaterly energy prices: December 2008 *Department for Business Enterprise and Regulatory Reform (BERR)* http://www.berr.gov.uk

[8] G. Strbac. *Quantifying the system costs of additional renewablesin 2020.* UK, October 2002.

[9] G. Strbac. *Challenges for market design to facilitate cost effective integration of renewables: a UK perspective.* presentation, Berlin, October 2007.

[10] G.Sinden. *Wind power and the UK wind resource.* Environmental Change Institute, University of Oxford, UK, 2005.

[11] G.Sinden. *Diversity in the electricity generating sector.* Environmental Change Institute, University of Oxford, UK, 2005.

[12] G.Sinden. *Diversified renewable energy portfolios for the UK.* Environmental Change Institute, University of Oxford, UK, 2005.

[13] S.Geman and D.Geman. *Stochastic relaxation, Gibbs distributions, and the Bayesian restoration of images.* IEEE, 1984.

[14] A.E.Gelfand and A.F.M.Smith. *Sampling-based approaches to calculating marginal densities.* Journal of the American Statistical Association, Vol.85, N410, 1990.

[15] M.A.Tanner and W.H.Wong. *The calculation of posterior distributions by data augmentation.* Journal of the American Statistical Association, Vol.82, N398, 1987.

[16] D.J.Allcroft and C.A.Glasbey. *A latent Gaussian Markov random field model for spatio-temporal rainfall disaggregation.* Applied Statistics, 52, 487-498, 2003.

[17] D.J.Allcroft and C.A.Glasbey. *Spatial disaggregation of rainfall using a latent Gaussian Markov random field.* Proceedings of the 17th International Workshop on Statistical Modelling, 2002.

[18] M.Durban and C.A.Glasbey. *Weather modelling using a multivariate latent Gaussian Markov random field.* Agricultural and Forest Meteorology, 109, 187-201, 2001.

[19] D.J.Allcroft, M.Durban and C.A.Glasbey. *Modelling weather data.* SCRI Annual Report, 192-195, 2001.

[20] British Atmospheric Data Center. *Surface wind speed measurements funded by Natural Environment Research Council.* http://mst.nerc.ac.uk/

[21] Utah Geological Survey. *Utah's Anemometer Loan Program.* http://geology.utah.gov/SEP/wind/anemometerdata/index.htm

[22] J.F.Manwell, J.G.McGowan and A.L.Rogers. *Wind Energy Explained. Theory, Design and Application.* John Wiley and Sons, Inc., 2002.

[23] B.Everett, G.Boyle and J.Ramage, editors. *Energy systems and sustainability.* The Open University, UK, 2003.

[24] G.Boyle. *Renewable electricity and the grid: the challenge of variability.* Earthscan, UK, 2007.

[25] J.R.Birge and F.Louveaux. *Introduction to stochastic programming.* Sringer-Verlag New York, USA, 1997.

[26] A.Prèkopa. *Stochastic Programming.* Springer, UK, 1995

[27] P.Kall and S.W.Wallace. *Stochastic Programming.* Wiley, Chichester etc., 1994.

[28] S.W.Wallace and W.T.Ziemba. *Applications of Stochastic Programming.* SIAM, USA, 2005

[29] D.Dentcheva, R.Gollmer, A. Möller, W.Römisch and R.Schultz. *Solving the Unit Commitment Problem in Power Generation by Primal and Dual Methods.* Preprint, Mathematik, 1996

[30] A.Möller, W.Römisch. *A Dual Method for the Unit Commitment Problem.* Preprint Nr 95-1, Humboldt-Universitat Berlin, Institut fur Mathematik, 1995

[31] S.Feltenmark, K.C.Kiwiel, P.Lindberg. *Solving Unit Commitment Problems in Power Production Planning.* Operations Research Proceedings, 1996

[32] C.C.Caroe and R.Schultz *A two-Stage Stochastic Program for Unit Commitment Under Uncertainty in Hydro-Thermal Power System.* Preprint SC 98-11, Konrad-Zuse-Zentrum fur Informationstechnik,1998

[33] D.Dentcheva and W.Römisch *Optimal Power Generation under Uncertainty via Stochastic Programming.* Stochastic Programming Methods and Technical Applications, 1997

[34] S.D.Flam. *Nonanticipativity in Stochastic Programming* Journal of Optimization theory and applications, Vol.46, No 1, 1985

[35] National grid electricity transmission. web-site www.nationalgrid.com, 2008.

[36] J.Hardenberg, M.S.Roulston, D.T.Kaplan and L.A.Smith. *Using medium-range weather forecasts to improve the value of wind energy production.* Renewable Energy, 28:585–602, 2003.

[37] R.W.Katz and A.H.Murphy, editors. *Economic value of weather and climate forecasts.* Cambridge University Press, UK, 2003.

[38] A.Costa, A.Crespo, J.Navarro, G.Lizcano, H.Madsen, E.Feitosa. *A review of the young history of the wind power short-term prediction* Renewable and Sustainable Energy Reviews, 12 (2008) 1725-1744

[39] P.R.J.Campbell and K.Adamson. *A novel approach to wind forecasting in the United Kingdom and Ireland* International Journal of Simulation: Systems, Science and Technology, Vol. 6, No 12-13, 2005

[40] U.Schlink and G.Tetzlaff. *Wind speed forecasting from 1 to 30 minutes.* Theoretical and Applied Climatology, No 60, 1998

[41] Report from the Environmental Audit Committee *Keeping the lights on: Nuclear, Renewables and Climate Change* Sixth report Session 2005-2006

[42] E.H.Huitema. *The analysis of Covariance and Alternatives.* John Wiley and Sons, Inc., USA, 1980.

[43] C.Chatfield. *The analysis of Time Series: an Introduction.* 6th edn., Chapman and Hall, London, UK, 2003.

[44] H.Schneider. *Truncated and Cencored samples from Normal Populations* Marcel Dekker, Inc., New York, USA, 1986.

[45] A.C.Johnson, N.T.Thomopoulos. *Characteristics and tables of the left-truncated normal distribution* Midwest Decision Sciences Institute, 2004 Annual Conference Proceedings, Cleveland, April 2004

[46] B.Flury. *A first course in Multivariate statistics* Springer-Verlag New York, USA, 1997.

[47] R.Fourer, D.M.Gay, B.W.Kernighan. *AMPL: A modelling language for mathematical programming* Springer-Verlag New York, USA, 2004.